MOLECULAR ANALYSIS OF INTERACTIONS BETWEEN NORMAL AND TRANSFORMED EPITHELIAL CELLS AT EARLY STAGES OF CANCEROGENESIS

KATARZYNA AGATA ANTON

This Thesis is Submitted to University College London
for the Degree of Doctor of Philosophy

October 2012

Department of Cell Biology
UCL Institute of Ophthalmology
11-43 Bath Street
London
EC1V 9EL

DECLARATION

I, Katarzyna Agata Anton, confirm that the work presented in this thesis is my own. Where information has been derived from other sources, I confirm that this has been indicated in the thesis.

London, October 2012

ABSTRACT

Carcinomas begin with a single transformed cell in an otherwise normal epithelial monolayer. To study the nature of interactions between a transformed cell and its neighbours at this initial stage of tumourigenesis a tetracycline-inducible system driving expression of a constitutively active form of oncogenic Ras (Ras^{V12}) was established in MDCK epithelial cells by the Fujita laboratory. Upon interaction with normal cells, Ras^{V12} cells most commonly undergo apical extrusion from an epithelial monolayer.

In order to identify proteins and pathways involved in interactions between normal and transformed cells, I have performed several biochemical screens described in this thesis. Firstly, I have shown that Hsp90β, identified previously in a 2D gel screen, is increased in Ras^{V12} cells surrounded by normal neighbours in a non-cell-autonomous fashion. By using inhibitors and a dominant negative form of Hsp90, I have shown that upregulation of this chaperone is most likely a part of a stress response delaying extrusion of transformed cells.

Secondly, I have performed a screen for tyrosine phosphorylated proteins and identified myosin IE and plectin as modified in mixed cultures of normal and transformed cells.

Finally, I have undertaken quantitative mass spectrometry of phosphorylated peptides using SILAC labelling to assess changes in Ras^{V12} cells upon their interaction with normal cells. In this screen I have found that an actin anti-capping protein, VASP, is phosphorylated on serine 239 in Ras^{V12} cells interacting with normal cells. This modification is known to inhibits its related to actin function. I have shown that depletion of VASP in Ras^{V12} cells results in their enhanced extrusion from normal monolayers, most likely due to their compromised attachment. The phosphorylation on serine 239 may be an early step in extrusion, contributing to disassembly of focal adhesions and stress fibres in transformed cells. I have also studied the role of another protein identified in the SILAC screen, MRCKβ, and shown that its depletion results in enhanced extrusion of Ras^{V12} cells from normal monolayers.

TABLE OF CONTENTS

TABLE OF FIGURES

LIST OF TABLES

LIST OF ABBREVIATIONS

17-AAG – 17-allylamino-17-demethoxygeldanamycin

ABL – Abelson leukemia virus tyrosine kinase

Akt – v-akt murine thymoma viral oncogene homolog 1

AMPK – AMP-activated protein kinase

APC – adenomatosis polyposis coli

Bak – BCL2-antagonist/killer

Bax – BCL2-associated x protein

Bcl-2 – B-cell lymphoma 2

BF – bright field

BLAST – Basic Local Alignment Search Tool

Bleb – blebbistatin

Brk – brinker

BSA – bovine serum albumin

Cdc37 – cell division cycle 37 homolog

Cdc42 – Rho GTP-ase cell division control protein 42

CDK1 – cyclin-dependent kinase 1

Cdk4 – cyclin-dependent kinase 4

cGMP – cyclic guanosine monophosphate

CHIP – C-terminus of Hsc70-interacting protein

COSMIC – Catalogue Of Somatic Mutations In Cancer database

CRIB – Cdc42/Rac interactive binding domain

Csk – C-terminal Src kinase

Ctrl – control

DAG – diacylglycerol

DAPI – 4',6-diamidino-2-phenylindole

DH – Dbl homology domain

DH5α – a strain of *Escherichia coli*

Dlg – discs large

DMEM – Dulbecco's Modified Eagle's Medium

DNA – deoxyribonucleic acid

DNHsp90β – dominant negative Hsp90β

Dpp – decapentaplegic

DTT – dithiothreitol

e.g. – for example

EGF – epidermal growth factor

EGFR – EGF receptor

EMT – epithelial to mesenchymal transition

Ensembl – a joint project between EMBL-EBI and the Wellcome Trust Sanger Institute to develop a software system which produces and maintains automatic annotation on selected eukaryotic genomes

ER – endoplamic reticulum

ERBB2 – erythroblastic leukemia viral oncogene homolog 2

ERK – extracellular-signal-regulated kinase

etc. – *Et cetera*; and other things

EthD-1 – ethdium homodimer-1

EVH1 - Ena/VASP homology 1 domain

EVH2 - Ena/VASP homology 2 domain

Exp – experiment

FAK – focal adhesion kinase

FBS – fetal bovine serum

FCS – fetal calf serum

FGF – fibroblast growth factor

FTase – farnesyltransferase

Fwe – flower

G12 – mutation of glycine in position 12 of Ras protein

G13 – mutation of glycine in position 13 of Ras protein

GA – Golgi Apparatus

GAPDH – glyceraldehyde-d3-phosphate dehydrogenase

GAPs – GTPase-activating proteins

GC – green fluorescent channel

GDI – guanine nucleotide dissociation inhibitors

GDP – guanosine diphosphate

GEFs – guanine nucleotide exchange factors

GF – growth factor

GFP – green fluorescent protein

GTP – guanosine triphosphate

GTPase – guanosine triphosphatase

H/M ratio – 'heavy' to 'medium' ratio

HA – human influenza hemagglutinin

HCD – higher energy collision dissociation

HEK293 – human embryonic kidney 293 cells

HGF – hepatocyte growth factor

Hid – head involution defective

HIF-1α – hypoxia-inducible factor 1

HILIC – hydrophilic interaction chromatography

Hop – Hsp70/Hsp90 organizing protein

H-Ras – Harvey rat sarcoma viral oncogene homolog

HRP – horseradish peroxidase-conjugated

HSC – hematopoietic stem cells

Hsp90 – heat shock protein 90

HSW – Hippo-Salvador–Warts pathway

IAA – iodoacetamide

ICMT – isoprenylcysteine carboxylmethyltransferase

IMAC – ion affinity chromatography

IP_3 – inositol 1,4,5-triphosphate

JNK – JUN N-terminal kinase

K-Ras – Kirsten rat sarcoma viral oncogene homolog

LAS - Leica Application Suite software

LB – Luria broth

LC-MS – liquid chromatography mass spectrometry

Lgl – lethal-giant larvae

Mahj – mahjong

MAPK – mitogen-activated protein kinase

MCF10A – Michigan Cancer Foundation 10A; a non-tumorigenic human epithelial cell line derived from a mammary gland

MCM2 – minichromosome maintenance complex component 2

MDCK – Martin-Darby canine kidney cells

MeCN – acetonitrile

MEK – MAP kinase kinase

MLC – myosin light chain

MLCK – myosin light chain kinase

MLK – mixed-lineage kinase

MMP – matrix metalloproteinase

MRCKβ – myotonic dystrophy kinase-related Cdc42-binding kinase β

MST – mammalian Ste20-like kinase

MTOC – microtubule organising centre

mTOR – mechanistic target of rapamycin

Myc – v-myc myelocytomatosis viral oncogene homolog

MYPT1 – myosin light chain phosphatase complex

N/I – not identified

N/Q – not quantified

NA – not available

NCBI – National Center for Biotechnology Information

NF1 – neurofibromin 1

NO – nitric oxide

NOS – nitric oxide synthetase

N-Ras – neuroblastoma *RAS* viral oncogene homolog

Opti-MEM – Reduced Serum Medium

PAKs – p21-activated kinases

PBS – phosphate buffered saline

PDGF – platelet-derived growth factor

PE – phorbol easter

PFA – paraformaldehyde

PH – pleckstrin homology domain

PI3K - phosphoinositide 3 kinase

PIP_2 – phosphatidylinositol 4,5-bisphosphate

PKC – protein kinase C

PKD1 – PI3K-dependent kinase-1

PKG – protein kinase G

PLCε – phospholipase C epsilon

PM – plasma membrane

pMLC – myosin light chain phosphorylated on serine 19

ppMLC – myosin light chain phosphorylated on both threonine 18 and serine 19

PRR – proline-rich region

PtdIns, PI – phosphatidylinositol

PTMs – post-translational modifications

PVDF – polyvinylidene fluoride membrane

PX – phox homology domains

Q61 – mutation of glutamine in position 61 of Ras protein

RA – Ras-association domain

Rab5 – Rab5 protein, member Ras oncogene family

Raf – v-raf murine sarcoma viral oncogene homolog

RalGDS – Ral guanine nucleotide dissociation stimulators

Rap1 – Rap1 protein, member Ras oncogene family

RasGRFs – guanine nucleotide-releasing factors

RasGRPs – guanyl nucleotide-releasing proteins

RASSF – Ras association domain family members

Ras^{V12} – a constitutively active form of Ras protein with a substitution on residue 12 from a glycine to a valine residue

Ras^{V12} cells – a stable cell line of MDCK cells transfected with a construct encoding a constitutively active form of H-Ras^{V12} expressed in an inducible manner under a tetracycline-controlled promoter

RBD – Ras/Rap binding domain

RBD – Ras-binding domain

RC – red fluorescent channel

RCE1 – endoprotease RAS-converting enzyme 1

REM – Ras-exchange motif

Rin – Ras and Rab interactor

RNA – ribonucleic acid

ROCK – Rho-associated protein kinase

RTK – receptor tyrosine kinase

s.d. – standard deviation

S239 – serine often phosphorylated in VASP protein

SARAH – Salvador/Rassf/Hippo domain

Scrib – scribble

SDS – Sodium dodecyl sulfate

SDS PAGE – sodium dodecyl sulfate polyacrylamide gel electrophoresis

SH2 – Src homology 2 domain

SH3 – Src homology 3 domain

SILAC – stable isotopomeric versions of amino acids

siRNA – small interfering RNA

SMART – simple modular architecture research tool

Sos – son of sevenless

SQSTM1 – sequestosome 1

Src – Rous sarcoma oncogene

Src cells – a stable cell line of MDCK cells transfected with a construct encoding a temperature sensitive mutant v-Src

SRF – serum response factor

STRING – Search Tool for the Retrieval of Interacting Genes/Proteins

TBS – Tris-buffered saline

TCS SPE – true point-scanning, spectral system from Leica

Tet – tetracycline

TFA – trifluoroacetic acid

TGFβ – transforming growth factor beta

TIAM1 – T-lymphoma and metastasis gene 1

TNF – tumour necrosis factor

TRP – tetratricopeptide repeat

VASP – vasodilator-stimulated phosphoprotein

VEGFR – vascular endothelial growth factor receptors

WASP – Wiskott-Aldrich syndrome protein

Wg, Wnt – wingless

WW – a protein domain with two highly conserved tryptophans

Yki – yorkie

ZONAB – ZO-1-associated nucleic acid-binding protein

CHAPTER 1:

INTRODUCTION

CHAPTER 1: INTRODUCTION

1.1 INTRODUCTION – THE IDEA BEHIND THE STUDY

Cancer is an ever-growing threat for everyone. Most cancers can only be detected at later stages of the disease, when they have accumulated a lot of mutations and start to form tumours. However we cannot underestimate the importance of early detection of the developing disease, as it correlates with much better prognosis for patients. In order to be able to detect cancer at earlier stages, we need to understand how it originates. Despite the general agreement in the field that carcinomas start off from a single mutated cell within a normal epithelial monolayer, not many studies have been carried out to clarify what exactly happens at the very beginning. Is a single transformed cell recognised by its neighbours and how do normal cells react to a sudden change in their environment?

Some of these questions have been addressed by the Fujita laboratory where, in a mammalian tissue culture system, cells transformed either by overexpression of an oncogene (H-Ras^{V12} or v-Src) or depletion of a tumour suppressor (Scribble) were mixed with normal cells. These studies revealed that transformed cells are recognised by their normal neighbours and either killed, as in the Scribble system (Norman et al., 2012), or extruded from the monolayer, as in the Ras^{V12} (Hogan et al., 2009) and v-Src (Kajita et al., 2010) systems (since the extruded cells remain alive the significance of these events is still unknown). This elimination phenomenon resembles cell competition in *Drosophila* (described in section 1.3) where less fit mutant cells are removed from imaginal discs of a developing embryo in order to maintain the integrity of the whole organ. A similar mechanism may function in mammalian epithelial monolayers leading to the removal of randomly appearing transformed cells.

Although some of the questions about extrusion in the Ras^{V12} system have already been addressed (described in section 1.5.4), unclear remains which signalling pathways are involved, how the recognition occurs and what the actual mechanism of extrusion is. The aim of my thesis is to identify novel proteins that

are important at early stages of extrusion using different biochemical screens and to understand their role.

1.2 RAS IN NON-TRANSFOMED CELLS AND AS AN ONCOGENE

1.2.1 DISCOVERY OF RAS PROTEINS

Ras genes were first identified in the late seventies in retroviruses (in this case, oncoviruses) that, as it was later clarified, hijacked them from non-transformed cells. The *ras* genes were subsequently mutated during viral replication and served as oncogenes upon reinfection and transformation of vertebrate cells. The Harvey sarcoma virus-associated oncogene was named H-*ras*, the Kirsten sarcoma virus-associated oncogene – K-*ras* (reviewed in (Karnoub and Weinberg, 2008)). Shortly after, mutated H-*Ras* and K-*Ras* genes were discovered in mouse and human cancer cell lines as well as in actual carcinoma samples. Another prominent member of the Ras family, N-*RAS*, was cloned from neuroblastoma and leukaemia cell lines.

Studies on human carcinomas revealed an association of particular mutations with different types of cancers: K-*RAS* was most commonly found mutated in pancreatic and colonic carcinomas, H-*RAS* in bladder carcinomas, and N-*RAS* in lymphomas and melanomas (reviewed in (Karnoub and Weinberg, 2008)) (more information in section 1.2.5).

1.2.2 RAS SUPERFAMILY AS SMALL GTPASES

In order to understand why mutations in *Ras* genes are crucial for some types of cancers, it is important to understand the function of Ras proteins in non-transformed cells.

The extended Ras superfamily, known up to date, comprises of more than 150 different proteins, playing vital roles in cell cycle progression (Ras and Rho), cell survival (Ras and Rho), actin cytoskeleton reorganisation (Rho), cell polarity and movement (Rho), vesicular (Rab, Arf) and nuclear (Ran) transport (reviewed in (Wennerberg et al., 2005)).

Ras proteins are small GTPases (20-25 kDa, 188-189 amino acids) that act as GTP-GDP regulated cellular switches. In contrast to heterotrimeric G proteins, another family of cellular GTPases, Ras consists of only one subunit, which is in fact similar to the α subunit of G proteins. The core G domain involved in GTP hydrolysis constitutes nearly 90% of the whole Ras protein (5-166 amino acids) and is conserved among all family members (Figure 1). Within this domain, five small G motives are responsible for binding of nucleotides (residues: 10-17, 35, 57-60, 116-119, 145-147). Upon GDP/GTP exchange, switches I and II (residues 32-38 and 59-67, respectively) undergo a conformational change that results in higher affinity of Ras proteins towards their effectors which can now bind to the core effector domain (32-40). The last segment of Ras proteins (residues 167-188,189) is highly variable and contains membrane targeting sequences that will be discussed later (section 1.2.3) (reviewed in (Cox and Der, 2010; Ellis and Clark, 2000; Wennerberg et al., 2005)).

Figure 1. Structure of Ras proteins.

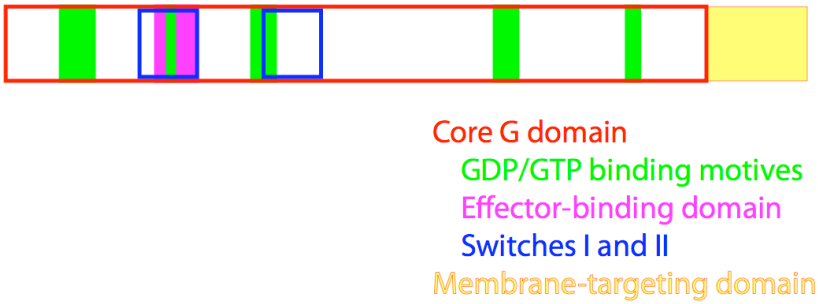

Since the intrinsic GTP binding and hydrolysis activities are weak, Ras proteins are regulated by guanine nucleotide exchange factors (GEFs) as activators stimulating GDP/GTP exchange, and GTPase-activating proteins (GAPs) as inactivators catalysing GTP hydrolysis (Rho and Rab proteins are also assisted by guanine nucleotide dissociation inhibitors) (reviewed in (Vigil et al., 2010)) (Figure 2).

All Ras GEFs contain a common catalytic domain called CDC25 homology domain (about 250 amino acids long) and a shorter Ras-exchange motif (REM). Additional sequences within different GEFs provide specificity for upstream regulators and activation mechanisms as well as further catalytic functions. Two

family members of the Ras GEFs, Sos (Son of Sevenless) and RasGRFs (guanine nucleotide-releasing factors), contain Dbl homology (DH) and pleckstrin homology (PH) domains, which allow them to catalyse guanine nucleotide exchange also on Rho family members, in particular Rac1. Proteins that belong to the third family of Ras GEFs, RasGRPs (guanyl nucleotide-releasing proteins), contain calcium-binding EF motives and a C1 domain with affinity for diacylglycerol (DAG) and phorbol easter (PE). These structures enable regulation by both DAG and PE of the catalytic activity of RasGRPs (reviewed in (Mitin et al., 2005)).

Ras GAPs are a more heterogeneous group compared to the GEFs. They contain only one common domain, RasGAP that stimulates GTP hydrolysis (±250 amino acids long), but share no other universal features. Although non-functional Ras GAPs can contribute to overactivation of Ras proteins and lead to cancer, they have been considerably less studied than the GEFs. The discovery of p120 RasGAP, provided an explanation why only particular residues within Ras proteins often undergo missense mutations in cancer (section 1.2.5). Mutations of the residues G12 (glycine in position 12) and Q61 (glutamine in position 61), which all main isoforms of Ras have in common, result in insensitivity of the protein to the GAP. As a consequence, Ras becomes permanently bound to GTP and is constitutively active (reviewed in (Mitin et al., 2005; Vigil et al., 2010)).

Figure 2. Regulation of Ras GTPases by their GAPs and GEFs. Ras proteins require the assistance of GEFs and GAPs to function as GTP-GDP regulated molecular switches. Known Ras GAPs – in red, Ras GEFs – in green.

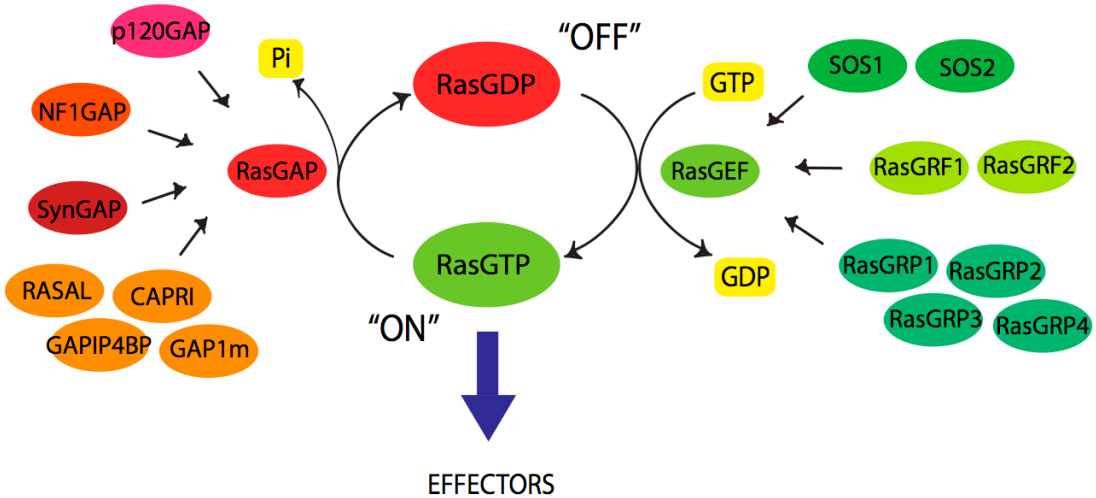

1.2.3 POST-TRANSLATIONAL MODIFICATIONS AND SUBCELLULAR LOCALIZATION OF RAS IS CRUCIAL FOR PARTICULAR FUNCTIONS

Apart from GAPs and GEFs, the function of Ras proteins is regulated by enzymes facilitating their post-translational modifications (PTMs). Directly after translation, Ras proteins exist in the cytoplasm as globular hydrophilic molecules. As their signalling function is primarily dependent on their association with cellular membranes, they require post-translational processing that results in converting their C-terminus into a hydrophobic tail that mediates their membrane insertion. Complex PTMs of Ras proteins control their localization to different cellular compartments, which in turn affects their transforming abilities (e.g. signalling downstream of Ras differs depending on its localization to the Golgi membranes and to the plasma membrane) (reviewed in (Ahearn et al., 2012)).

The first signal for a constitutive modification of the C-terminal end of Ras proteins is the CAAX motif (where C is cysteine, A – aliphatic, X – any amino acid) that is recognised by farnesyltransferase (FTase). FTase catalysis the addition of a farnesyl isoprenoid to the cysteine residue in a newly translated Ras protein. This modification directs the protein to the endoplasmic reticulum (ER), where the CAAX motif is processed by two other enzymes: endoprotease RAS-converting enzyme 1 (RCE1) and isoprenylcysteine carboxylmethyltransferase (ICMT). Firstly, RCE1 removes the AAX part of the motif, leaving farnesylcysteine at the C-terminus, then ICMT catalyses the methyl esterification of the α-carboxyl group of farnesylcysteine. The end product of all three modifications is a membrane-associated Ras protein with a hydrophobic C-terminus. However, at this stage Ras is still not hydrophobic enough to facilitate translocation to the plasma membrane (PM) (reviewed in (Ahearn et al., 2012)).

In order to become a PM component, Ras proteins require a second signal within the amino acid sequence that undergoes modifications, another cysteine residue (in case of H-RAS, N-RAS and one isoform of K-RAS – K-RAS4A) or a lysine-rich region (in case of KRAS4B). The cysteine residue can be palmitoylated in a reversible manner by palmitoyl acyltransferase DHHC9–GPC16 that resides in the Golgi Apparatus (GA) (Swarthout et al., 2005). This modification increases the affinity of Ras proteins for membranes over 100-fold comparing to only

farnesylated Ras. In case of KRAS4B, the lysine-rich region itself stabilizes association of this protein with the PM. Moreover, it can be further modified by PKC, which phosphorylates serine 181 within the lysine-rich region. This modification is known as farnesyl-electrostatic switch: once phosphorylated, KRAS4B looses the affinity for membranes, dephosphorylation brings it back (Silvius et al., 2006).

Among other known Ras modifications are acylation/deacylation (linked to RAS trafficking to and from the GA), peptidyl-prolyl isomerization, ubiquitylation (regulates trafficking of HRAS to and from endosomes) and S-nitrosylation (reviewed in (Ahearn et al., 2012)).

1.2.4 Molecular and cellular effects of Ras activation

In non-transformed cells, in which Ras proteins are not constitutively active, upstream signalling of Ras starts at the PM. Firstly, growth factors, such as EGF, FGF, PDGF, bind appropriate receptor tyrosine kinases, stimulating receptor dimerization, autophosphorylation and activation. This event leads to the recruitment of a cytoplasmic complex of a RasGEF with an adaptor protein containing an SH2 domain, which binds phospho-tyrosine on the active receptor (e.g. SOS RasGEF and Grb2 adaptor). The now membrane-associated RasGEF complex is positioned in close proximity to membrane-bound Ras and can facilitate GDP/GTP exchange and activation of this small GTPase (reviewed in (Mitin et al., 2005)).

Ras activation triggers many distinct cellular pathways (summarised in Figure 3). Most of the downstream effectors share a Ras-binding domain (RBD) or a Ras-association domain (RA) that enables them to be recruited to the membrane by GTP-bound Ras (reviewed in (Cox and Der, 2010)).

The first identified Ras effector is Raf-1, the top kinase in the mitogen-activated protein kinases (MAPK) cascade, a major mechanism by which mitogens stimulate cell proliferation. Raf proteins (A-Raf, B-Raf, Raf-1 also known as c-Raf) are Ser/Thr kinases that upon activation act as MAPK kinase kinases (MAP3K) by phosphorylating MAPK kinases (here MEKs), which in turn activate the MAPK extracellular-signal-regulated kinases (here ERKs). After translocation to the nucleus, ERK proteins activate various transcription factors, among them the well-

described Elk-1 protein. Active Elk-1 forms a ternary complex with serum response factor (SRF) on promoters of genes containing serum response elements (SRE), e.g. the growth-related *cFos* and *JunB* genes (reviewed in (Sharrocks, 2001)).

The second best characterised downstream effector of Ras is phosphoinositide 3 kinase (PI3K), which is important for numerous cellular processes, such as cell cycle progression, growth, survival, migration, and intracellular vesicular transport. PI3K phosphorylates the 3-hydroxyl group of the inositol ring of phosphatidylinositol lipids (PtdIns, PI). Depending on the phosphorylation state of other hydroxyl groups in the inositol ring, 3-phosphorylated PtdIns molecules can subsequently bind effector proteins containing various lipid binding domains: PH domains, phox homology domains (PX) and FYVE domains (reviewed in (Vanhaesebroeck et al., 2010)). Binding of 3-phosphoinositides coordinates the localization and function of effector proteins, among them are Akt family Ser/Thr kinases, PI3K-dependent kinase-1 (PKD1), as well as some GEFs for Rho and Ras (reviewed in (Kyriakis, 2009)).

The Ral guanine nucleotide dissociation stimulators (RalGDS) family of Ras effectors consists of four members: RalGDS, RGL, RGL2/Rlf and RGL3. All of them share high sequence homology as well as three conserved domains: a CDC25 homology domain, an upstream Ras exchange motif (REM), and a C-terminal Ras/Rap binding domain (RBD). The CDC25 domain allows RasGDS to act as GEFs for Ral proteins (members of the Ras family), while the RBD part mediates their interaction with Rap and Ras themselves. Due to the presence of both sequences, RalGDS are a unique link between different small GTPases allowing them to regulate each other. Activated Ral proteins bind and regulate Sec5, filamin, RalBP1, and ZONAB, thereby, play a role in the regulation of endocytosis, exocytosis, actin organization, and changes in gene expression (reviewed in (Ferro and Trabalzini, 2010)).

Another Ras effector with a GEF activity is T-lymphoma and metastasis gene 1 (TIAM1), which stimulates Rac1 activation. Through Rac1, TIAM1 contributes to actin cytoskeleton rearrangements, activation of p21-activated kinases (PAKs) and JUN N-terminal kinase (JNK) (reviewed in (Minard et al., 2004)).

A particularly powerful Ras effector is phosphoinositide-specific phospholipase C epsilon (PLCε), which directly generates inositol 1,4,5-

triphosphate (IP_3) and diacylglycerol (DAG) from phosphatidylinositol 4,5-bisphosphate (PIP_2). Production of these secondary messengers stimulates two cellular events: release of calcium from the ER into the cytosol as well as activation of PKC signalling cascades. Consequently, this results in the modulation of important cellular processes, such as cell division and differentiation. On a physiological level, these second messengers are important for correct heart and kidney function. Similarly to RalGDS and TIAM1, PLCε has a CDC25 domain, which enables it to act as a GEF for Rap1 and Ras, creating a positive regulation loop that results in prolonged activation of PLCε (reviewed in (Smrcka et al., 2012)).

The Rin family is another group of Ras effectors with GEF activity, this time towards Rab proteins, in particular, they have an ability to stimulate Rab5-dependent endocytosis (Kajiho et al., 2011; Kimura et al., 2006; Tall et al., 2001). Rin1 has also been implicated in activation of ABL tyrosine kinase and as a consequence actin remodelling (Hu et al., 2005).

Ras association domain family members (RASSF) are a recently discovered group of Ras effectors that were implicated in activation of cell death, but also stabilization of microtubules and regulation of the cell cycle. RASSF are a unique group of effectors without any catalytic activity, instead serving as adaptor proteins for various signalling molecules. The two best studied members of the family, RASSF5A as well as RASSF1A, have been shown to promote apoptosis through interactions *via* their SARAH domain with the kinases MST1 and MST2. This association leads to activation of the kinases and their translocation to the nucleus, where they contribute to the DNA damage response (reviewed in (Gordon and Baksh, 2011; Pfeifer et al., 2010)).

Figure 3. **Ras effectors.** Main pathways triggered by Ras activation downstream of a growth factor (GF) binding to a receptor tyrosine kinase (RTK). Further explanation in the text (1.2.4).

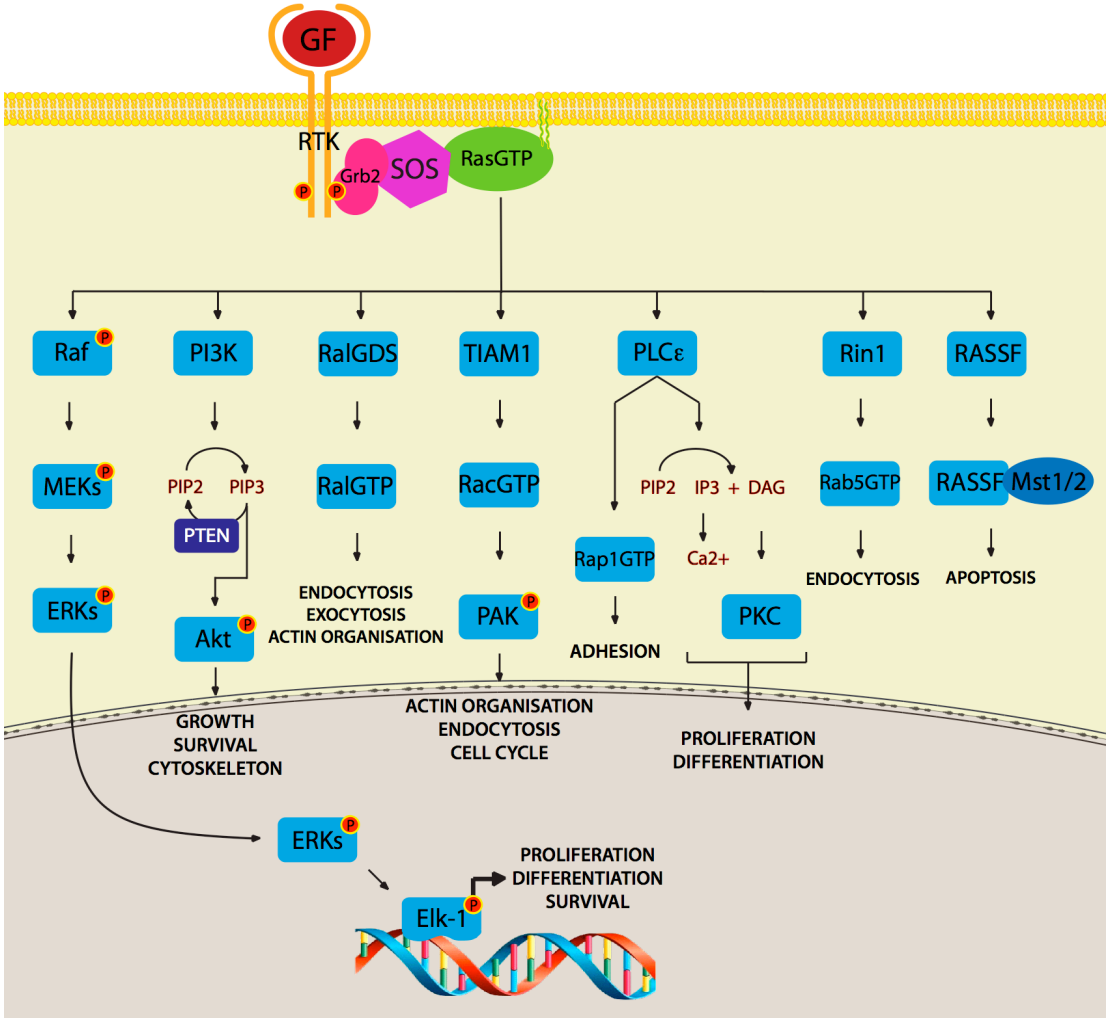

1.2.5 RAS ONCOGENES IN CANCER

CANCER AS A MULTISTEP PROCESS

Early studies on Ras function in cancer revealed that oncogenic *Ras* was unable to transform primary cells, e.g. freshly isolated rodent embryos, on its own (Land et al., 1983). However introduction of H-Ras^{V12} (a mutant with a glycine to valine substitution on residue 12) led to transformation of cells already immortalised (Newbold and Overell, 1983) or those that had undergone other predisposing modifications (Land et al., 1983). The finding supported the idea of carcinogenesis as a graduate, multistep process.

After decades of research, there is an agreement in the field that development of cancer requires a set of basic cellular processes to be altered. In their review, Hanahan and Weinberg enumerate the hallmarks of cancer: cells have to become independent of growth signals, but still be able to proliferate, they need to develop insensitivity to growth inhibition and cell death, as well as change their metabolism. At later stages, tumours require sustained angiogenesis, and eventually gain invasive and metastatic properties (Hanahan and Weinberg, 2000; Hanahan and Weinberg, 2011). Interestingly, most of these features can be reached *via* mutations in *Ras* genes themselves, their regulators and effectors. Therefore Bar-Sagi calls the Ras pathway a "tumourigenic web" that captures numerous changes required for cancer to arise and progress (Pylayeva-Gupta et al., 2011).

MUTATIONS IN RAS GENES

RAS proteins are mutated in 33% of human cancers (from COSMIC database, June 2012). Most common mutations are missense substitutions (over 98% of all sequenced *RAS* mutations) that usually occur in three particular positions of RAS proteins: glycine 12 (G12), glycine 13 (G13) and glutamine 61 (Q61) (Figure 4). These changes impair the ability of RAS to hydrolyse GTP through either interfering with GAP binding (G12, G13) or preventing water molecules to access GTP, an event that is essential for GTP hydrolysis. As a result these oncoproteins become permanently bound to GTP and constitutively activate their downstream effectors (reviewed in (Pylayeva-Gupta et al., 2011)).

Figure 4. Frequency of particular mutations in different *RAS* genes found in human cancers. [COSMIC database, June 2012]

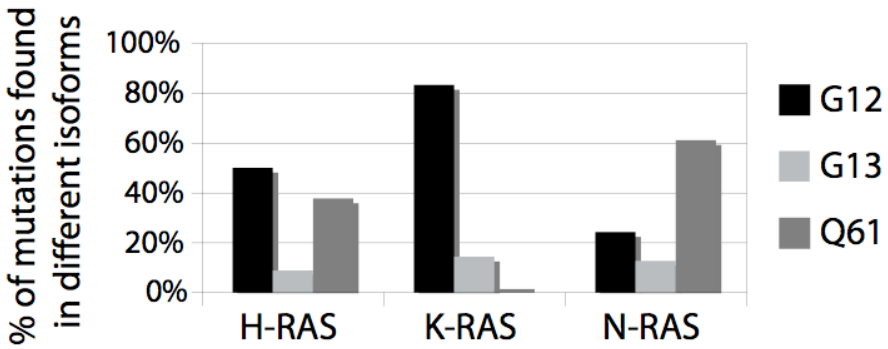

In human cancers, K-*RAS* is mutated most commonly in malignancies of lungs, intestines and pancreas. Changes in H-*RAS* are found in cancers arising from skin, head and reproductive organs, while N-*RAS* – in diseases of haematopoietic tissues and skin (Table 1). It is unclear why certain type of cancer would benefit from mutations in particular RAS isoforms. According to some available data, tissue specific expression levels of different Ras proteins matter most, and if the promoters are replaced, the isoforms can be functionally redundant (Potenza et al., 2005). Conversely, other studies suggest that RAS proteins have separate cellular functions (Haigis et al., 2008). Further research is necessarily to clarify the differences between K-RAS, H-RAS and N-RAS in normal as well as pathological conditions.

Table 1. Frequency of mutations in *RAS* genes found in different types of human cancers. NA – not available. Shaded fields – found in over 5% of samples. * - Data from the COSMIC database from 5/6/2012. Numbers in brackets indicate total number of unique samples sequenced. ** - Data from the US National Cancer Institute SEER Cancer Statistics Review. The rates are shown as per 100,000 people per year within a period 2005-2009.

Primary Tissue	H-RAS % Mutated*	K-RAS % Mutated*	N-RAS % Mutated*	Incidence Rate**	Mortality Rate**
Adrenal gland	1% (136)	0 (211)	5 (171)	NA	NA
Autonomic ganglia	0% (63)	3 (63)	6 (102)	NA	NA
Biliary tract	0% (153)	28 (1766)	2 (287)	NA	NA
Bone	2% (199)	1 (252)	0 (207)	0.9	0.4

Breast	1% (759)	3 (974)	2 (548)	124.3	23.0
Central nervous system	0% (964)	1 (1184)	1 (1074)	6.5	4.3
Cervix	9% (264)	7 (637)	2 (132)	8.1	2.4
Endometrium	1% (314)	14 (2312)	1 (337)	23.9	4.1
Eye	0% (33)	4 (108)	2 (127)	0.8	0.1
Haematopoietic and lymphoid tissue	0% (3171)	5 (6265)	10 (9155)	40.8	17.5
Kidney	0% (273)	1 (706)	0 (435)	15.1	4.0
Large intestine	0% (757)	35 (39774)	3 (2197)	46.3	16.7
Liver	0% (271)	6 (537)	3 (310)	6.9	4.2
Lung	0% (2118)	17 (19130)	1 (3637)	62.6	50.6
Meninges	0% (62)	0 (62)	0 (62)	NA	NA
Oesophgus	1% (161)	3 (375)	0 (161)	4.5	4.3
Ovary	0% (152)	14 (3193)	3 (191)	12.7	8.2
Pancreas	0% (279)	58 (5838)	2 (306)	12.1	10.8
Parathyroid	0% (100)	0 (100)	0 (100)	NA	NA
Penis	7% (28)	4 (28)	0 (28)	0.8	0.2
Peritoneum	0% (3)	7 (87)	-	0.7	0.3
Pituitary	3% (300)	0 (300)	0 (300)	NA	NA
Prostate	5% (558)	8 (1009)	1 (558)	154.8	23.6
Salivary gland	15% (164)	3 (173)	0 (48)	1.3	0.2
Skin	6% (2466)	2 (1829)	16 (5939)	23.0	3.6
Small intestine	0% (5)	17 (380)	0 (6)	2.0	0.4
Soft tissue	5% (745)	6 (1145)	5 (514)	3.3	1.3
Stomach	4% (384)	7 (2822)	2 (216)	7.6	3.6
Testis	4% (130)	4 (432)	3 (283)	5.4	0.2
Thymus	2% (46)	2 (186)	0 (46)	0.7	0.3
Thyroid	4% (4327)	2 (5446)	7 (4943)	11.6	0.5
Upper aerodigestive track	9% (1202)	3 (1734)	3 (860)	10.8	2.5
Urinary track	9 % (1765)	4 (1099)	1 (873)	21.1	4.5
TOTAL	**3% (22379)**	**23% (100428)**	**7% (34554)**	**465.2 (All sites)**	**178.7 (All sites)**

MUTATIONS IN OTHER COMPONENTS OF THE RAS PATHWAY

Apart from RAS itself, many of its regulators as well as effectors have been implicated in tumourigenesis. This includes the oncogenes *EGFR*, *BRAF*, *PI3KCA* (catalytic domain) and *RALGDS* that are mutated in 20%, 20%, 12% and 1% of human cancers, respectively (from COSMIC database, June 2012). Another two important RAS effectors, PLCε and TIAM1, are not recognised as proto-oncogenes; however, they have been shown to contribute to tumour progression in mice (TIAM1 was shown to be essential for Ras-dependent transformation) (Bai et al., 2004; Malliri et al., 2002). Importantly, among RAS effectors we can also find tumour suppressors, namely RIN1 and RASSF. RIN1 blocks Ras signalling by stimulating endocytosis of EGFR (Tall et al., 2001), while RASSF can trigger apoptosis (Khokhlatchev et al., 2002). Both have been found silenced through methylation in cancer cell lines (reviewed in (Milstein et al., 2007; Richter et al., 2009)) and in case of RASSF also in primary tumours (Meng et al., 2012).

Upstream of Ras, GEFs could theoretically be overactivated in cancer. This type of mutations however is found very rarely in malignant tissues for any of the traditional GEFs (excluding PLCε, which functions as both Ras effector and activator) (Swanson et al., 2008). Another possibility leading to Ras activation would be eliminating its GAPs. In case of Neurofibromin 1 (NF1) RasGAP, this event indeed occurs in many glioblastomas. Moreover, patients suffering from neurofibromatosis type 1, an inherited condition in which expression of NF1 is lost, have increased risk of developing tumours (McClatchey, 2007).

IN SEARCH OF A CURE

Studies on *Ras* genes and their effectors encouraged researches to look for inhibitors of these signalling pathways that could be used for treatments. The search started off from GTP antagonists, that were suggested in hope to repeat the success of molecules mimicking ATP used for inhibition of kinases. The idea fell quite quickly upon realisation that GTP has much higher affinity to Ras than ATP to kinases. Attempts to restore GAP activity towards Ras mutants failed as well, leading to diversion of the search towards more indirect ways of inhibition (reviewed in (Baines et al., 2011)).

Given that membrane recruitment is crucial for Ras to function, researches looked for inhibitors of enzymes facilitating its association with the PM. FTase inhibitors, though efficient for H-Ras, did not have an effect on K-Ras, due to differences in processing of these two proteins as well as additional mechanisms within the cells replacing the missing activity. The multitude of other farnesylated proteins that were inhibited together with Ras, including some tumour suppressors, eventually forced scientists to look for a cure elsewhere (reviewed in (Rowinsky, 2006)). Other modifications of Ras proteins leading to their PM localization have been considered; however, no major progress has been reported thus far. Preventing insertion of Ras proteins into cellular membranes may also be achieved through modification of relevant signals within this oncoprotein. Inhibition of prenyl insertion sites using salirasib, proved efficient for dislodging Ras from the PM. The drug is now undergoing clinical trials (reviewed in (Baines et al., 2011)).

Since mutations in RAS effectors are often associated with cancer, various studies considered targeting signalling downstream of RAS for treatment. Two pathways in particular were the main object of interest: Raf-MEK-ERK and PI3K-AKT-mTOR.

Sorafenib was considered a promising candidate against RAF and was indeed approved for treatment of some types of cancers. It appears, however, that the mechanism behind the success of this compound is most likely blocking angiogenesis, as opposed to targeting tumour cells directly, and seems to involve inhibition of other than RAF kinases, including vascular endothelial growth factor receptors (VEGFR) (reviewed in (Baines et al., 2011)). A more successful attempt to inhibit RAF is based on vemurafenib, a selective inhibitor of B-RAF kinase activity. Vemurafenib proved to rapidly reduce melanomas with mutated B-RAF; however, patients developed resistance to the drug relatively quickly (Flaherty et al., 2010). Another potential complication is that the inhibitor can lead to activation of ERK, instead of inhibition, in cancer cell lines with mutated RAS (Heidorn et al., 2010; Rajakulendran et al., 2009). Vemurafenib, together with many other inhibitors against RAF and MEK, is still undergoing clinical trials (details on http://www.clinicaltrials.gov).

From the PI3K-AKT-mTOR pathway, all three types of proteins have been targeted and inhibitors against them are undergoing clinical trials. Most

successful so far are temsirolimus and everolimus, compounds compromising mTOR activity, which have already been approved for treatment of advanced renal cell cancer (reviewed in (Fasolo and Sessa, 2012)).

In view of the recent discovery that Ral GTPases are essential for some RAS-dependent tumours, inhibition of this group of proteins has been investigated as well with some success, leading to current clinical trials (reviewed in (Baines et al., 2011)).

As tumours consist of heterogeneous groups of cells, a reasonable and most effective approach to treatment is using several different methods, so called combination therapy. It can rely on two different inhibitors, but most commonly includes chemotherapy (compounds interfering with DNA replication or cell division, such as doxorubicin or taxol) or radiotherapy combined with inhibitors (reviewed in (Baines et al., 2011)).

1.3 Cell competition in Drosophila

1.3.1 Minute Mutants

The idea of cell competition appeared in cell biology for the first time in 1975, when Genes Morata and Pedro Ripoll published their study on *Minute* mutant fly cells, later identified as carrying a mutation in ribosomal proteins (Kongsuwan et al., 1985). Slower proliferating *Minute* cells were eliminated from imaginal discs of mosaic *Drosophila* embryos comprising of normal and *Minute* heterozygous mutant cells, while embryos consisting of *Minute* mutant cells alone were viable and could develop into healthy flies (Morata and Ripoll, 1975). The new phenomenon was shown to depend on cell growth and proliferation: starved cells did not compete as effectively and competition did not occur after the completion of growth (Simpson, 1979). Since it did not cross developmental boundaries (Simpson and Morata, 1981), cell competition was proposed to be a mechanism that regulates robustness of the organ size control in flies.

1.3.2 dMyc Driven Cell Competition

The next step in understanding cell competition was identifying proto-oncogene dMyc (*Drosophila* Myc) as a super-competitor. Myc is a transcription factor controlling expression of genes which products are involved in proliferation, apoptosis, energy metabolism and protein biosynthesis (reviewed in (Luscher and Vervoorts, 2012)). Cells carrying *diminutive*, a hypomorphic version of *dmyc*, are eliminated from imaginal discs of developing *Drosophila* embryos by their wild-type neighbours through induction of apoptosis dependent on the pro-death factor Hid (de la Cova et al., 2004; Moreno and Basler, 2004). More interestingly, when a mosaic contains cells overexpressing dMyc in addition to normal cells, the roles reverse and former wild-type "winners" become "losers". These studies indicate that the relative levels of dMyc appear to be a source of cell competition in *Drosophila*; for that reason dMyc was labelled a super-competitor (de la Cova et al., 2004; Moreno and Basler, 2004).

More recently, another set of genes involved in cell competition was identified: the tumour suppressor components of the Hippo-Salvador–Warts

(HSW) pathway, which is involved in the regulation of cell proliferation and apoptosis (Tyler et al., 2007). When mutated, HSW genes (*expanded*, *fat*, *salvador*, *hippo*, *warts*) are known to transform fly cells into super-competitors. The same was observed upon overexpression of the downstream effector of the HSW pathway, Yorkie (Yki) (Neto-Silva et al., 2012), (Ziosi et al., 2012). Yki is a transcription co-factor negatively regulated by the HSW pathway. Experiments have revealed that active Yki supports cell growth, most likely by directly promoting *dmyc* expression (Neto-Silva et al., 2012). A definite proof that cell competition driven by HSW pathway occurs via dMyc was demonstration that in the absence of dMyc, cells overexpressing Yki were no longer super-competitors (Neto-Silva et al., 2012). Moreover, *diminutive* heterozygotes overexpressing Yki remained outcompeted when confronted with wild-type cells (Ziosi et al., 2012).

Although ribosomal genes and *dmyc* are involved in cell growth, it was shown that not all growth related genes initiate cell competition. Overexpression of neither phosphatidylinositol 3-kinase (PI3K) nor cyclin D together with cyclin-dependent kinase 4 (Cdk4) resulted in triggering competitive interactions in *Drosophila* (de la Cova et al., 2004). These observations suggest that differences in growth rates between neighbouring cells are not sufficient to drive cell competition.

1.3.3 Wnt pathway-dependent competitive behaviour – away from dMyc

The next breakthrough in the field of cell competition was the demonstration that not all competitive behaviour is related to dMyc. Unexpectedly, help arrived from one of the vital and conserved pathways, the Wnt signalling pathway, a known regulator of cell survival and growth often over activated in tumours. When Wingless (Wg), the ligand of the Wnt pathway, or its receptor Frizzled are mutated in some cells of a developing wing disc, they frequently die. However when the whole compartment is lacking Wnt signalling, cells survive. On the other hand, when Wnt signalling is overactivated due to the mutation of its negative suppressors APC and axin, cells become super-competitiors and induce apoptosis in their neighbours (Vincent et al., 2011). Cell competition triggered by this conserved pathway was shown to be completely independent of dMyc; in fact, high levels of Wnt activation repress *dmyc*

expression in both APC and axin mutants. In the same study another novel concept was introduced to the field of cell competition: Notum, a secreted inhibitor of Wnt signalling, was found to be produced by super-competitors in order to compromise the Wnt response in their neighbours and lead to their apoptotic death (Vincent et al., 2011).

1.3.4 POLARITY PROTEINS IN CELL COMPETITION

Oncogenic alterations in cells do not necessarily provide a competitive advantage. Potentially tumourigenic cells with mutations in their apical-basal polarity genes *discs large* (*dlg*), *scribble* (*scrib*) or *lethal-giant larvae* (*lgl*), which on their own overproliferate and lose their epithelial integrity, are out-competed from mosaic imaginal discs of developing fly embryos (Brumby and Richardson, 2003; Grzeschik et al., 2007). Further studies on *scribble* and *lgl* mutants revealed that normal cells produce and secrete Eiger (a fly TNF), which induces pro-apoptotic JNK activity in the mutant cells (Igaki et al., 2009). Growth of *scribble* mutants is also inhibited upon signalling downstream of Eiger: JNK itself was found to promote HSW activity and consequently inhibit Yki and prevent *dmyc* expression (Chen et al., 2012). In line with these results are previous findings that *lgl* and *scribble* mutant cells can be rescued from elimination in a mosaic wing disc by overexpression of dMyc (Chen et al., 2012; Froldi et al., 2010). It has been suggested that fitness of the cells surrounding these polarity markers mutants determines whether they will be eliminated from the fly imaginal discs or not.

Related to polarity complexes is another protein triggering cell competition in *Drosophila*, an Lgl binding protein Mahjong (Mahj). Flies carrying a homozygous mutation in *mahj* develop more slowly than wild-type animals and die at a late pupal stage. Mutant larvae however are not exhibiting any visible morphological defects. In contrast, when found in a mosaic environment in a *Drosophila* wing disc, m*ahj* mutant cells become apoptotic through activation of the JNK pathway. Moreover, overexpression of Mahj prevents JNK phosphorylation in *lgl* mutants and rescues them from being outcompeted (Tamori et al., 2010). Up to date, the role of Mahj in polarity formation and its relation to Lgl remains unknown.

1.3.5 UNDERSTANDING THE MECHANISM OF CELL COMPETITION

Several mechanisms of cell competition have been proposed. Early studies on *Minute* and *dmyc* mutants pointed towards ribosomal proteins and the efficiency of protein synthesis as an outcome that could be compared between the neighbours and result in competitive behaviour.

Later on, Moreno and colleagues suggested another possible explanation of how ribosomal and *dmyc* mutations could trigger cell competition. They have shown that "loser" cells upregulate repressor Brinker (Brk), what in turn leads to JNK activation and apoptosis. In "winner" cells Brk is downregulated due to high activity of the decapentaplegic (Dpp) pathway. Dpp is a secreted morphogen, a member of the TGFβ family, produced in a part of the fly wing disc and taken up *via* receptor-mediated endocytosis. Moreno and colleagues suggested that cells in *Drosophila* imaginal discs compete for survival factors and that those with a slower endocytic uptake, for example due to impaired ribosomal activity, may not activate Dpp signalling as efficiently as the wild type cells (Moreno et al., 2002). This hypothesis cannot explain all the types of cell competition, however, since some of them have been proven to be independent of Dpp signalling (de la Cova et al., 2004).

The possibility that cell competition is mediated by different from Dpp secreted soluble factors was proposed by de la Cova and colleagues after they noticed that close proximity, but not direct contact was required to induce cell death of normal cells by dMyc super-competitors (de la Cova et al., 2004). This hypothesis was further investigated in an *in vitro* system with *Drosophila* S2 cells overexpressing *dmyc* (Senoo-Matsuda and Johnston, 2007). The authors used a cell culture system in which they co-cultured S2 normal cells with S2 cells overexpressing *dmyc* so that they could not have direct physical contact by separating them with a membrane filter. Although not in contact with each other, cells were still competing, leading to increased death rates of normal cells. Consequently, conditioned media from mixed competing cocultures had the ability to induce cell death in naive normal cells grown alone. It is not known whether soluble factors also play a role *in vivo*, and, if yes, what their nature is or whether they are important for other types of cell competition.

One of the biggest questions in understanding cell competition is how do cells recognise each other and decide which of them will end up as a "loser" and which as a "winner". Gene arrays comparing expression patterns of competing cells revealed that a calcium channel Flower (Fwe) is expressed in three different isoforms, two of which, Fwe^{Lose-A} and Fwe^{Lose-B}, are specific for "loser" cells while the third one, Fwe^{Ubi}, always marks a "winner" (Rhiner et al., 2010). The pattern was confirmed in dMyc super-competitors as well as *Minute* mutants. Importantly, overexpression of one of the "loser" isoforms of Fwe in an otherwise normal wing disc in a mosaic fashion was sufficient to induce their elimination. Even reducing expression levels of Fwe^{Ubi} itself in some of the cells within the fly epithelium led to their apoptosis. Rhiner et al. proposed that Fwe labelling is a downstream event of a mechanism aiming to compare fitness of the cells and marking them for death or survival. What the upstream mechanism is and how exactly cell death is executed remains to be elucidated.

In the same screen in which Fwe was implicated in cell competition, another gene with altered expression was identified: dSparc, a secreted acidic protein rich in cysteine. dSparc is also known as osteonectin and was recently suggested to be a molecular chaperone for collagen IV (Martinek et al., 2007). dSparc was found upregulated and secreted to the basement membrane by "loser" cells in cell competition triggered by altered expression or mutations in ribosomal proteins, dMyc, and the polarity genes *scribble*, *lgl, dlg* (Portela et al., 2010). dSparc is enriched at an early stage of the cell competition and its expression transiently protects "loser" cells from activation of caspases and delays their apoptosis (Portela et al., 2010). Since dSparc is also expressed upon serum depravation in non-competitive conditions (Portela et al., 2010) or in hemocytes invading tissues (Martinek et al., 2002), it has been proposed a part of a general stress response rather than a specific competition marker.

In human cancers SPARC has been studied with conflicting results: in some tumours it was found upregulated, in others downregulated (Lapointe et al., 2004; Mantoni et al., 2008). It is however generally believed to promote metastatic growth and cancer progression (reviewed in (Podhajcer et al., 2008)). Most recently, Moreno and colleagues have found SPARC to be upregulated at the boundaries of several types of tumours and normal tissues consistent with the idea that cell competition may play a role in cancer (Petrova et al., 2011).

1.4 Activation of Ras and Src in Drosophila

Cancer has been extensively studied in *Drosophila* and not only in the context of cell competition. This model organism is very well characterised with multiple tools for genetic manipulation available to researchers. Despite genetic and structural differences between these invertebrates and humans, for example, the lack of blood vessels, many basic processes as well as most of the major signalling pathways involved in mammalian cancerogenesis, can be modelled in flies (reviewed in (Rudrapatna et al., 2012; Stefanatos and Vidal, 2011)).

The most relevant for this thesis studies relate to oncogenic activation of Src and Ras proteins. Direct activation of Src in flies through overexpression of either wild-type or constitutively active forms of this protein leads to increased proliferation as well as apoptosis (Pedraza et al., 2004). In contrast, activation of Src achieved through a knockdown of an inhibitor of Src family kinases, C-terminal Src kinase (dCsk), results in blocking of apoptosis accompanied by decreased adhesion and overproliferation (Vidal et al., 2006). Interestingly, the latter occurs only when the loss of dCsk is widespread. Discrete, local deficits of this regulator have a non-cell-autonomous effect within the fly epithelium and lead to basal exclusion and apoptotic death of cells with overactivated Src. This phenomenon is mediated by dE-cadherin, p120-catenin, Rho1, JNK and MMP2 (Vidal et al., 2006). The mystery of the opposite outcomes of two different ways of activation of Src can be explained by the nature of Src signalling itself. Low levels of Src activity, similar to these achieved through depleting dCsk, trigger antiapoptotic pathways, whereas high levels promote cell death. In tumours, however, higher Src activation is often coupled with mutations in other oncogenes or tumour suppressors abolishing the apoptotic response and ultimately resulting in overgrowth and metastasis of the transformed tissues (Vidal et al., 2007).

Abnormal activation of Ras obtained by overexpressing its constitutively active form $dRas^{V12}$ in *Drosophila* results in overgrowth of the affected tissue and formation of benign 'tumours'. These highly proliferative cellular masses acquire metastatic-like behaviour upon gaining additional oncogenic mutations, for example, as mentioned earlier, loss of the polarity marker Scribble (Brumby and Richardson, 2003; Pagliarini and Xu, 2003). Strikingly, cooperation between the two

mutants was observed even when the mutations occurred in separate neighbouring cells. Studies have shown that downstream of Scribble, active JNK is sufficient to cooperate with Ras, drive extracellular matrix remodelling and enable invasion through MMP1 (Uhlirova and Bohmann, 2006). Further exploration of oncogene cooperation revealed the importance of the tumour microenvironment in invasion of *dRas^{V12}, scrib$^{-/-}$* cells. A cytokine called tumour necrosis factor (TNF), in *Drosophila* known as Eiger, is also required for JNK activation and promotion of invasive growth (Cordero et al., 2010). Remarkably, both JNK and Eiger have been found to play contradictory roles in cancer progression depending on the genetic context. Promotion of cancer progression by these two proteins is evident in double mutants of *Ras* and *scribble*, which invade surrounding tissues in a JNK- and Eiger-dependent fashion. Conversely, in *scrib$^{-/-}$* cells exposed to cell competition within a normal fly epithelium, JNK and Eiger act as tumour suppressors and drive apoptotic cell death of these cells (reviewed in (Rudrapatna et al., 2012; Vidal, 2010)).

Apart from *scrib$^{-/-}$* other mutations were found to cooperate with Ras^{V12} in driving tumour progression. High levels of active Src itself promote malignant growth and metastasis in concert with Ras, which does not come as a surprise, since the JNK pathway contributes to dCsk-mediated phenotypes (Vidal et al., 2007).

From the studies of cancer and competition in *Drosophila,* a picture emerges that depicts a fine balance between elimination of transformed cells from a normal epithelium and their escape followed by hijacking of the whole organism. It appears that one mutation in one cell is often not enough to drive tumourigenesis. With greater numbers or more mutations, transformed cells gain an advantage over the normal cells. The artificial divisions introduced by researchers between cancer and competition studies are bound to be shattered in the future.

1.5 Cell Competition and related phenomena Mammalian Cells

1.5.1 Competition in non-transformed cells

In two recent reports, cell competition was identified in mammalian non-transformed cells (Bondar and Medzhitov, 2010; Marusyk et al., 2010). The authors used lethally irradiated mice to study mechanisms of repopulation of haematopoietic stem cells (HSC). When two non-irradiated populations of HSC are mixed, they reconstitute the haematopoietic lineages according to their starting ratios. However, if one of the groups is treated with a low dose of ionizing irradiation causing mild DNA damage (at the level that still allows them to reconstitute haematopoietic lineage when they are introduced on their own), they become outcompeted by the non-irradiated group. This type of competition was shown to be dependent on p53 levels in the two populations. Low levels of p53 are sufficient for HSC to outcompete cells with higher p53 levels, which normally correlates with DNA damage, even without previous irradiation. In the process, outcompeted cells do not undergo apoptosis, but express growth arrest and senescence-related genes, such as p16 (Bondar and Medzhitov, 2010).

Since downregulation of p53 often occurs in cancer, there is a risk that p53-mutants could overtake the HSC niche. Hence, an additional protective mechanism was assumed, but not characterised so far, helping with elimination of the transformed cells with a competitive advantage (reviewed in (Green, 2010)).

1.5.2 Early studies on cocultures of normal and transformed cells

Interactions between normal and transformed mammalian cells have been studied for over fifty years. In the early reports, fibroblasts transformed with either viruses (Stoker, 1964), carcinogens (Borek and Sachs, 1966) or oncogenes (Alexander et al., 2004) were cocultured with normal fibroblasts. As a result of the mixing, growth of the transformed cells was inhibited. GAP junctions were implicated in (Bignami et al., 1988) and out of (Alexander et al., 2004) the role in transmission of the inhibitory signal from normal to transformed cells. Not clear remains what sort of signals would be transduced. The relevance of these studies

to cancer can also be questioned, since most of cancers originate from epithelial tissues, not fibroblasts.

1.5.3 POLARITY PROTEINS-RELATED CELL COMPETITION

The first tumour suppressor that when depleted has been shown to cause cell competition in mammalian cells was *scribble* (Norman et al., 2012). In a mammalian cell culture system based on Martin-Darby Canine Kidney (MDCK) cells, downregulation of Scribble results in the elimination of these cells from monolayers of normal cells. Similarly to the events in the *Drosophila* imaginal discs, Scribble-knockdown cells (hereafter referred as Scribble cells) undergo apoptosis upon interaction with normal cells. Active Caspase-3, Bak and Bax can be detected in extruded Scribble cells, suggesting that their cell death occurs as a result of mitochondrial apoptosis. It has been shown that apoptotic death of Scribble cells is independent of their extrusion: treatment with myosin II inhibitor blebbistatin inhibits extrusion but does not prevent activation of caspases. While active JNK has been implicated in the competitive elimination of Scribble cells in *Drosophila*, it does not seem to play a role in the mammalian system. Instead activation of p38 mitogen activated protein kinase (p38 MAPK) is required for apoptotic elimination of Scribble cells (Norman et al., 2012).

Another polarity related protein studied in *Drosophila* has also been shown to induce cell competition in mammalian cells. MDCK cells with depleted Mahj, a Lgl binding partner that is conserved among species, are capable of not only forming monolayers but also cysts with well defined lumen and correctly localized polarity markers. In contrast, plating *Mahj*-knockdown cells within a monolayer of normal cells results in their apoptotic death followed by apical extrusion, which, analogically to the *Drosophila* system, occurs *via* activation of the JNK pathway (Tamori et al., 2010).

Although the pathways triggering apoptosis in mammalian cells downregulating Scribble differ from their *Drosophila* counterparts, both described above phenomena can be classified as mammalian cell competition. After all, the ultimate result of the interaction between two otherwise viable populations is elimination of one of them via cell death.

1.5.4 INTERACTIONS OF NORMAL AND RAS^{V12}-TRANSFORMED CELLS

In 2009, the first study on interactions between H-Ras^{V12}-transformed and normal MDCK cells was published (Hogan et al., 2009). The system was created to imitate early stages of cancerogenesis during which a single mutation transforms a single cell within an otherwise normal monolayer. H-Ras^{V12} was expressed in MDCK cells (hereafter referred as Ras^{V12} cells) in an inducible manner under a tetracycline-controlled promoter. Upon mixing of Ras^{V12} cells with normal cells at a ratio 1 to 100 on a collagen gel, two phenomena occurred: apical extrusion of transformed cells from the normal monolayer (the most common event) or formation of basal protrusions by Ras^{V12} cells under their normal neighbours. Apical extrusion was also confirmed in an *in vivo* system based on *Drosophila* imaginal discs in which some of the cells expressed Ras^{V12}. In the tissue culture system, extruded Ras^{V12} cells remained alive and proliferated on top of the normal monolayer. In contrast to the competition known from *Drosophila*, extrusion of transformed cells was independent of apoptosis and, for that reason, it is difficult to classify it as cell competition without knowing the fate of extruded cells in a living organism.

Two aspects of apical extrusion of Ras^{V12} cells have been studied so far: signalling downstream of Ras that leads to the extrusion events and some of the cytoskeletal rearrangements that occur during the process. The MAPK pathway was shown to be required for apical extrusion, while PI3K was not involved (both of these pathways were important for formation of basal protrusions). At the top of the MAPK pathway, Raf (serine/threonine protein kinase, also known as MAP kinase kinase kinase) was required, but not sufficient, in its active form for apical extrusion to take place.

During apical extrusion various cytoskeletal rearrangements occur. Prior to extrusion Ras^{V12} cells increase their height, accumulate Ras^{V12}, actin and E-cadherin at the junctions between each other. These changes happen in a non-cell-autonomous manner. Hogan and colleagues have studied in details the role of myosin and actin in this process. They have shown that inhibition of myosin activity or actin polymerization both supress apical extrusion. Phosphorylated myosin (Thr-18, Ser-19) was upregulated in Ras^{V12} cells surrounded by normal cells

24 hours after induction of Ras^{V12} expression. Upstream of myosin, Rho-associated protein kinase (ROCK) and the Rho GTP-ase cell division control protein 42 (Cdc42), but not the Rho GTP-ase Rac, were shown to take part in extrusion. The dominant negative mutants of both of ROCK and Cdc42 proteins inhibited extrusion. Cdc42 was also shown to be active in Ras^{V12} cells prior to extrusion using recombinant protein for the Cdc42-binding domain (CRIB) of WASP. The molecular mechanism that links Cdc42 signalling to ROCK activation is not known.

Further studies are required to clarify whether what happens in this system is related to cell competition known from the Scribble and Mahjong downregulation systems, if similar pathways are involved, and what the role of this process is in a living organism.

1.5.5 Interface between normal and v-Src-transformed cells

Another oncogene study quickly followed the Ras^{V12} paper and confirmed that extrusion of transformed cells from mammalian epithelia is a phenomenon occurring *in vivo* in vertebrates, in particular in a Zebra fish embryo (Kajita et al., 2010). The object of this analysis was the Rous sarcoma virus *src* gene (*v-src*), the first oncogene ever identified (Hunter, 1980). Src is a non-receptor tyrosine kinase that regulates various cellular process, including remodelling of the actin cytoskeleton, cell adhesion and proliferation (reviewed in (Yeatman, 2004)). In order to study interactions between v-Src-transformed and normal epithelial cells, Kajita and colleagues used a temperature sensitive mutant of v-Src in MDCK cells (hereafter referred as Src cells): Src becomes active after moving the cells from 40.5°C to 35°C. Upon mixing Src cells with normal cells at a ratio 1 to 100 followed by Src activation, transformed cells become extruded from a normal monolayer in the same way as Ras^{V12} cells. However, they were never observed to form basal protrusions. Similarly to Ras^{V12} cells, extrusion of Src-transformed cells was independent of apoptosis and extruded cells remained alive, loosely attached to a normal monolayer.

Since the events in the Src system closely resembled what happened to Ras^{V12} cells, Kajita and colleagues decided to investigate whether there were any common pathways activated upon interactions with normal cells. Firstly, they noticed that before extrusion Src cells undergo shape changes similar to Ras^{V12}

cells. They became taller than their normal neighbours or Src cells grown on their own; their shape also changed into more rounded. Myosin II was shown to be involved in extrusion: blebbistatin along with the inhibitors of myosin light chain kinase (MLCK) and ROCK prevented the process. What differed from the Ras^{V12} extrusion was the site of accumulation of phosphorylated myosin, as increased phospho-myosin staining was found at the plasma membrane.

Secondly, the authors discovered that Ras itself played a role in the extrusion of Src cells by using a dominant negative form of this protein. Downstream of Ras, the MAPK pathway, but not PI3K, was required for extrusion of Src cells. In contrast to Ras^{V12} cells, however, Src cells when surrounded by their normal neighbours accumulated active MAPK along the cell cortex.

Downsteam of Src, active focal adhesion kinase (phospho-FAK) was shown to be necessary for extrusion to occur and, strikingly, also accumulated along the membranes. Further experiments revealed that although FAK and myosin II were activated independently of each other, they both contributed to MAPK activation. Interestingly, E-cadherin and β-catenin were mislocalized in Src cells prior to extrusion from the apical to the basal part of cell-cell adhesions, a change that was not reported in the Ras^{V12} system.

Taking into consideration the early reports about communication between normal and transformed cells through the GAP junctions, the authors examined and subsequently excluded their involvement in the phenomenon.

Although a lot of similarities were reported between Ras^{V12}- and v-Src-driven extrusion of transformed cells from the normal monolayers, there is also evidence that different pathways are regulated upon interactions with normal neighbours in each of the cell types. It is possible that the recognition and signalling from normal cells might be common and conserved in mammalian cells. We can speculate that in a living organism after extrusion transformed cells are exposed to harsh conditions (as flow of urine or stool) and removed from the organism. When the transformation happens in other niches (for example, breast epithelium), extruded cells could become a target for the immunological clearance mechanisms.

1.5.6 INTERACTIONS OF NORMAL AND ONCOGENE-TRANSFORMED CELLS IN ORGANOTYPIC CULTURES

An alternative possibility to cell removal *via* extrusion was suggested in a recent study on interactions between normal and transformed cells in three-dimensional (3D) organotypic cultures of MCF10A, a non-transformed human mammary epithelial cell line (Leung and Brugge, 2012). The authors propose that the clonal outgrowth of oncogene-transformed single cells from the growth-arrested acinar structures, that they observe, might be an early step in tumour progression.

In this study, oncogenes were classified into two groups: those that when activated were sufficient to drive clonal expansion of the transformed cells on their own, as erythroblastic leukemia viral oncogene homolog 2 (ERBB2), and those that upon activation were not capable of releasing the cells from the growth inhibition within the acni, as c-MYC or AKT (also known as protein kinase b). The latter group could be divided further if the attachment of the transformed cells was modified, e.g., by overexpressing matrix metalloproteinases (MMP). In this situation, cells with active AKT that had translocated to the lumen could proliferate, whereas cells overexpressing c-MYC could not.

Interestingly, clonal outgrowth of ERBB2 overexpressing cells was dependent on the same pathways as extrusion of Ras^{V12} and Src cells from normal epithelial monolayers of MDCK cells. Activation of the MAPK kinase pathway was required for this phenomenon to occur, while PI3K inhibition did not affect the process.

In this study, the authors separate extrusion from subsequent proliferation or apoptosis. It is a notable distinction which may tell us about the fate and ultimately the role of this process in mammals. In the future, research looking at extrusion in living adult organisms with developed immune systems will clarify the fate of extruded cells, whether the outcome of extrusion depends on the environment and if some primary tumours are already metastatic.

1.6 THE AIM OF THIS THESIS

The general goal of my thesis is gaining a better understanding of the process of extrusion of transformed cells from a normal epithelial monolayer. In particular, in this project I aimed to identify and clarify the role of novel proteins important for interactions between normal and Ras^{V12}-transformed cells at an early stage of extrusion using an unbiased approach of biochemical screening. In the first result chapter, I present validation of a 2D gel screen performed previously, in which Hsp90β was identified as a molecule altered in cocultures of normal and transformed cells. In the following chapters, I describe two other biochemical screens I performed in the course of my studies. The aim of both of these screens was to pinpoint novel signalling pathways regulated by phosphorylation in cocultures of normal and transformed cells. Firstly, a traditional approach of immunoprecipitation of tyrosine-phosphorylated proteins from cocultures of normal and transformed cells was used. This method was then perfected in the last screen, through utilisation of a SILAC labelling technique, which allowed for quantitative analysis of changes in phosphorylation levels of proteins in just one of the cell types from cocultures (here, in transformed cells). In this thesis, I present results of both screens as well as preliminary validation data supporting the involvement of two identified molecules in the process of extrusion.

CHAPTER 2:

MATERIALS AND METHODS

CHAPTER 2: MATERIALS AND METHODS

2.1 MOLECULAR BIOLOGY AND BIOCHEMISTRY

2.1.1 TRANSFORMATION OF COMPETENT CELLS

Escherichia coli DH5α chemically competent cells (Invitrogen) were thawed on ice. To 50 µl of the cell suspension ± 1 µg of plasmid DNA was added for a further 30-minute-incubation on ice. Cells were then heat-shocked at 42°C for 45 seconds and returned to ice for 3 minutes. 1 ml of fresh LB medium was added to the cells followed by a 1 hour incubation at 37°C. 100 µl of the cell suspension were then plated on LB agarose plates supplemented with 100 µg/ml ampicillin and incubated overnight at 37°C.

2.1.2 PREPARATION OF PLASMID DNA

Colonies obtained after plating transfected bacteria were picked, inoculated into 200 ml LB media supplemented with 100 µg/ml ampicillin and incubated overnight at 37°C. Plasmid DNA for transfection was isolated from bacterial cells using Plasmid Maxi Kit (Qiagen) using the manufacturer's instructions.

2.1.3 SDS SAMPLE PREPARATION

Confluent cells were washed with ice-cold PBS and lysed in the well with an appropriate amount of lysis buffer (20 mM Tris-HCl [pH 7.5], 150 mM NaCl, and 1% Triton X-100) supplemented with protease inhibitors (details in chapter 2.1.8), e.g. 300 µl or 80 µl of the lysis buffer per well in a 6-well or 48-well culture dish, respectively. Lysates were collected in 1.5 ml tubes and SDS buffer was added (one third of final volume). Samples were boiled at 99°C for 10 minutes.

2.1.4 SDS POLYACRYLAMIDE GEL ELECTROPHORESIS (SDS-PAGE)

SDS polyacrylamide gels were prepared using the ingredients listed in table 2 (proportions for a most commonly used 10% gel are shown).

Table 2. Composition of SDS-PAGE gels used throughout the thesis.

	Resolving gel 10%		Stacking gel	
	Mini	**Maxi**	**Mini**	**Maxi**
Water	3 ml	12 ml	3.2 ml	9.5 ml
1.5 M Tris/Cl (pH 8.8)	2.5 ml	10 ml	x	x
0.5 M Tris/Cl (pH 6.8)	x	x	1.25 ml	3.75 ml
50% glycerol	2 ml	8 ml	x	x
40% acrylamide /bisarylamide solution	2.5 ml	10 ml	500 µl	1.5 ml
10% SDS	100 µl	400 µl	50 µl	150 µl
TEMED	15 µl	50 µl	5 µl	15 µl
10% APS	30 µl	120 µl	50 µl	150 µl
Total Volume	**10 ml**	**40 ml**	**5 ml**	**15 ml**

Large gels were run overnight at 18 mA (per two gels) in a PROTEAN II xi gel electrophoresis tank (Bio-Rad). Small gels were run for 1-2 hours at 40 mA (per two gels) in a Mini-PROTEAN II gel electrophoresis tank (Bio-Rad). Protein size was assessed by comparison with PageRuler™ Prestained Protein Ladder (Fermentas).

2.1.5 IMMUNOBLOTTING

Proteins resolved in SDS-PAGE were subsequently transferred onto polyvinylidene fluoride membrane (PVDF, Millipore) in Bio-Rad Trans-Blot cells at 70 V for 2 hours or at 220 mA overnight at 4°C. Before transfer, membranes were soaked for at least 5 minutes in methanol and briefly washed in transfer buffer (100 mM glycine, 10 mM Trizma base, 10% methanol). A transfer sandwich was prepared as follows: the PVDF membrane and the polyacrylamide gel, which had been washed in transfer buffer, were placed in between four sheets of soaked in transfer buffer Whattman blotting paper and two sponges. After removing air bubbles, the whole cassette was placed in a tank filled with transfer buffer.

Membranes were then stained with 0.1% amido black (MERCK Millipore) for 30 seconds, briefly washed with ultrapure water and agitated with a destaining buffer (20% methanol, 7.5% acetic acid) for 30 minutes at room temperature.

Membranes were blocked with 3% skimmed milk (Marvel) in PBST (0.05% Tween20 in PBS from Fisher Bioreagents) for 2 – 3 hours. Primary antibodies were diluted in 3% milk/PBST and incubated with membranes overnight at 4°C or for at least 3 hours at room temperature. Next, membranes were washed three times for 10 minutes in PBST and incubated with secondary antibodies for a further 1 to 4

hours. Horseradish peroxidase-conjugated (HRP) secondary antibodies were also diluted in 3% milk/PBST. Goat anti-mouse and goat anti-rat antibodies (Jackson Immunoresearch) were used at a dilution 1:2000, goat anti-rabbit (Jackson Immunoresearch) was used at 1:5000 and mouse anti-goat (Sigma) was used at 1:1000. Membranes were washed three time with PBST and bands were visualised using ECL detection reagents (solution I: 2.5 mM luminol, 0.45 mM p-coumaric acid, 0.1 M Tris/Cl pH 8.5; solution II: 0.02% hydrogen peroxide, 0.1 M Tris/Cl pH 8.5) combined in a 1 to 1 ratio applied onto membranes. High performance chemiluminescence film (Hyperfilm, Kodak) was used to capture the images.

2.1.6 ANTIBODIES

Table 3. List of primary antibodies used throughout the thesis for immunofluorescence, immunoblotting and immunoprecipitation.

Antigen	Catalog number	Company	Species	Concentration used
Hsp90α	SPA-840	Stressgen	Rat	IF – 1:100
Hsp90β	ab2927	Abcam	Rabbit	IF – 1:50 WB – 1:1000
Raf-1	ab32025	Abcam	Rabbit	WB – 1:1000
Erbb2	610161	BD Biosciences	Mouse	WB – 1:500
GAPDH	MAB374	Millipore	Mouse	WB – 1:5000
pERK	M9692	Sigma-Aldrich	Mouse	WB – 1:1000
ERK2	34680	Qiagen	Mouse	WB – 1:1000
Plectin	sc-33649	Santa Cruz Biotechnology	Mouse	IF – 1:100
VASP	3132	Cell Signaling	Rabbit	IF – 1:200
pVASP Ser239	3114	Cell Signaling	Rabbit	IF – 1:100
pVASP Ser239	sc-101439	Santa Cruz Biotechnology	Mouse	IF – 1:100
Vinculin	V9131	Santa Cruz Biotechnology	Mouse	IF – 1:200
MRCKβ	sc48834	Santa Cruz Biotechnology	Rabbit	IB – 1:1000
Myosin IIA	M8064	SIGMA	Rabbit	IF – 1:200

pMLC	3675	Cell Signaling	Mouse	IF – 1:100
ppMLC	3674	Cell Signaling	Rabbit	IF – 1:50
p-Tyrosine 4G10	16-638	Millipore	Mouse	IP – Agarose-conjugated beads
p-Tyrosine	9419	Cell Signaling	Mouse	IP – Sepharose Bead Conjugate

2.1.7 GEL STAINING WITH SYPRO® RUBY

After SDS-PAGE large gels were transferred into a clean box, washed briefly with ultrapure water and fixed in 200 ml of fixing solution (50% methanol, 7% acetic acid) twice for 1 hour at room temperature. The gels were then stained in SYPRO® Ruby dye (Invitrogen) overnight at 4°C. The following day, the gels were distained with 200 ml of wash solution (10% methanol and 7% acetic acid) for 1 hour and stored in ultrapure water. Images were taken using default settings for SYPRO® Ruby stained gels on a Molecular Imager FX (BioRad).

2.1.8 IMMUNOPRECIPITATION

Cells were plated under three conditions: normal MDCK cells alone, Ras^{V12} cells alone and a 1 to 1 mixed population. 1.2 x 10^7 cells were plated in a 15-cm plate and two plates were used for analysis for each condition. After 6-8 hours of plating, tetracycline (2 μg ml^{-1}) was added to induce GFP-Ras^{V12} expression. After 14 hours, the cells were washed with ice-cold PBS, scraped and lysed in 1 ml Triton X-100 lysis buffer (20 mM Tris-HCl [pH 7.5], 150 mM NaCl, and 1% Triton X-100) containing leupeptin (5 μg ml^{-1}), phenylmethylsulfonylfluoride (50 mM), aprotinin (7.2 trypsin inhibitor units), as well as phosphatases inhibitors: sodium orthovanadate (1 mM), ammonium molybdate (0.1 mM) and sodium fluoride (10 mM) (all inhibitors were from Sigma). The cells were then lysed for 20 minutes at 4°C. After centrifugation at 14,000 x g for 10 minutes at 4°C, the supernatants were incubated with prewashed sepharose beads for 30 minutes at 4°C for preclearing. This step was repeated 3 times. 50 μl of the precleared supernatants were taken as 'total cell lysate' fraction. The rest of the supernatants was subjected to immunoprecipitation for 4 hours with 50 μl of prewashed beads with conjugated anti-phospho-tyrosine antibodies (Millipore and Cell Signalling, mixed in a ratio 1:1).

The beads were subsequently washed twice with the lysis buffer, and bound proteins were eluted with 200 µl of SDS sample buffer for 10 minutes at 95°C. Eluted fractions were analysed by perfoming sodium dodecyl sulfate-polyacrylamide gel electrophoresis (SDS-PAGE), followed by SYPRO® Ruby protein gel staining (Invitrogen) or Western blotting with anti-phospho-tyrosine-antibody.

2.2 CELL BIOLOGY

2.2.1 CELL CULTURE

MDCK cells were cultured in Dulbecco's modified Eagle's medium (DMEM, Gibco) supplemented with 10% fetal calf serum (FCS; Sigma), 1% Glutamax™ (Gibco) and penicillin/streptomycin (PAA Laboratories) at 37°C and ambient air supplemented with 5% CO_2. MDCK cells stably expressing GFP-Ras^{V12} in a tetracycline inducible manner were made by Catherine Hogan (Hogan et al., 2009). These cells were maintained in selective medium containing 10% FCS (tetracycline-free; PAA Laboratories, Pasching, Austria), 5 µg ml^{-1} of blasticidin (PAA Laboratories) and 400 µg ml^{-1} of zeocin (Invitrogen). To induce GFP-Ras^{V12} expression, 2 µg ml^{-1} tetracycline was added to the culture medium.

2.2.2 CELL STORAGE

For storage, cells (in their second generation since thawing) were trypsinised, spun down at 1000 rpm for 5 minutes, resuspended in fresh medium supplemented with 10% DMSO to a concentration (1-2) x 10^6 cells/ml and transferred to cryovials. Initial freezing took place in a isopropanol bath at -80°C overnight. Cells were subsequently transferred to liquid nitrogen for long term storage (-150°C).

2.2.3 PREPARATION OF COLLAGEN COATED PLATES AND COVERSLIPS

Type–I collagen solution was obtained from Nitta Gelatin (Nitta Cellmatrix type 1–A), and was neutralized on ice to a final concentration of 2 mg ml^{-1} according to the manufacturer's instructions. Glass coverslips in 6–well culture dishes were coated with 1 ml of neutralized collagen and allowed to solidify for 30 minutes at 37°C. Alternatively, for time-lapse experiments 6-well glass-bottom dishes were

coated with 400 µl of neutralized collagen. For each assay, between 0.8 x 10^6 and 2 x 10^6 cells were plated per well onto the collagen gel. Ras^{V12} cells were combined with MDCK cells at a ratio of 1:100 or 1:50. After incubation for 6–16 hours at 37°C, tetracycline was added to induce Ras^{V12} expression. Cells were incubated for the indicated times.

2.2.4 TRANSFECTION METHODS

LIPOFECTAMINE 2000

Lipofectamine 2000 (Invitrogen) was used for creating stable cell lines (described below) as well as extrusion studies with the following constructs: pcDNA3-HA-Hsp90β, pcDNA3-HA-DNHsp90β (both purchased from Addgene), pcDNA/T0/GFP (Dupre-Crochet et al., 2007), pcDNA/T0/GFP-Ras^{V12} (Hogan et al., 2009). MDCK cells were split into collagen coated 6-well plates at 0.5 x 10^6 per well and allowed to recover overnight. The following day, the medium was replaced with fresh DMEM without antibiotics. Transfection mixtures were prepared as follows: 2 µg of DNA were resuspended in 250 µl of Opti-MEM (Invitrogen), while 5 µl of Lipofectamine 2000 was added to another 250 µl of Opti-MEM. After 5 minutes both mixtures were combined and allowed to form transfection complexes for 20 minutes at room temperature. The mixture was then added to the cells. After 4-6 hours, the medium was replaced with fresh DMEM, and the cells were fixed with 4% PFA after a further 18-20 hours.

CALCIUM PHOSPHATE

HEK293 cells were used for confirming expression of Hsp90β and DNHsp90 from purchased constructs. Cells were split into 10-cm culture dishes at 2.0 x 10^6 cells per plate. The following day a transfection mixture was prepared as follows: to 450 µl sterile water 50 µl of 2.5 M $CaCl_2$ solution was added together with 5 µg of plasmid DNA. DNA was then precipitated by adding dropwise 500 µl 2x HEPES buffer (280 mM NaCl, 10 mM KCl, 1.5 mM Na_2HPO_4, pH 7.05) while vortexing. After 5 minutes, the mixture was applied onto the cells. After 4-6 hours, the medium was replaced with fresh DMEM, and the cells were lysed and used for Western blot analysis after 18-20 hours.

INTERFERIN

Interferin (Polyplus-transfection) was used for transfection of siRNAs into MDCK, Ras^{V12} or GFP cells. Cells were plated in 48-well plates at 0.5-1 x 10^4 cells per well. After 16-18 hours (for next-day-transfections) or immediately afterwards (for trypsin-transfection), the transfection procedure was carried out. 0.5 µl of 20 µM siRNA (Table 4) was added to 50 µl of Opti-MEM. Next, 1 µl of Interferin was added to the mixture, which was then incubated at room temperature for 25 minutes. Complete medium was added to the transfection mixture, which was afterwards applied onto the cells up to the final transfection volume of 250 µl. After 2 days, cells were split and combined with normal cells in 6-well plates (one knockdown well with 1 x 10^6 MDCK cells) on collagen coated coverslips or collagen coated time-lapse dishes. After overnight incubation, tetracycline (2 µg ml^{-1}) was added to induce GFP-Ras^{V12} expression and cells were either fixed at 8 hours or 24 hours from *GFP-Ras^{V12}* induction or followed using time-lapse microscopy.

Table 4. Sequences of siRNA molecules used in this thesis. All siRNA reagents were ordered from Thermo Scientific, resuspended to a final concentration of 20 µM in 1X siRNA buffer (20 mM KCl, 0.2 mM $MgCl_2$, 6 mM HEPES, pH 7.5) and stored at -80°C.

siRNA name	siRNA sequence
Control_si_RNA	MISSION siRNA Universal Negative Control 1 and 2 mixed in a 1 to 1 ratio (Sigma)
VASP_dog_oligo_1	GGAAATAAGATGAGGGAGA
VASP_dog_oligo_2	CCACAGGGCTCCAGAAGAT
VASP_dog_oligo_3	CCAGAATGGTCCCGCCTCA
MRCK_pan _dog_oligo_1	AGAGAAGACTTTGAGATAT
MRCK_alpha _dog_oligo_2	AAGATATGGCTCGATTTTA
MRCK_beta _dog_oligo_3	AAAGAATTCTGAAACGATG

2.2.5 GENERATION OF STABLE CELLS LINES

MDCK-GFP-Ras^{V12} cells stably expressing HA-Hsp90β were produced as follows. MDCK-GFP-Ras^{V12} cells were transfected with pcDNA3-HA-Hsp90β (Addgene) using Lipofectamine 2000 (Invitrogen) according to the manufacturer's instructions,

followed by selection in medium containing 800 µg ml^{-1} of G418 (Calbiochem), 5 µg ml^{-1} of blasticidin and 400 µg ml^{-1} of zeocin. Overexpression of Hsp90β-HA was analysed by immunofluorescence and immunoblotting.

2.2.6 Fluorescent labelling of cells

For some experiments cells were labelled with CellTracker Red CMTPX dye (Molecular Probes). Supplied powder was reconstituted in DMSO up to 0.67 mg/ml. 25 µl of the dye was then added to a 80% confluent 6 cm dish of MDCK cells in FCS free medium. After 25-30 minutes cells were washed with PBS and recovered in normal medium for a further 30 minutes before being trypsinised and used for experiments.

2.2.7 Inhibitors

All the inhibitors were added to mixed cultures or Ras^{V12} cells alone together with tetracycline, which due to the 2 hour incubation time for GFP-Ras^{V12} expression accounted for pre-incubation. Two Hsp90 inhibitors (both from Sigma-Aldrich) were used in this thesis: 17-Allylamino-17-demethoxygeldanamycin (17-AAG) used for most experiments at 100 nM and celastrol used for most experiments at 1 µM (unless indicated otherwise). Myosin II inhibitor, blebbistatin, was used at 60 µM (Toronto Research Chemicals).

2.2.8 HGF assay

In the HGF assay, 1 $x10^5$ MDCK cells were plated and in 35 mm wells and cultured for 24 hours in the presence of 100 nM HGF (Chmicon) and with Hsp90 inhibitor 17-AAG (50, 75, 100 nM).

2.2.9 Time-lapse microscopy

MDCK cells stably expressing GFP–Ras^{V12} with or without indicated siRNA knockdown were trypsinized and combined with wild type MDCK cells at a ratio of 1 : 50. Cells were plated at a density of 1 x 10^6 cells per well or 2 x 10^6 cells per well in 35 mm glass-bottom culture dishes (MatTek Corporation) for all experiments. Mixed cells were incubated for 16 hours or 4 hours, respectively, at 37°C before being transferred to a tetracycline-containing medium. 4 hours after tetracycline addition, the cells were filmed for up to 48 hours with pictures taken every 10 minutes. Only groups smaller than four cells at the beginning of the

movie were chosen. To assess cell viability ethdium homodimer-1 (EthD-1, Molecular Probes) was added to the medium while imaging at 400 nM.

To obtain time-lapse images, a Zeiss Axiovert 200 M microscope was used with a Ludl Electronic Products Biopoint Controller and a Hamamatsu C4742−95 Orca camera (Hamamatsu). Images were captured and analysed using Volocity software (Improvision).

2.2.10 FIXATION METHODS

PFA

PFA fixation was performed after 8, 18 and 24 hours from tetracycline addition. Confluent monolayers were washed with PBS before 4% PFA in PBS was applied for 5 to 15 minutes at room temperature (depending on cell density, matrix and primary antibody used afterwards). Cells were then washed 3 times with PBS and either permeabilised straight away or left at 4°C for no longer than for 3 days until staining.

METHANOL

Cells plated on glass were in some cases fixed with methanol (for certain antibodies). Fixation was performed after 8, 18 and 24 hours from tetracycline addition. Confluent monolayers were washed with PBS before pure methanol (-20°C) was applied for 5 to 8 minutes at -20°C. Cells were then rehydrated for 10 minutes with PBS, and either permeabilised immediately afterwards or left at 4°C for no longer than for 3 days until staining.

COMBINED PFA AND METHANOL METHOD

Cells plated on collagen used for stainings with antibodies typically working only in methanol fixed cells were first washed with PBS, then treated for 5 to 10 minutes with 4% PFA/PBS at room temperature, washed 3 times with PBS, and finally fixed for further 3 to 5 minutes in pure methanol (-20°C) for 3 to 5 minutes. Rehydration and further immunostaining steps followed.

2.2.11 IMMUNOFLUORESCENCE

Primary antibodies used for stainings are listed in table 3.

ON GLASS

After fixation, cells on glass were permeabilized in 0.5% Triton X-100/0.3% BSA/PBS for 10 minutes. If fixed with PFA, the cells were then washed once in quenching solution (20 mM glycine, 0.5% BSA in PBS) and left in the same solution for 30 minutes. Next, the cells were incubated with blocking buffer (0.5% BSA, 0.2% Triton X-100 in PBS) for over 3 hours. Primary antibodies diluted in blocking buffer were applied overnight. The following day, coverslips were washed three times for 10 minutes each with blocking buffer, and incubated with secondary antibodies Alexa-568-, Alexa-555- and Alexa-647-conjugated secondary antibodies (1 : 600, Molecular Probes) and/or phalloidin-647 (1 : 200 - Molecular Probes, 1 : 2000 Sigma) for 2–4 hours at room temperature. The cells were then washed three times for 10 minutes in blocking buffer and were incubated with Hoechst in PBS for 3 minutes, followed by washing in PBS and mounting onto mowiol on a glass slide.

ON COLLAGEN

After fixation, cells on collagen were permeabilized in 0.5% Triton X-100/PBS for 10 minutes. The cells were then washed once in PBS followed by three 10-minute washes in glycine wash buffer (7 mM Na_2HPO_4, 3.5 mM NaH_2PO_4, 130 mM NaCl and 100 mM glycine). The cells were blocked for more than 2 hours in blocking buffer (7 mM Na_2HPO_4, 3.5 mM NaH_2PO_4, 130 mM NaCl, 0.2% Triton X-100, 0.05% Tween-20, 10% FCS, 0.02% BSA and 7.7 mM NaN_3), and incubated with primary antibodies for 16 hours at 4°C. This was followed by three 10-minute washes with gentle agitation in blocking buffer before incubation with Alexa-568-, Alexa-555- and Alexa-647-conjugated secondary antibodies (1:200, Molecular Probes) and/or phalloidin-647 (1:200 - Molecular Probes, 1:2000 - Sigma) for 2–4 hours at room temperature. Cells were then washed three times for 10 minutes in blocking buffer and were incubated with Hoechst/PBS for 3 minutes, followed by washing in PBS and mounting onto a glass slide with mowiol and an additional cover glass on top.

2.2.12 PHASE CONTRAST MICROSCOPY

Cells for the HGF assay were examined using a Bio-Rad Radiance 2100 MP system mounted on a Nikon 800 microscope using Lasersharp software (Biorad).

2.2.13 CONFOCAL MICROSCOPY

Cells cultured on collagen gels were examined using a Leica TCS SPE, SPE2 or SPE3 confocal microscope and Leica Application Suite (LAS) software.

2.3 DATA ANALYSIS

2.3.1 QUANTIFICATION OF IMMUNOFLUORESCENT IMAGES

Images were analysed using Leica Application Suite (LAS) software while pixel intensity was quantified using Metamorph 6.0 digital analysis software (Universal Imaging).

FLUORESCENCE INTENSITY

A defined circular region was created in the cytoplasm of the indicated cells in xz confocal sections. For each cell, 10 regions were created. The total pixel intensity within each region was determined and the mean pixel intensity was calculated for each cell.

ACTIN ACCUMULATION AT JUNCTIONS

A defined circular region was created on along the phalloidin stained junction of the indicated cells in xz confocal sections. For each junction, 2-3 regions were created. The total pixel intensity within each region was determined and the mean pixel intensity was calculated for each type of junction. The value was then multiplied by the average length of particular types of junctions determined for the same cells with the LAS software.

NUCLEAR LIFT

Position of each nucleus in Ras^{V12} cells was assessed in xz confocal sections through the middle of the cells. Depending on their proximity to the apical and basal membrane were classified into three groups:

1) lifted – the upper edge of the nuclear envelope very close to the apical membrane, visible difference between position of the nucleus in Ras^{V12} cells comparing to the position of nuclei in surrounding normal MDCK cells,

2) moving – elongated shape, generally closer to apical membrane, visible difference between position of the nucleus in Ras^{V12} cells comparing to the position of nuclei in surrounding normal MDCK cells,

3) at the same level as in normal cells – the lower edge of the nuclear envelope very close to the basal membrane, no visible difference between position of the nucleus in Ras^{V12} cells comparing to the position of nuclei in surrounding normal MDCK cells.

2.3.2 QUANTIFICATION OF IMMUNOBLOTS

Immunoblots were quantified using ImageJ software.

2.3.3 QUATIFICATION OF EXTRUSION RATES

GFP-Ras^{V12} cells that were apically extruded or formed basal protrusions were counted and expressed as a ratio relative to total cells. Cells were counted following 24 hours of tetracycline and inhibitor addition.

2.3.4 QUANTIFICATION OF TIME-LAPSE MOVIES

Ras^{V12} cells visible throughout the movie were taken into consideration while quantifying time lapse images. Each Ras^{V12} cell was followed for the duration of the movie and the time of its extrusion was recorded. Extrusion rates were quantified by dividing total number of cells at the end by total number of extruded cells. Proliferation rates were quantified by dividing total number of cells at the end by total number of cells at the beginning. Average group size at the end of the movie was also registered.

2.3.5 STATISTICAL METHODS

Two-tailed Student's *t* tests were used to determine P values. All data were analysed in Microsoft Excel.

2.4 SILAC SCREEN METHODS

2.4.1 SILAC LABELLING

MEDIUM PREPARATION

Medium for SILAC labelling was prepared as follows: 13.26 g of arginine- and lysine-deficient DMEM powder (Caissons Lab) was mixed with 3.7 g of sodium bicarbonate and dissolved in 1 L ultrapure autoclaved water. pH was adjusted to 7.1 and the medium was filtered. Before culturing MDCK cells the medium was

supplemented with dialysed FBS (30 MWCO) (Invitrogen), as well as penicillin/streptomycin and GlutaMax, as before. Labelled amino acids (Sigma Isotopes) were added at a final concentration of 50 µg/L: for a 'light' label lysine-0 (unlabelled) and arginine-0 (unlabelled), for a 'medium' label lysine-4 ($^{2}H_4$-labelled) and arginine-6 ($^{13}C_6$-labelled), for a 'heavy' label lysine-8 ($^{13}C_6$, $^{15}N_4$-labelled) and arginine-10 ($^{13}C_6$, $^{15}N_4$-labelled).

LABELLING OF RAS^{V12} AND MDCK CELLS

MDCK and two sets of Ras^{V12} cells were labelled for five generations in SILAC medium with 'light', 'heavy' and 'medium' amino acids, respectively. Cells were plated in 15 cm culture dishes and split accordingly: first split 1 to 5, second – 1 to 4, third – 1 to 3, fourth – 1 to 2 (cells grew slower in medium with dialysed FBS).

Labelling efficiency was calculated from MS analysis of labelled lysates. In short, cell lysates were mixed ('heavy' to 'light' in a 1 to 1 ratio or 'medium' to 'light' in a 1 to 1 ratio), separated by SDS-PAGE, and two gel bands of high and low molecular weight were excised, digested and analysed by LC-MS. Relative quantification of 'heavy' to 'light' ratio and 'medium' to 'light' ratio in these proteins, revealed a labelling efficiency of 98% for both arginine and lysine within the proteins contained the isotopic labels.

2.4.2 CELL CULTURE

For an experiment, cells were trypsinised, counted and plated at 4 x 10^7 cells per a 15 cm plate. In these confluent conditions, they formed a monolayer very quickly. Cells were grown in two conditions: 'medium' Ras^{V12} cells were plated alone in two plates, while 'heavy' Ras^{V12} cells were mixed in a 1 to 1 ratio with 'light' MDCK cells in four plates. All the cells were kept in 'light' medium, to minimise negative effects of label exchange during the experiment. After 2 hours, tetracycline was added (2 µg ml^{-1}) to the medium. After 6 hours, cells were harvested. We confirmed that during an 8 hour incubation in 'light' medium, label exchange was not higher than 10-20%.

2.4.3 CELL LYSIS

After 6 hours from adding tetracycline, cells were washed with TBS and lysed in a total amount of 10 ml of 9 M Urea / 100 mM Tris/Cl pH 8 supplemented with 0.2 mM sodium vanadate. Lysates were scraped, combined in a tube and sonicated

(three times for 15 seconds each until the lysate was clear). After spinning down for 10 minutes at 20,000 rcf, the supernatant was moved to a fresh tube. To reduce disulfide bonds DTT was added to the lysates at 5 mM final concentration and the tube was incubated in a water bath at 55°C for 15 minutes. After cooling down, alkylating agent iodoacetimide was added up to a final concentration of 10 mM, and the tube was incubated for a further 15 minutes in the dark. Finally, the lystates were topped up to 45 ml volume with 100 mM Tric/Cl pH 8.0 and 20 µg trypsin was added to digest isolated proteins into peptides. Digestion lasted 48 hours, after which peptides were kept at 4°C until isolation (no longer than for 3 days).

2.4.4 PURIFICATION OF PEPTIDES

Sep-Pak C18 Plus Short Cartridges (Waters) were used to purify peptides. Each column was firstly activated by application of 5 ml acetonitrile (MeCN), then washed twice with 7 ml 0.1% trifluoroacetic acid (TFA). TFA was added to the peptide solution at a final concentration of 1%. The lysate was then spun down for 5 minutes at 2000 rpm, room temperature, the supernatant was moved to a fresh tube and loaded onto the column. Pressure was applied and air bubbles were removed during extraction. The column with bound peptides was subsequently washed twice with 0.1% TFA 10ml. Peptides were eluted with 8 ml 50% MeCN / 0.1% TFA. Eluates were aliquated into screw cap microcentrifuge tubes, frozen for at least 30 minutes on dry ice and finally dried in a Savant SC250EXP SpeedVac concentrator (Thermo Scienctific). Dried peptide pellets were store at -20°C.

2.4.5 ISOLATION OF PHOSPHO-PEPTIDES

For isolation of phosphopeptides, dried peptide pellets were resuspended in 25%MeCN / 0.1% TFA to a concentration of 20 mg/ml. Phos-Select Iron Affinity gel (Sigma) was used for selective purification of phosphorylated peptides. 300 µl of the beads, were washed with 0.1% TFA, followed by two washes with 25% MeCN / 0.1% TFA. 100 µl of the peptide solution (2 mg of peptides) was diluted to a concentration of 5 mg/ml in 150 µl 25% MeCN / 0.1% TFA and applied onto the gel for 2-hour long rotation at room temperature. The gel with bound phosphorylated peptides was then spun down for 30 seconds at 800 rcf and washed with following buffers: twice with 0.1% TFA, once with 0.1% TFA/ 50%

MeCN, twice with 1% TFA / 50% MeCN and finally once with ultrapure water. The elution was performed twice with 250 µl of 100 mM ammonium bicarbonate (ABC) pH 9.5 for 10 minutes at room temperature. Eluted fractions were combined, phosphorylated peptides were stabilised with 20 µl 20% TFA, frozen on dry ice for 30 minutes and dried in a vacuum centrifuge.

2.4.6 HYDROPHILIC INTERACTION CHROMATOGRAPHY (HILIC)

Phosphorylated peptides isolated from 10 mg of total peptides were resuspended in 500 µl of 80 % ACN prior to injection and purified using HILIC chromatography (Ultimate 3000 HPLC system, Thermo) to fractionate the sample. The following solvents were used: A (0.005 % TFA), B (90 % ACN/0.005 % TFA) and C (0.04 % TFA). Samples were loaded in 90% solvent B. Phosphopeptides were fractionated on a 2.1 x 150 mm TSKgel Amide column. Following gradient steps were performed: 100% B for 3 min, to 90% B in 2 min, to 70% B in 20 min, up to 20% in 10 min while solvent C increased from 0 to 20%. Between 12 and 44 min 16 fractions of 300 µl were colleted and lyophilized for LC-MS analyses. [Experiment was performed by John Sinclair, Jorgensen's lab, ICR]

2.4.7 LIQUID CHROMATOGRAPHY TANDEM MASS SPECTROMETRY (LC-MS/MS)

Phosphorylated peptides were identified by Liquid Chromatography Tandem Mass Spectrometry (LC-MS/MS) using nanoflow capillary reversed-phase LC on an Eksigent NanoLC-Ultra 2D with a cHiPLC-nanoflex system (Eksigent, Dublin, California) coupled to an LTQ Orbitrap Velos mass spectrometer (Thermo Fisher Scientific, Hemel Hempstead, UK). 'Trap and elute' configuration was chosen on the NanoFlex system, and two type of columns were used: a trap column (200 µm x 0.5 mm) and an analytical column (200 µm x 15 cm), both packed with ChromXP C18-CL 3 µm 120 Å. Samples dried after HILIC were resuspended in 10 µl of 0.1% FA and loaded at a flow rate of 5 µl/min for 5 min. Elution was performed at a flow rate of 300 nl/min in a linear gradient of 5 % to 30% of ACN, 0.1 % FA solution in 120 min. Data-dependent mode switching automatically between Orbitrap MS and MS/MS acquisition was used. Acquisition of survey full scan MS spectra (from m/z 400-2000) was performed in the Orbitrap Velos using a resolution of 30,000 at m/z 400. Isolation and fragmentation of top 10 most intense ions with charge states greater than 2 was performed to a value of 3e4 in a higher energy collision dissociation (HCD) cell. Normalized collision energy was

set at 42%. Fragments were detected in the Orbitrap with a resolution of 7,500. Ions were selected up to 2,000 counts while ion accumulation times reached a maximum of 500 ms for full scans and 400 ms for HCD. The dynamic exclusion parameters were: width of 5 ppm with 1 repeat lasting 8 seconds for a duration of 60 seconds. [Experiment was performed by John Sinclair, Jorgensen's lab, ICR]

2.4.8 DATA ANALYSIS

Peptide identification was performed using raw data obtained in Xcalibur software (Thermo) through processing in Proteome Discover v1.3 software (Thermo Scientific) with Mascot v2.2 search engine (Matrix Science) and Ensembl dog database. The following Mascot search parameters were used: precursor mass tolerance – 10 ppm; fragment mass tolerance – 0.6 Da; trypsin missed cleavage – 2; static modifications: carbamidomethylation (C); variable modifications: oxidation (M), deamidated (NQ), phosphophorylation (STY), arginine $^{13}C_6$ (R6), arginine $^{13}C_6{}^{15}N_4$ (R10), lysine $^{2}H_{D4}$ (K4), and lysine $^{13}C_6{}^{15}N_4$ (K8). Filters applied to obtained peptide sequence matches (PSMs) were: a mascot significance threshold of at least 0.05, peptide score of at least 20, peptide maximum rank of 1 and pRS phosphorylation site probabilities ≥ 85 % (PhosphoRS1.0). The false discovery rate (FDR) was set to a q-value ≤ 0.01 (Percolator) for peptides.

Identified peptides with a 'heavy' to 'medium' ratio higher than 2 or lower than 0.5 in any of the three performed experiments were chosen for preliminary search and the ratios were compared between experiments. For some peptides, the ratio was not quantified due to the stringent parameters of the search. In that case, spectra were analysed manually and the ratios assessed from the raw data. Phosphorylated peptides for which a 'heavy' to 'medium' ratio was reproduced in two biological repeats were chosen for further analysis.

The identity of chosen peptides was confirmed by comparing them against the dog protein database with Basic Local Alignment Search Tool (BLAST, NCBI). Identified phosphorylation sites were aligned to sites in human, mouse and rat proteins. Current knowledge concerning characterisation of these sites (regulators, function) was obtained from the PhosphoSitePlus website. Other types of analysis were performed using databases such as STRING, SMART, Pfam, etc.

CHAPTER 3:

HSP90

CHAPTER 3: HSP90

3.1 INTRODUCTION

Apical extrusion of Ras^{V12}-transformed epithelial cells has been discovered and briefly characterised in the Fujita laboratory (the findings are summarised in section 1.5.4). Although some of the pathways downstream of Ras activation as well as a few proteins regulating cytoskeletal rearrangements have been both implicated or excluded from the process, answers to many questions remain unknown. Up to date, we cannot explain how normal and transformed cells recognise each other, what receptors mediate recognition, what signalling pathways are activated before and during extrusion, what is the mechanism and nature of this process and finally, what is the significance and fate of extruded transformed cells in an organism.

Faced with so many questions, Dr Fujita resorted to unbiased biochemical screens, which would allow him to identify molecules regulated in normal or transformed cells only when they were interacting with each other. In the course of my PhD studies, I have contributed to several types of experiments that were performed in line with this train of thought. One of the screens, however, was undertaken before I joined the laboratory, and I was later asked to characterise the results. This experiment was a 2D gel screen, in which all the proteins isolated from MDCK and Ras^{V12} cells plated alone were compared to all the proteins isolated from mixed cultures of these two cell types. Total cell lysates obtained after growing cells in these three conditions for 16 hours from inducing GFP-Ras^{V12} expression were firstly separated in non-denaturing conditions in which most of the proteins remain in the complexes that they form *in vivo*. A second round of separation was performed in denaturing conditions using standard SDS-PAGE in which proteins are separated according to their size. The final gels were subsequently stained with a SYPRO Ruby dye, and visualised patterns were analysed. Comparison of the dots in different conditions revealed that one of them was found repeatedly enhanced only in mixed cultures of MDCK and Ras^{V12} cells (Figure 5A). The protein was identified by mass spectrometry (MS) as heat

shock protein 90 beta (Hsp90β), and subsequently validated by immunoblotting (Figure 5B).

Figure 5. Hsp90β forms a different type of complex in mixed cultures compared to MDCK and Ras^{V12} cells alone. (A) Total cell lysates from MDCK cells alone, Ras^{V12} cells alone and mixed cultures were separated on 2D gels according to the size of the complexes formed in the cells (native PAGE) and according to the size of denatured proteins (SDS PAGE). (B) Total cell lysates were separated on 2D gels and analysed by immunoblotting using anti-Hsp90β antibody.

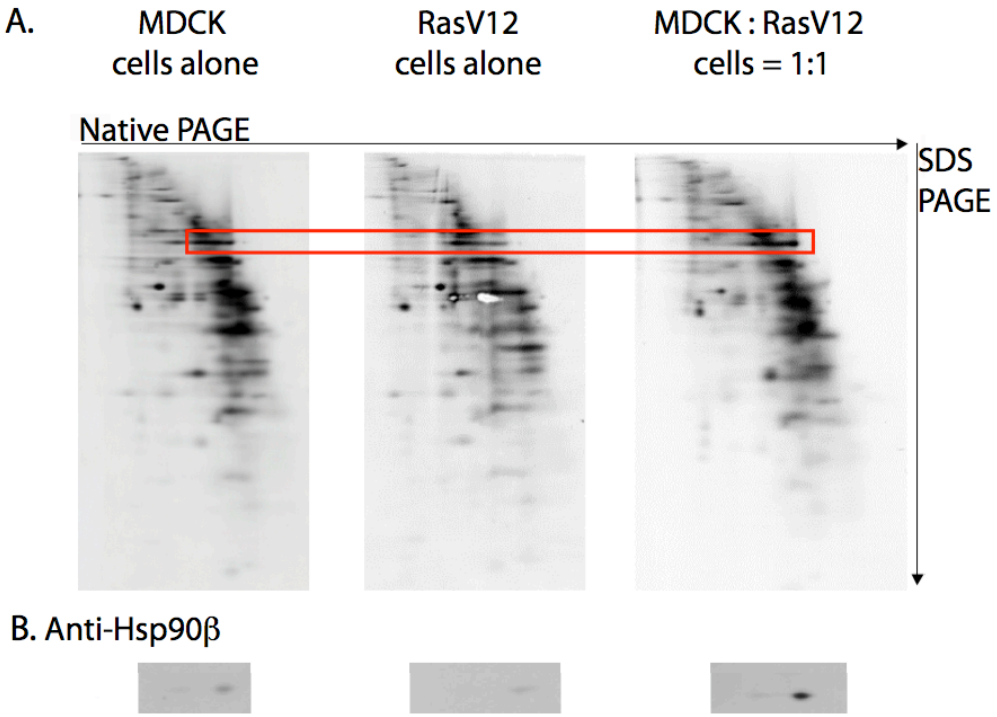

Hsp90 is an evolutionarily conserved molecular chaperone, a protein that assists in folding as well as stabilization of other proteins, collectively known as its 'clients'. According to the definition, a client is a molecule that without the help of a chaperone is degraded; in case of Hsp90, its clientele is estimated to encompass as much as 10% of the yeast proteome (Zhao and Houry, 2005). To facilitate this colossal task Hsp90 is very abundant in the cytosol, constituting about 1% of total protein mass in mammalian cells (Lai et al., 1984). Although the name of this protein suggests that it is expressed upon heat shock, this chaperone is in fact quite poorly induced above already high basal levels. Out of the two known vertebrate cytosolic isoforms, alpha and beta, only the former is

upregulated in heat-inflicted stress conditions, while the latter is generally believed to be constitutively expressed, and just occasionally induced by growth factors (Meng et al., 1993; Zhang et al., 1999). Despite these differences, a lot of cellular roles are common for both Hsp90 isoforms (Millson et al., 2007). Among a few known exceptions are regulation of B-cell lymphoma 2 (Bcl-2) dependent stabilization of hypoxia-inducible factor 1 (HIF-1α), which is performed exclusively by Hsp90β (Trisciuoglio et al., 2010), or secretion of α, but not β, isoform to the cell surface as well as cell culture medium to facilitate maturation of matrix metalloproteinase 2 (MMP2) (Sims et al., 2011).

In vivo Hsp90 most commonly forms flexible homodimers, although the β isoform can also be found in monomers (Minami et al., 1991). Each unit within a dimer contains their own N-terminal ATP-binding domain, middle domain where co-chaperones and client proteins bind, as well as a C-terminal dimerisation domain (this part also contains a MEEVD motif which anchors co-chaperones with tetratricopeptide repeat, TRP) (reviewed in (Li et al., 2012)).

To perform its chaperoning function, Hsp90 requires ATP. Interestingly, the ATP-binding pocket in this chaperone adopts a unique Bergerat fold geometry with a deep cavity characteristic only to few ATPases (e.g gyrase, histidine kinase). This unusual conformation explains high specificity of Hsp90 inhibitors interfering with the ATP-binding site (Bergerat et al., 1997; Travers et al., 2012). The nucleotide-binding domain preferentially binds ATP having over 100 times higher affinity to triphosphates comparing to diphosphates (Grenert et al., 1997). Upon binding of ATP, a "lid" closes over the molecule promoting N-terminal dimerisation of Hsp90, enforcing a conformational change from a V-shaped "open" state to a "closed" form. This in turn stimulates ATPase activity leading to ATP hydrolysis, opening of the lid, releasing ADP and returning to the initial V-shaped state (reviewed in (Prodromou, 2012)).

The ATPase cycle is coupled with sequential association and dissociation of different co-chaperones required for the Hsp90 function (reviewed in (Li et al., 2012)). Over 20 of these regulatory proteins have been found to affect Hsp90 function or deliver the clients. A prominent group mentioned earlier are TRP co-chaperones binding the C-terminal domain of Hsp90. Among them are Hop and CHIP binding Hsp90 in a mutually exclusive manner. These two co-chaperones have the ability to direct the function of the complex to either promotion of

folding (Hop) or degradation (CHIP) of assisted clients, respectively (Kundrat and Regan, 2010). Another worth mentioning co-chaperone is Cdc37, known as a chaperone of kinases. It recognises these signalling proteins with its N-terminal domain to subsequently bind Hsp90 and deliver the clients to the machinery (reviewed in (MacLean and Picard, 2003)).

Additionally Hsp90 activity is known to be regulated through not yet very well characterised posttranslational modifications, e.g. phosphorylation (Duval et al., 2007), acetylation (Kovacs et al., 2005) or S-nitrosylation (Retzlaff et al., 2009).

Unknown up to date remains where exactly client proteins fit in the ATPase/co-chaperone cycle or even how most of them are recognized by the machinery.

Since many of the over 200 confirmed client proteins assisted by Hsp90 (current list can be found on http://www.picard.ch) are signalling molecules often required for cell proliferation and survival, the function of this chaperone is particularly crucial for cancer cells. Among the known Hsp90 clients implicated in carcinogenesis are ERBB2, C-RAF, CDK4, AKT/PKB, steroid hormone receptors, mutant p53, HIF-1α, survivin and telomerase. Hsp90, in particular isoform α, has been found upregulated in cancer cells (Kubota et al., 2010; Neckers, 2002) and, not surprisingly, inhibition of its function was shown to be especially toxic towards transformed cells (Price et al., 1977; Sasaki et al., 1979).

Anti-tumour activity of geldanamycin (GA), a naturally occurring compound isolated in 1970s from a soil bacterium *Streptomyces hygroscopicus* (DeBoer et al., 1970), has been the first to be linked with inhibition of Hsp90 (Whitesell et al., 1994). Multiple studies followed this discovery, leading to identification as well as synthesis of new Hsp90 inhibitors, over 20 of which entered clinical trials during the past two decades. Unfortunately, none of them has been approved for clinical use due to their toxicity, side effects, or insufficient data supporting their anti-tumour activity. Nonetheless, gaining insight into intrinsic properties of Hsp90 allows researchers to design ever better inhibitors giving hope for a forthcoming treatment (reviewed in (Neckers and Workman, 2012)).

Several reasons are often mentioned to explain unusual sensitivity of cancer cells to Hsp90 inhibition. According to some, but not all, biochemical

studies, Hsp90 present in transformed cells has higher affinity towards both ATP and ATP-mimicking inhibitors like GA (Kamal et al., 2003). Moreover, Hsp90 in these cells forms much bigger, more active 'superchaperone' complexes (Kamal et al., 2003) coordinating cancer-specific networks (Moulick et al., 2011). Another explanation for the essential role of Hsp90 in cancer can be inferred from the inherent characteristics of tumour cells themselves. By escaping the control of growth factors and cell cycle they become prone to different types of cellular stress: insufficient nutrients, proteotoxicity, hypoxia, genetic instability, or attacks from the immune system (reviewed in (Neckers and Workman, 2012)). According to the latter hypothesis, in transformed cells Hsp90 acts as a buffer helping to overcome cellular stress. Interestingly, a buffering role has also been suggested for Hsp90 in evolution, where is it believed to decrease a negative impact of mutations leading to higher variation between genotypes (Jarosz and Lindquist, 2010).

3.2 RESULTS

3.2.1 HSP90 IS INCREASED IN RAS CELLS WHEN THEY ARE SURROUNDED BY NORMAL CELLS

Due to the important role of Hsp90 in stress management, particularly in cancer cells, we decided to investigate the role of this protein in interactions between normal and transformed cells. From the data obtained in the 2D gel screen, we concluded that Hsp90 in mixed cultures either forms a different type of complex or undergoes altered posttranslational modifications comparing to Ras^{V12} or MDCK cells alone. As a consequence of the nature of the screen, it could not be determined in which cell type from the mixed cultures Hsp90 was altered. Moreover, at this point it was not clear whether a biochemical screen in which transformed and normal cells were mixed in a ratio 1 to 1 could be utilised to gain insight into a situation studied up to date, where fewer transformed cells were plated within a monolayer of normal cells.

Since imitating early stages of cancerogenesis was the original purpose of the study, Ras^{V12} cells were now plated together with normal cells in a ratio 1 to 100 on collagen type I matrix, as well as alone. In order to assess differences in Hsp90 amount and localization between mixed and single cell type cultures, immunostaining with an anti-Hsp90β antibody was performed at two different time points from inducing GFP-Ras^{V12} expression. In experiments performed after 7 hours from addition of tetracycline to the culture medium, a significant increase in Hsp90β staining was observed in Ras^{V12} cells surrounded by normal cells, but not in Ras^{V12} cells alone (Figure 6B, D). Hsp90β localized in these cells to their apical, enlarged during extrusion, part. A similar increase was also detected after 24 hours from addition of tetracycline to the medium (Figure 6E), in Ras^{V12} cells that had already undergone extrusion, suggesting that high levels of Hsp90β were maintained throughout the process.

As Hsp90 in vertebrates exists in two distinct cytosolic isoforms, α and β, of which function is often redundant towards client proteins, mixed and singe cell type cultures were immunostained with an anti-Hsp90α antibody. A comparable

enhancement in the staining intensity in Ras^{V12} cells surrounded by normal cells was recorded (Figure 6A, C).

Figure 6. Hsp90β and Hsp90α are both increased in Ras^{V12} cells surrounded by normal cells, but not in Ras^{V12} cells alone. (A, B) Confocal images of xz sections of Ras^{V12} cells surrounded by normal cells and Ras^{V12} cells alone on collagen. Cells were fixed after 7 hours of incubation with tetracycline (2 µg ml^{-1}) and stained with anti-Hsp90α (A) and anti-Hsp90β (B) antibodies (red). (C, D, E) Quantification of accumulation of Hsp90α (C) and Hsp90β after 7 hours (D) and 24 hours (E) of incubation with tetracycline, in the cytoplasm of Ras^{V12} cells surrounded by normal cells and Ras^{V12} cells alone. In each experiment, approximately 24 (C), 15 (D), 9 (E) Ras^{V12}-expressing cells were counted per condition. Data are mean of the means of four independent experiments ± s.d.; *P < 0.05, ***P < 0.0001 (data in graph (E) represents two independent experiments).

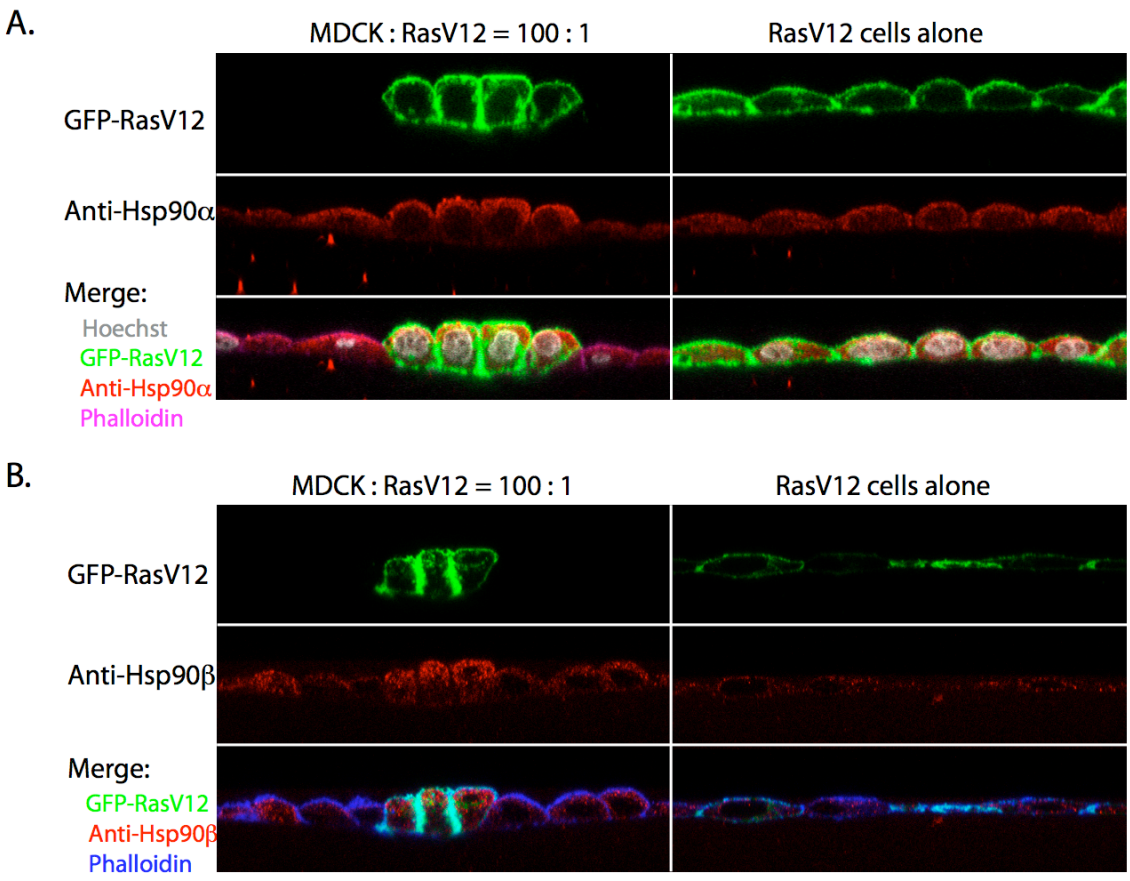

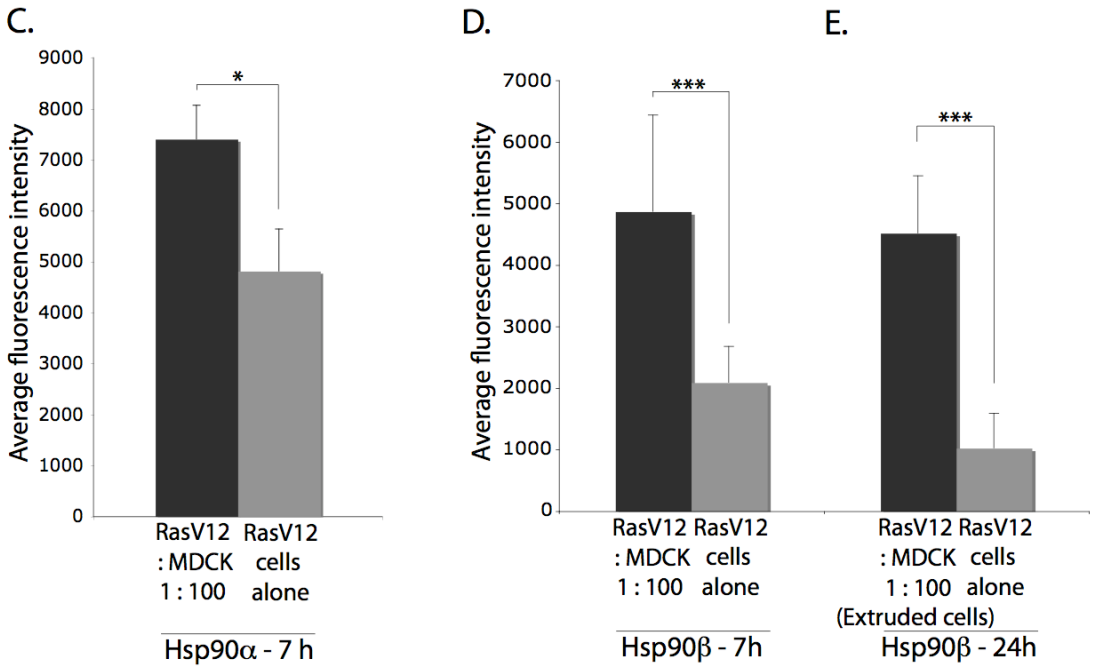

In order to assess whether upregulation of Hsp90 was a common phenomenon in transformed cells surrounded by normal cells, another system studied in the Fujita laboratory was examined by immunostaining with the anti-Hsp90β antibody. Stable cell lines carrying a tetracycline-inducible construct with GFP-v-Src, analogous to Ras^{V12} cells, created by Mihoko Kajita, were mixed with normal MDCK cells on collagen. GFP-v-Src expression was induced for 8 hours and immunostaining was performed. In contrast to Ras^{V12} cells, in v-Src cells surrounded by normal cells reproducible enhancement of Hsp90β staining was not observed (Figure 7).

Figure 7. Hsp90β is not reproducibly increased in v-Src cells surrounded by normal cells. Confocal images of xz sections of v-Src cells surrounded by normal cells and v-Src cells alone on collagen. Cells were fixed after 8 hours of incubation with tetracycline (2 μg ml^{-1}) and stained with anti-Hsp90β antibody (red).

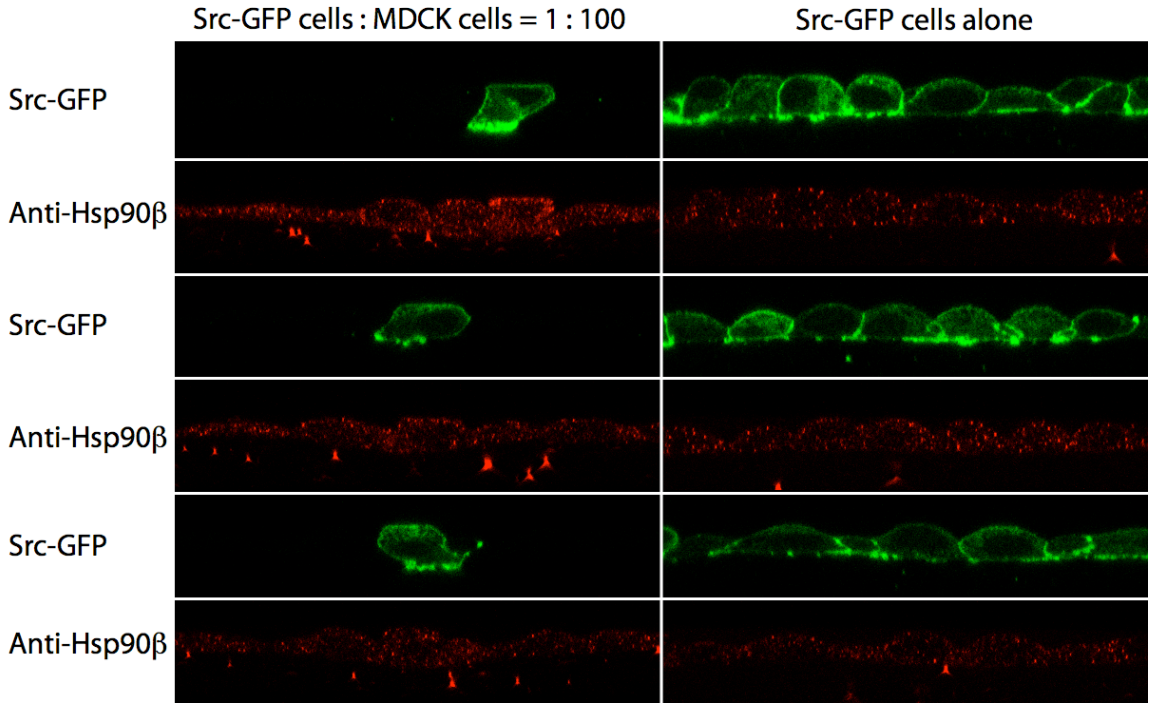

3.2.2 HSP90 INHIBITOR 17-AAG BLOCKS EXTRUSION

Knowing that both isoforms of cytosolic Hsp90 are upregulated in Ras^{V12} cells upon their interaction with normal cells prior to their extrusion, we took advantage of a variety of commercially available inhibitors of this chaperone to uncover its role in extrusion.

After a naturally existing Hsp90 inhibitor geldanamycin was found particularly toxic in cancer treatment, various modifications of this compound were synthesised in order to avoid this unwanted side effect. One of the derivatives was 17-N-allylamino-17-demethoxygeldanamycin (17-AAG), a more successful, less toxic inhibitor which similarly to the original geldanamycin replaces ATP in the nucleotide binding pocket, interfering with the ATPase activity necessary for the function of this chaperone (Schulte and Neckers, 1998).

Firstly, to confirm that 17-AAG was active in MDCK cells, a hepatocyte growth factor (HGF) assay was performed. The idea behind the assay is an observation that treatment with geldanamycin as well as its derivatives prevent sparsely plated MDCK cells from scattering in response to HGF (Shen et al., 2005). Although the HGF response is mediated by the Met receptor, a client of Hsp90, it is not clear whether inhibition of this chaperone is responsible for the anti-scattering effect. Upon addition of HGF alone to the cell culture medium, MDCK underwent visible epithelial to mesenchymal transition within 24 hours, however, treatment with as little as 50 nM 17-AAG, not only prevented them from scattering, but also visibly repressed their proliferation (Figure 8A). The decreased cell numbers can be explained by inhibition of Hsp90, a chaperone of many proteins involved in the cell cycle (eg. CDK1, CDK2, cyclin B etc.). Inhibition of Hsp90 chaperoning activity upon treatment with 17-AAG, was further confirmed by immunoblotting of total cell lysates of MDCK cells cultured in the presence of this inhibitor with an anti-ErbB2 antibody (Figure 8B). As 100 nM concentration of 17-AAG was the most efficient in inducing degradation of ErbB2, an established client of Hsp90, it was chosen for further analysis.

Figure 8. Hsp90 inhibitor 17-AAG inhibits Hsp90 activity in MDCK cells. (A) Phase contrast images of MDCK cells cultured for 24 hours at low density with or without HGF (100 nM) and with Hsp90 inhibitor 17-AAG (50, 75, 100 nM). (B) Total cell lysates of MDCK cells cultured with an Hsp90 inhibitor and analysed by immunoblotting using anti-ErbB2 antibody.

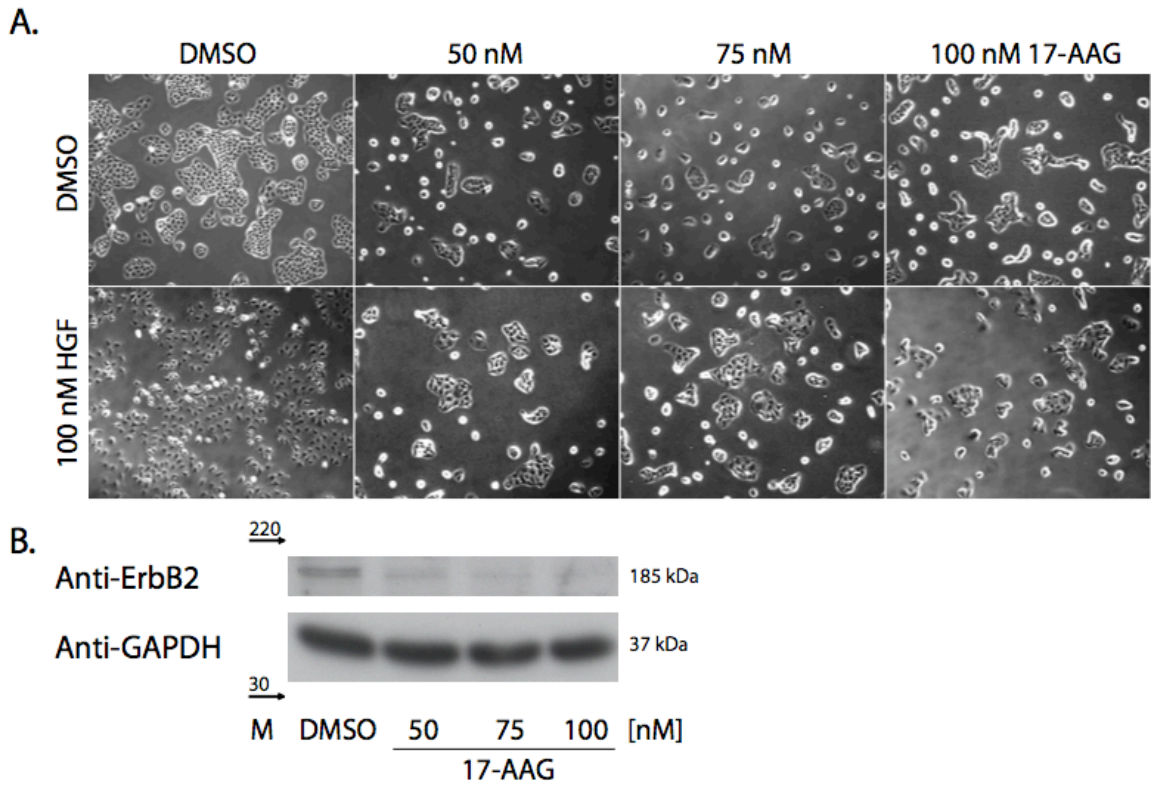

Secondly, to assess the effect of Hsp90 inhibition on extrusion, Ras^{V12} cells were mixed with normal cells in a ratio 1 to 100. After allowing them to form a monolayer for around 6 hours, cells were treated with tetracycline together with 100 nM 17-AAG. Following a 24-hour treatment, cells were fixed and examined by immunofluorescence (Figure 9A). The effect observed after inhibition of Hsp90 with 17-AAG was striking: extrusion of Ras^{V12} cells from normal monolayers was nearly completely blocked by the treatment (Figure 9B). No signs of toxicity were detected for either of the cell types at that time point.

Figure 9. Hsp90 inhibitor 17-AAG blocks extrusion of Ras^{V12} cells from a monolayer of normal cells. (A) Confocal images of xz and xy sections of Ras^{V12} cells surrounded by normal cells on collagen. Cells were fixed after a 24-hour incubation with tetracycline (2 μg ml^{-1}) and the Hsp90 inhibitor 17-AAG (100 nM), and stained with phalloidin-647 (grey). (B) Quantification of frequency of apical extrusion and formation of basal protrusions of Ras^{V12} cells in a monolayer of MDCK cells in the presence of Hsp90 inhibitor 17-AAG. In each experiment, approximately 13 groups of Ras^{V12} cells were counted per condition. Data are mean ± s.d. of four independent experiments; $^{**}P < 0.005$.

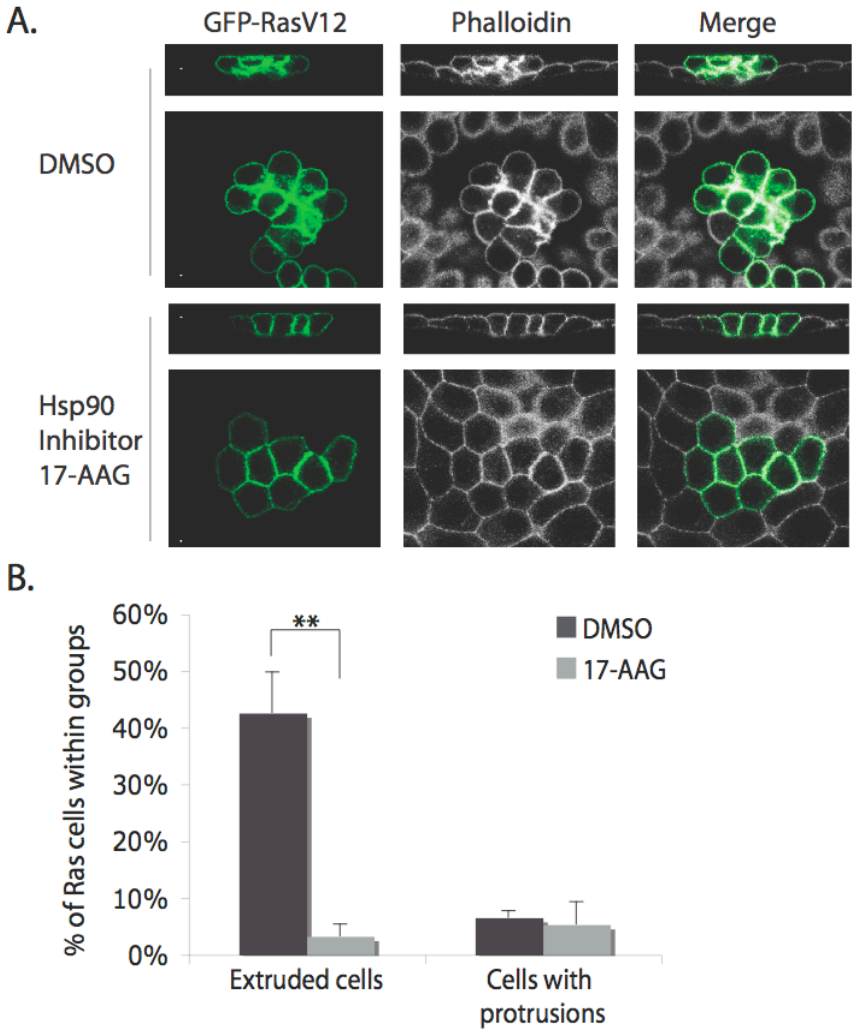

3.2.3 PHOSPHORYLATION OF ERK IS COMPROMISED BY HSP90 INHIBITOR 17-AAG

Apart from blocking extrusion, treatment with 17-AAG visibly affected the phenotype of transformed cells. Although Ras^{V12} cells continued to increase their cell height comparing to their normal neighbours as reported by Hogan and colleagues (Hogan et al., 2009), they resembled normal cells to a much greater extent than Ras^{V12} cells treated just with DMSO. Accumulation of both actin and E-cadherin was visibly reduced on the junctions between Ras^{V12} cells in a monolayer of normal cells (Figure 10A, B). In fact, a decrease in the intensity of junctional actin and E-cadherin staining, as well as in the signal from junctional GFP-Ras^{V12} itself, was also noticeable in Ras^{V12} cells alone (Figure 10A, B), suggesting that under these conditions transformation itself might have been impaired.

Figure 10. Accumulation of junctional actin and E-cadherin in Ras^{V12} cells is affected by treatment with Hsp90 inhibitor 17-AAG. (A, B) Confocal images of xy sections of Ras^{V12} cells surrounded by normal cells and Ras^{V12} cells alone on collagen. Cells were fixed after a 24-hour incubation with tetracycline (2 µg ml^{-1}) and the Hsp90 inhibitor 17-AAG (100 nM), and stained with either phalloidin-647 (A) or anti-E-cadherin antibody (B) (purple).

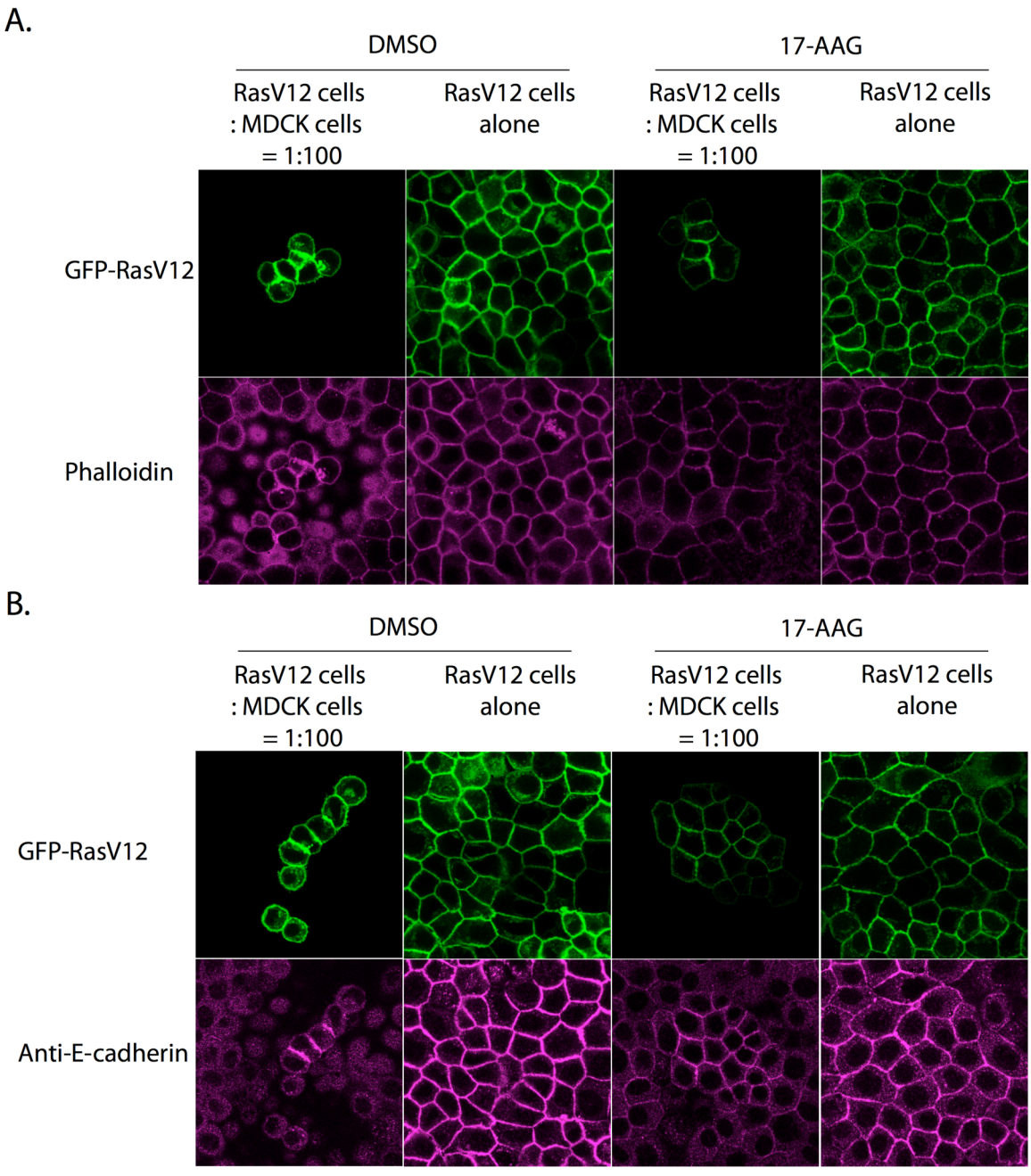

Indeed, it has been reported previously that knock-down of Hsp90α compromised MAPK signalling (Bandyopadhyay et al., 2010). Given that MAPK activation downstream of Ras^{V12} is required for extrusion to occur (Hogan et al.,

2009), we decided to check whether levels of phosphorylated ERK were changed by addition of 17-AAG to the culture media of either MDCK or Ras^{V12} cells.

Firstly, characterisation of ERK activation upon tetracycline addition in Ras^{V12} cells was performed. GFP cells, a stable cell line transfected with an original construct into which Ras^{V12} encoding fragment was subsequently inserted, was used as a control. To cells plated at three different densities, tetracycline was added. Cells were lysed at three different time points from inducing GFP-Ras^{V12} expression, and lysates were analysed by immunoblotting with anti-phospho-ERK, and anti-ERK antibodies. Activation of ERK was only noted at 7 hours from adding tetracycline (Figure 11 A), but not at any of the later time points (Figure 11 B, C), suggesting that MAPK signalling downstream of Ras^{V12} is only activated transiently in these cells (Figure 11 D). Additionally, higher activation of ERK was observed in cells plated in less confluent conditions.

Figure 11. Upon induction of Ras^{V12} expression ERK is activated transiently. (A, B, C) Total cell lysates of pTR-GFP cells and pTR-GFP-Ras^{V12} cells analysed by Western blotting using anti-pERK, anti-ERK and anti-GAPDH antibody. Cells were grown in 6-well plates at three different cell densities: 0.5 x 10^6 (an equivalent of ± 50% confluent cells), 0.75 x 10^6 (± 75% confluent cells), and 1 x 10^6 (cells forming a monolayer). Cells were lysed at different time points from adding tetracycline: 7 hours (A), 18 hours (B), 24 hours (C). (D) Quantification of the data presented in (A, B, C). The ratios of pERK to ERK representing level of ERK activation at different time points were plotted. Each value represents pERK to ERK ratio in Ras^{V12} cells normalised to pERK to ERK ratio in GFP cells plated at the same density and lysed at the same time.

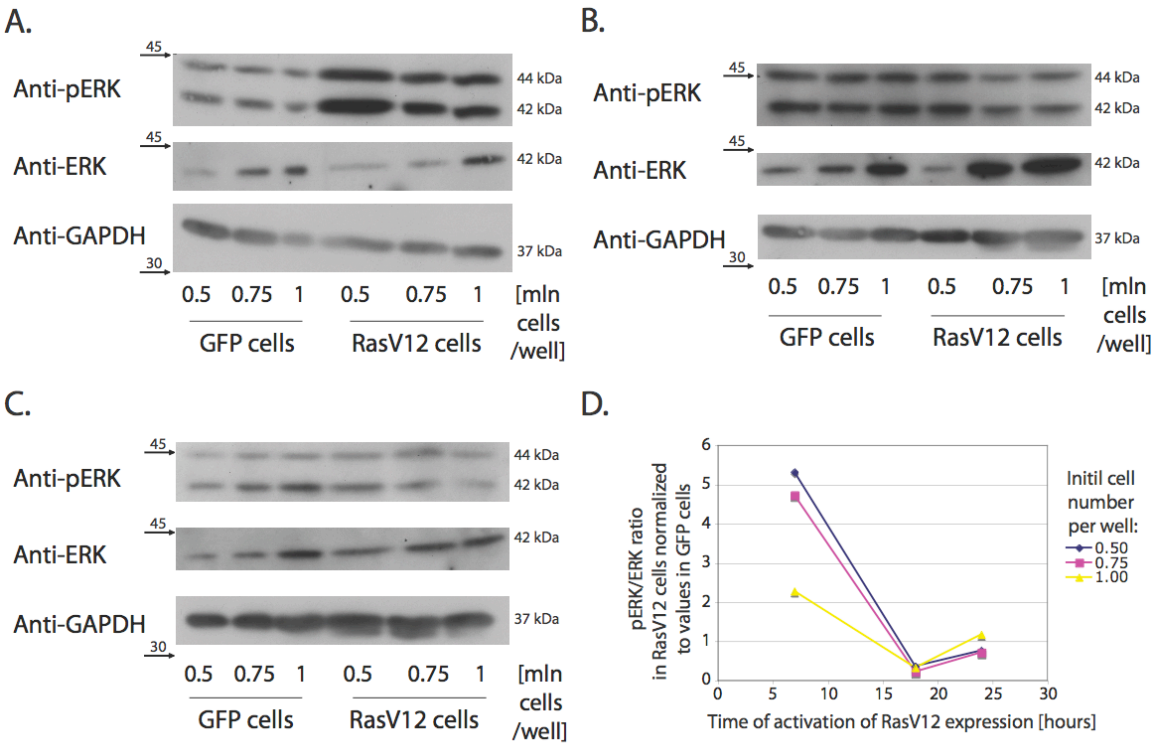

To investigate the impact of 17-AAG on activation of MAPK signalling upon Ras^{V12} expression, lysates of both MDCK and Ras^{V12} cells were analysed by immunoblotting with anti-phospho-ERK antibody 7 and 24 hours after addition of tetracycline to the media. In lysates treated for 7 hours with tetracycline and 17-AAG of both MDCK as well as Ras^{V12} cells, a remarkable reduction in the signal of phosphorylated ERK was recorded (Figure 12A). Consistently with previous findings concerning the time line of ERK activation in Ras^{V12} cells, no difference was seen in the amount of phosphorylated ERK after 24 hours from addition of tetracycline between cells treated or non-treated with 17-AAG (Figure 12B).

Figure 12. Hsp90 inhibitor 17-AAG blocks ERK activation in MDCK and Ras^{V12} cells. (A, B) Total cell lysates of MDCK cells and pTR-GFP-Ras^{V12} cells treated with Hsp90 inhibitor 17-AAG analysed by immunoblotting using anti-pERK and anti-GAPDH antibodies. Cells were lysed at different time points from adding tetracycline: 7 hours (A) and 24 hours (B).

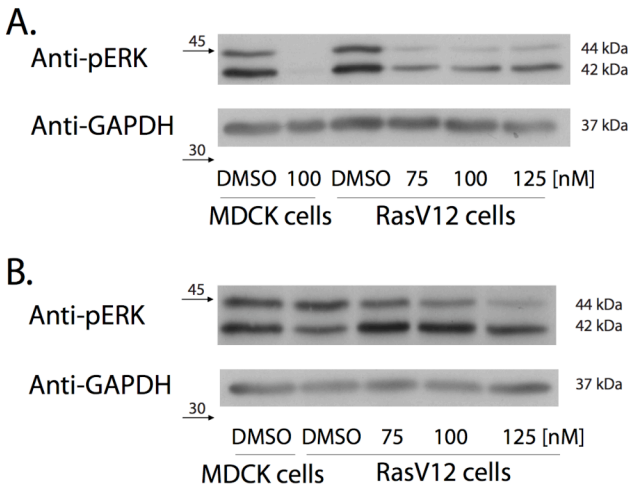

Taken together, these data indicate that treatment with 17-AAG affects activation of MAPK signalling downstream of Ras^{V12}, possibly though inhibiting chaperoning function of Hsp90 towards one of the proteins upstream of MAPK pathway, e.g. B-Raf.

3.2.4 PHOSPHORYLATION OF ERK IS NOT AFFECTED BY HSP90 INHIBITOR CELASTROL

Inhibition of ERK activation was previously found to prevent extrusion of Ras^{V12} cells from a monolayer of normal cells (Hogan et al., 2009). As treatment with Hsp90 inhibitor 17-AAG resulted in hindering ERK phosphorylation in Ras^{V12} cells, we decided to use a compound impairing Hsp90 function *via* a different mechanism.

Celastrol is a guinone methide triterpene isolated from a Chinese vine *Tripterygium wilfordii*, which has been used for thousands of years to treat fever, chills, edema and carbuncle. Only recently, celastrol was linked to inhibition of Hsp90 following a gene expression signature-based screen (Hieronymus et al., 2006). Interestingly, celastrol, unlike most other Hsp90 inhibitors, including 17-AAG, does not interfere with the ATP-binding site in this chaperone. Despite the fact that ATP can still be bound to the Hsp90-celastrol complex, ATPase activity is inhibited (Zhang et al., 2009). According to some reports, celastrol binds to C-terminal domain of Hsp90, disrupting its interaction with a kinase co-chaperone Cdc37 (Sreeramulu et al., 2009; Zhang et al., 2008; Zhang et al., 2009). Importantly, treatment with celastrol does not preferentially affect kinase clients of Hsp90 (Zhang et al., 2010) and therefore, according to some studies, the effect of this molecule on Hsp90 is in fact less specific (Chadli et al., 2010).

We decided to test celastrol in extrusion, hoping that due to a different mechanism of inhibiting Hsp90, treatment with celastrol would result in altered client sensitivity, and possibly allow for ERK activation in our system.

Firstly, inhibition of Hsp90 in Ras^{V12} cells was confirmed by immunoblotting of total cell lysates treated with celastrol for 18 hours. Both tested client proteins, Raf-1 as well as ErbB2 were degraded upon treatment with celastrol, but in line with previous findings, their individual sensitivity to the inhibitor differed from one client to the other (Figure 13A). In contrast to treatment with 17-AAG however, incubation with celastrol did not result in reduction of phosphorylated ERK after 7 hours from adding tetracycline (Figure 13B). Furthermore, treatment with higher concentrations of celastrol had a stabilizing effect on phosphorylated ERK at later time points from induction of GFP-Ras^{V12} expression (Figure 13C).

Figure 13. Hsp90 inhibitor celastrol blocks Hsp90 activity in Ras^{V12} cells, but does not inhibit ERK activation. (A, B, C) Total cell lysates of Ras^{V12} cells treated with different concentrations of Hsp90 inhibitor celastrol analysed by immunoblotting using anti-Raf, anti-ErbB2, anti-Ras, anti-GFP, anti-GAPDH (A), anti-pERK, anti-ERK (B, C) antibodies. Cells were lysed at different time points from adding tetracycline: 7 hours (B), 18 hours (A, C).

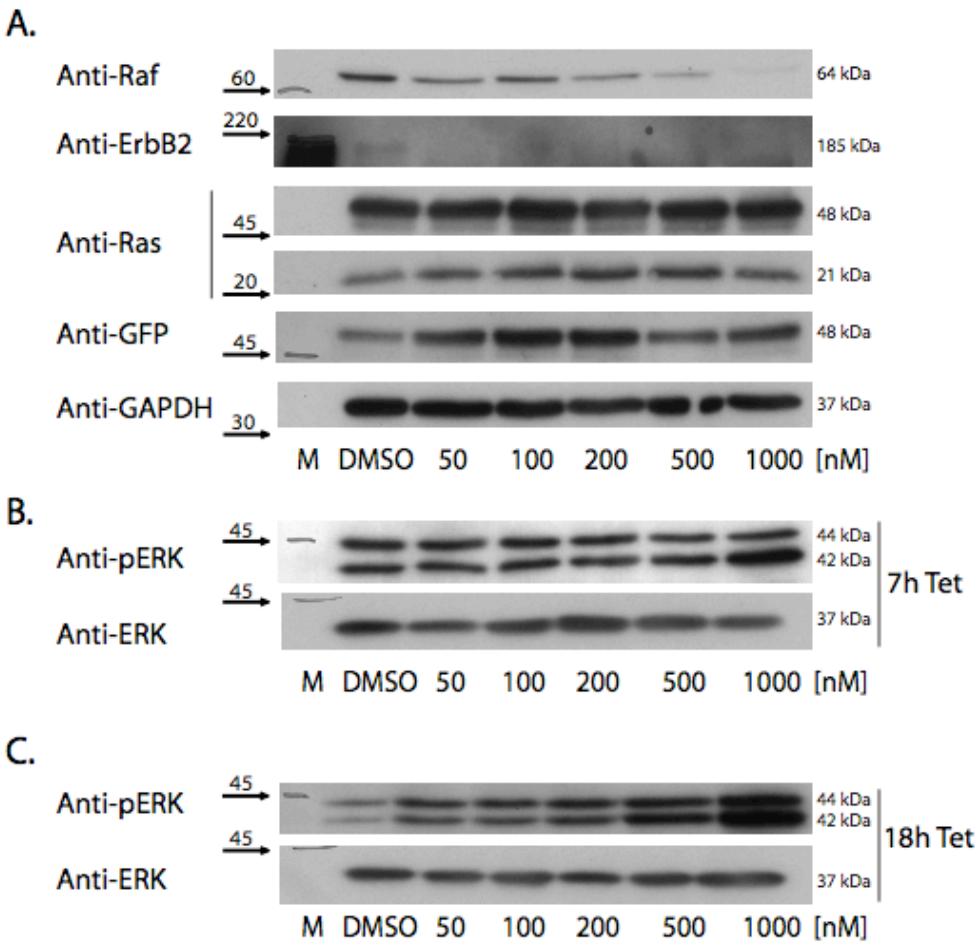

3.2.5 HSP90 INHIBITOR CELASTROL ENHANCES EXTRUSION ON COLLAGEN

Knowing that celastrol does not prevent ERK activation downstream of Ras^{V12} expression, we decided to use this inhibitor to study the effect of Hsp90 inhibition on extrusion.

Ras^{V12} cells were plated together with MDCK cells in a ratio 1 to 100 on collagen type I matrix. After 6 hours, tetracycline together with 1 μM celastol was added to the cell culture medium, followed by a 24-hour incubation. Cells were subsequently fixed with 4% PFA, and examined by immunoflourescence. Treatment with celastrol did not prevent extrusion of Ras^{V12} cells from a monolayer of normal cells (Figure 14A). Instead transformed cells were extruded around 10% more efficiently at this time point (Figure 14B).

Ras^{V12} cells treated with celastrol both in mixed and single cell type cultures produced GFP positive intracellular vesicles, and generally appeared less fit than control cells (Figure 14A). In order to confirm that increase in extrusion of these cells did not occur following their cell death upon treatment with celastrol, we performed time lapse experiments. Ras^{V12} cells were plated on collagen among normal cells in a ratio 1 to 50. After overnight incubation, tetracycline was added to the cultures together with 1 μM celastrol. Four hours later groups of Ras^{V12} cells no larger than 4 neighbouring transformed cells were randomly chosen and followed using time lapse microscopy for further 48 hours. During that time both control and celastrol-treated Ras^{V12} cells underwent extrusion from normal monolayers in a similar fashion (Figure 15A). In control conditions groups of extruded Ras^{V12} cells after 48 hours of imaging formed a compact mass without visible in the bright field junctions, while cells incubated with celastrol appeared more separated (images 48:00-BF in Figure 15A). Nonetheless, in both conditions cells continued to proliferate after extrusion, indicating that even upon treatment with this Hsp90 inhibitor, they remained alive. Their viability was further confirmed by addition of ethidium homodimer-1 to the culture medium, a cell-impermeant nucleic acid stain, which was not incorporated into extruded Ras^{V12} cells up to 48 hours from tetracycline addition (Figure 15B).

Figure 14. Hsp90 inhibitor celastrol enhances extrusion of Ras^{V12} cells from a monolayer of normal cells. (A) Confocal images of xz and xy sections of Ras^{V12} cells surrounded by normal cells and Ras^{V12} cells alone on collagen. Cells were fixed after a 24-hour incubation with tetracycline (2 μg ml^{-1}) and the Hsp90 inhibitor celastrol (1 μM), and stained with phalloidin-647 (magenta) and Hoechst (grey). (B) Quantification of frequency of apical extrusion of Ras^{V12} cells from a monolayer of MDCK cells in the presence of Hsp90 inhibitor celastrol. In each experiment, approximately 11 groups of Ras^{V12} cells were counted per condition. Data are mean ± s.d. of four independent experiments; *$P < 0.05$.

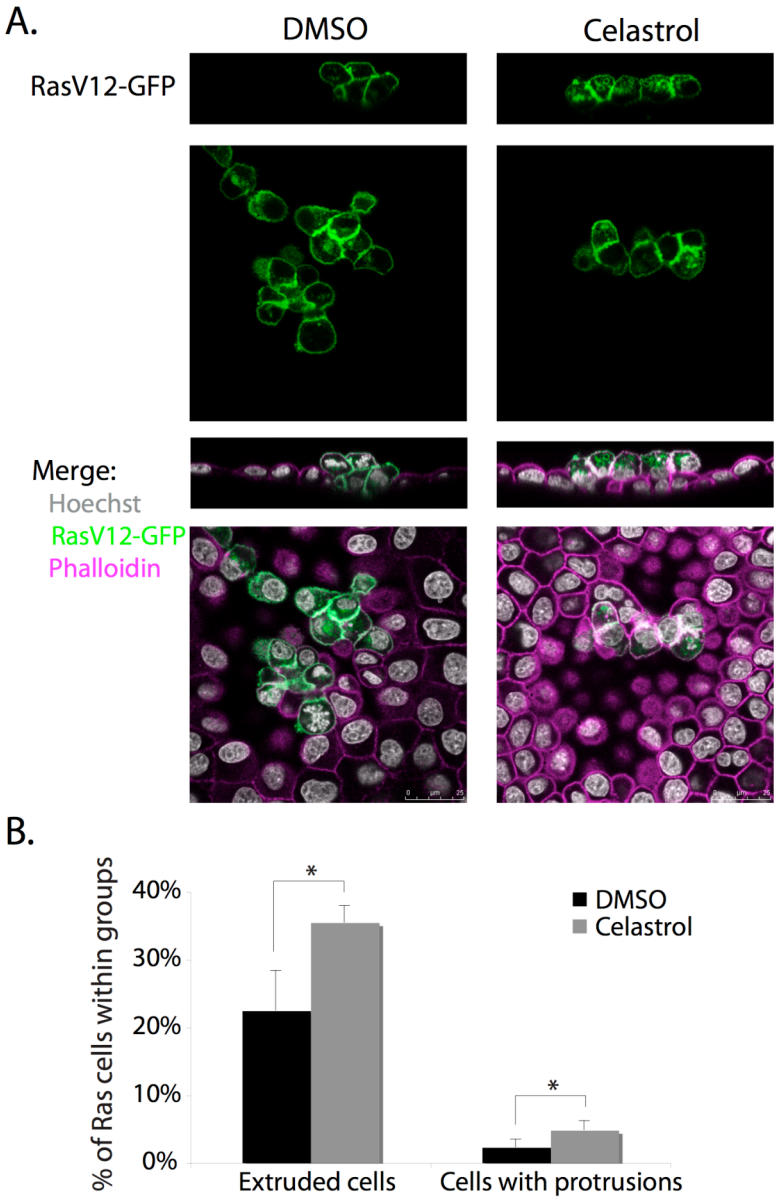

Figure 15. Ras^{V12} cells treated with celastrol for 48 hours on collagen remain alive after extrusion. (A, B) Ras^{V12} cells treated with 1 μM celastrol continued to proliferate after extrusion from a monolayer of normal cells (A), and did not incorporate ethidium dye after 48 hours from tetracycline addition (B). Ras^{V12} cells were combined with normal MDCK cells at a ratio of 1 to 50 and cultured on type-I collagen gels, followed by tetracycline and celastrol treatment. Images were extracted from a representative time-lapse analysis as an overlay of bright field (BF), green fluorescent channel (GC), and red fluorescent channel (RC), as indicated.

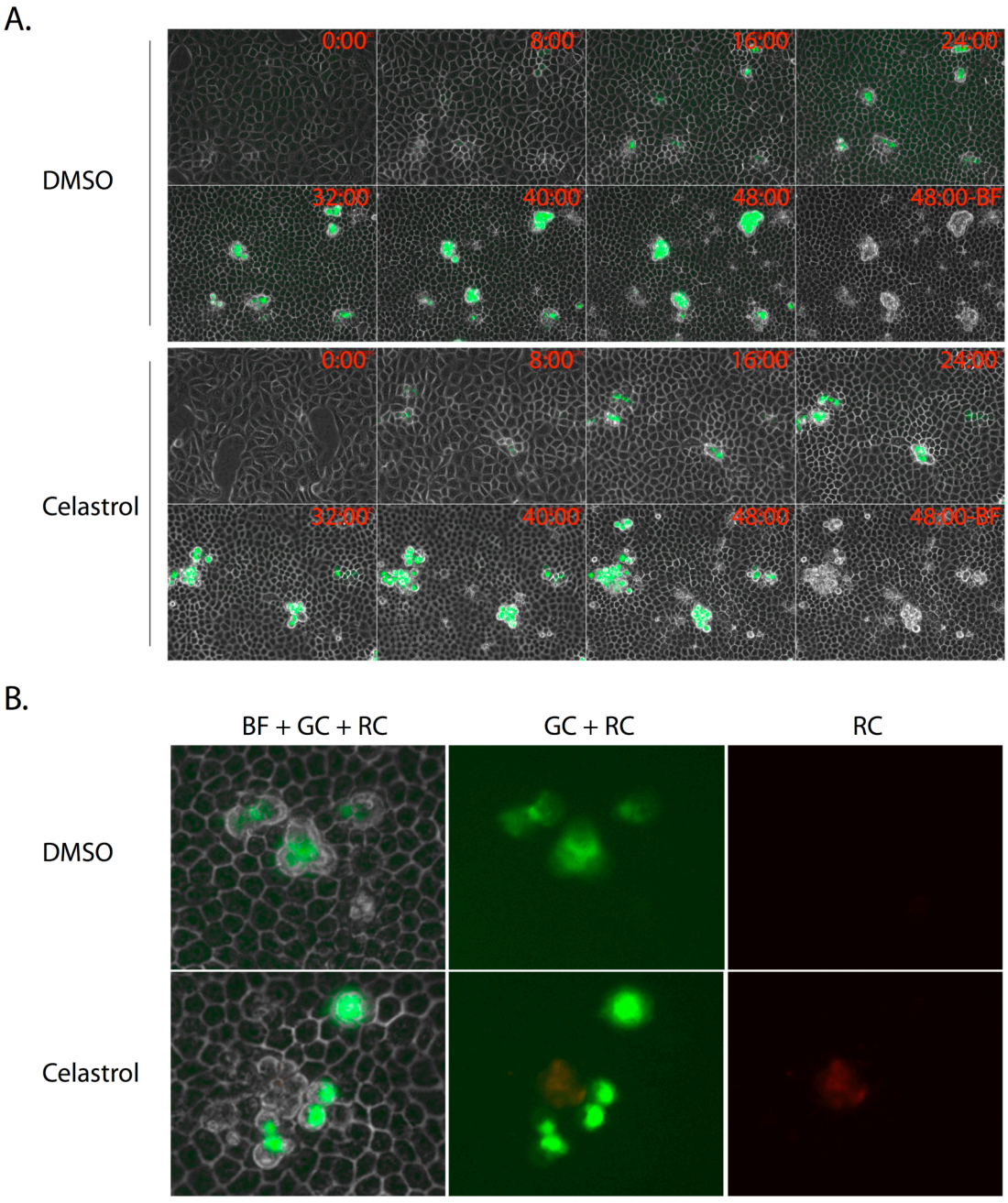

3.2.6 DOMINANT NEGATIVE FORM OF HSP90 ENHANCES EXTRUSION ON COLLAGEN

Since treatment with Hsp90 inhibitors used in this study had contradicting effects on extrusion of Ras^{V12} cells from normal monolayers, we decided to use a different approach to elucidate what role Hsp90 plays in this process.

A dominant negative form of Hsp90β created by site directed mutagenesis within the ATP-binding pocket was previously shown to inhibit VEGF-induced phsphorylation of Akt, eNOS and dependent on them NO release in endothelial cells (Miao et al., 2008). In order to clarify whether inhibition of Hsp90 indeed resulted in higher extrusion rates of Ras^{V12} cells surrounded by normal neighbours, we purchased commercially available constructs encoding the dominant negative form of this chaperone as well as a wild type form tagged with an HA tag in mammalian expression vectors (Addgene). Unfortunately, an attempt to create a stable cell line expressing the dominant negative form of Hsp90 failed, possibly due to toxicity of long term inhibition of this protein in Ras^{V12} cells. As a result, both constructs were instead transiently transfected into MDCK cells together with original GFP-Ras^{V12} and GFP constructs in six possible combinations (Figure 16B). 24 hours from transfection cells were fixed and immunostained with an anti-HA antibody, Hoechst and phalloidin (Figure 16A). Cells positive for both GFP signal and anti-HA staining with non-fragmented nuclei were chosen for quantification of extrusion.

While over 15% of cells transfected with a GFP-Ras^{V12} construct alone underwent extrusion at this time point, and over 45% had a tall phenotype characteristic for cells immediately before extrusion, cotransfection with constructs encoding either of the Hsp90 forms, increased these numbers. 30% of cells transiently expressing wild type of Hsp90β and over 45% of cells expressing the dominant negative form of this chaperone (DNHsp90β) underwent extrusion by 24 hours from transfection (Figure 16B). Importantly, cells cotransfected with control GFP plasmid and either of Hsp90 constructs, remained within normal monolayers.

In order to exclude higher expression levels of the dominant negative form of Hps90β as the cause for higher extrusion rates, we immunoblotted total lysates of transfected MDCK cells with anti-Hsp90β, anti-HA, anti-GFP and anti-Ras

antibodies. After 24 hours from transfection, detected levels of DNHsp90 form were in fact lower than of the wild type form (Figure 16C). In lysates obtained from cells cotransfected with *GFP-Ras^{V12}*, the amount of DNHsp90 further deceased comparing to cotransfection with GFP-plasmid alone, possibly due to loose attachment to the monolayer of some of the extruded groups, which subsequently might have been lost before the lysis. ERK activation was not affected in Ras^{V12} cells expressing DNHsp90 comparing to Ras^{V12} cells expressing Hsp90β (Figure 16D).

From the presented above data we concluded that inhibition of Hsp90 leads to higher extrusion rates of transformed cells from normal monolayers, a result confirmed with Hsp90 inhibitor celastrol as well as DNHps90β.

Figure 16. MDCK cells transiently transfected with Ras^{V12} and a dominant negative form of Hsp90β are more efficiently extruded from a monolayer of normal cells than MDCK cells co-transfected with Ras^{V12} and wild-type Hsp90β. (A) Confocal images of xz sections of MDCK cells transiently transfected with constructs driving expression of GFP, GFP-Ras^{V12}, Hsp90β-HA, DNHsp90β-HA in indicated combinations, plated on collagen. Cells were fixed after 24 hours since transfection, and stained with anti-HA antibody (red), phalloidin-647 (magenta) and Hoechst (grey). (B) Quantification of frequency of apical extrusion of cells co-transfected with GFP or Ras^{V12} with either wild-type Hsp90β or DNHsp90β from a normal monolayer. In each experiment, approximately 20 cells were counted per condition. Data are mean ± s.d. of five independent experiments; **P* < 0.05, ***P* < 0.005, ***P < 0.0001. (C) Total cell lysates of MDCK cells co-transfected 24 hours (C) earlier with GFP or Ras^{V12} with either wild-type Hsp90β or DNHsp90β analysed by immunoblotting using anti-Hsp90β, anti-HA, anti-Ras, anti-GFP and anti-GAPDH antibodies. (D) Confocal images of xy sections of Ras^{V12} cells transiently transfected with constructs driving expression of Hsp90β-HA, DNHsp90β-HA and subsequently plated with MDCK cells in a 1 to 1 ratio on collagen. Cells were fixed after 32 hours from transfection with an 8-hour incubation with tetracycline (2 μg ml^{-1}), and stained with anti-pERK (red) and anti-HA-tag antibodies (magenta).

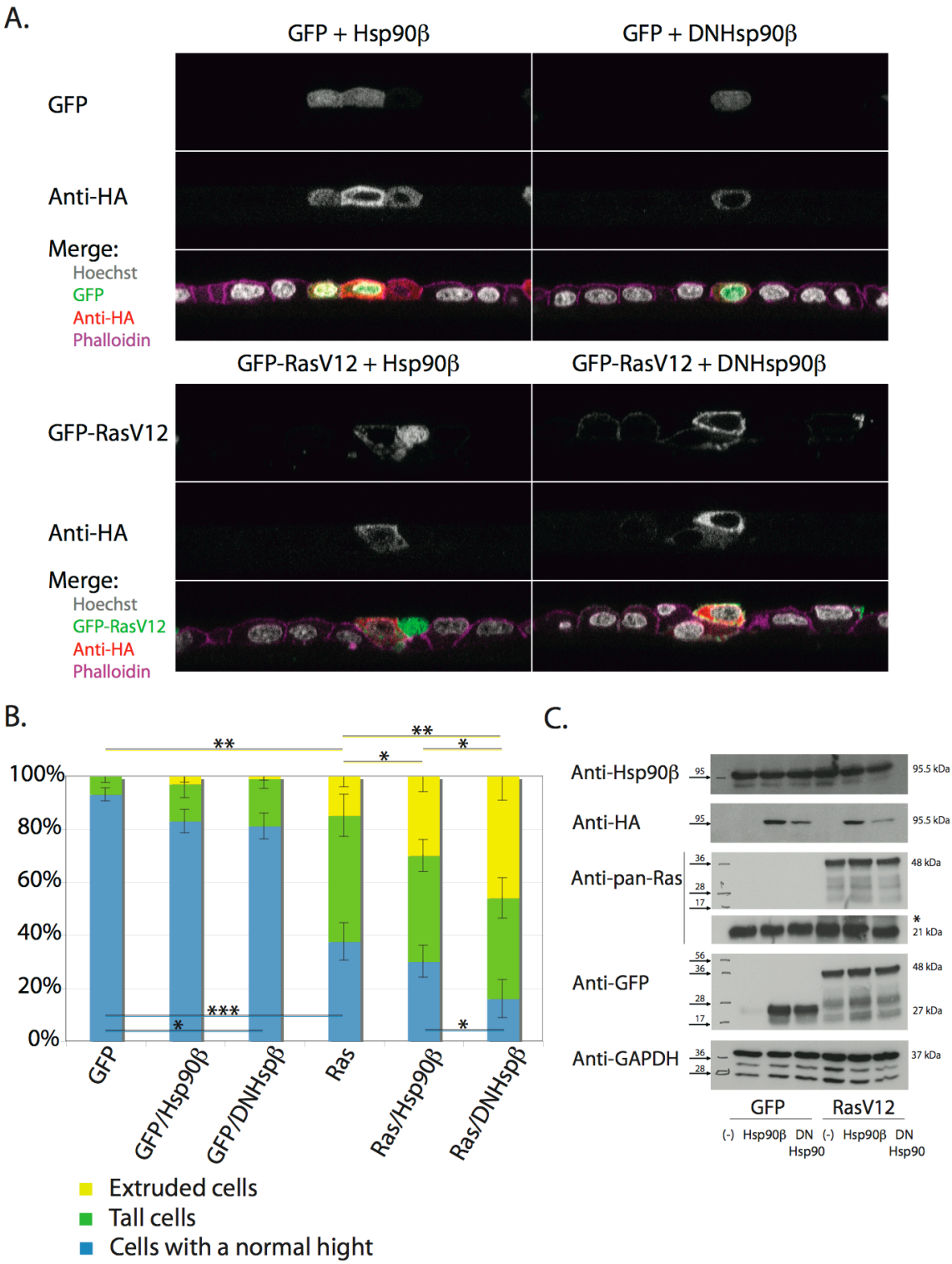
A.
GFP + Hsp90β
GFP + DNHsp90β
GFP
Anti-HA
Merge:
Hoechst
GFP
Anti-HA
Phalloidin
GFP-RasV12 + Hsp90β
GFP-RasV12 + DNHsp90β
GFP-RasV12
Anti-HA
Merge:
Hoechst
GFP-RasV12
Anti-HA
Phalloidin
B.
100%
80%
60%
40%
20%
0%
GFP
GFP/Hsp90β
GFP/DNHspβ
Ras
Ras/Hsp90β
Ras/DNHspβ
Extruded cells
Tall cells
Cells with a normal hight
C.
Anti-Hsp90β
Anti-HA
Anti-pan-Ras
Anti-GFP
Anti-GAPDH
95.5 kDa
48 kDa
21 kDa
27 kDa
37 kDa
GFP
RasV12
(-) Hsp90β DN Hsp90
(-) Hsp90β DN Hsp90

D.

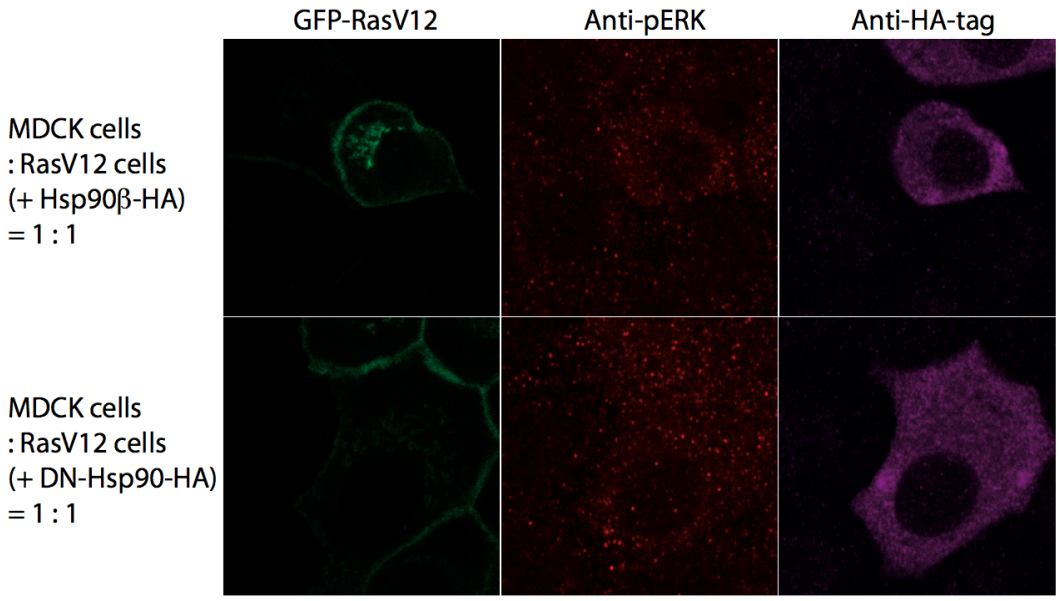
GFP-RasV12
Anti-pERK
Anti-HA-tag
MDCK cells
: RasV12 cells
(+ Hsp90β-HA)
= 1 : 1
MDCK cells
: RasV12 cells
(+ DN-Hsp90-HA)
= 1 : 1

3.9 DISCUSSION

In this study, I benefited from a 2D gel screen previously done in the Fujita laboratory, in which Hsp90 was identified as a protein altered in mixed cultures of normal and transformed cells, compared to these two cell types grown separately. Using Hsp90 antibodies and a system imitating early stages of cancerogenesis established by Catherine Hogan (Hogan et al., 2009), I found that both cytosolic isoforms of Hsp90, alpha and beta, present in mammalian cells were upregulated and localized apically in Ras^{V12} cells surrounded by normal cells early after inducing oncogene expression. Conversely, a similar level of upregulation was not reproduced in Src cells plated within normal monolayers, indicating that Hsp90 overexpression or stabilization is not a common phenomenon in all types of extruding transformed cells. Interestingly, although Hsp90α has been previously found upregulated in stress as well as in some types of cancers cells, Hsp90β is believed to remain at a constant level. According to one study, Hsp90β expression might be regulated by PKC epsilon (Wu et al., 2003); however, none of the available PKC inhibitors affected Hsp90 upregulation in our system (data not shown).

To study the role of Hsp90 in extrusion, we took advantage of two commercially available inhibitors, each hindering the chaperoning activity of this protein *via* a different mechanism. 17-AAG, a derivative of the better known geldanamycin, nearly completely blocked extrusion, possibly due to inhibition of ERK activation detected at 8 hours from adding tetracycline. Treatment with MAPK inhibitors was previously shown to prevent extrusion (Hogan et al., 2009); hence, it is likely that by affecting this pathway, 17-AAG interfered with Ras-dependent transformation itself. This hypothesis is further supported by the results of treatment with the second Hsp90 inhibitor, celastrol. Upon addition of this compound to mixed cultures of Ras^{V12} and MDCK cells, both extrusion and ERK activation not only still occurred, but were enhanced. In the case of ERK, its phosphorylated form was stabilised. It remains unclear why treatment with two inhibitors of the same protein, resulted in opposite effects on MAPK activation. One possible explanation is that by acting on Hsp90 *via* different mechanisms, these inhibitors target slightly different pools of client proteins. Variable

sensitivity of client proteins to inhibition of Hsp90 has been reported before, although a theory behind this phenomenon is yet to be proposed. If Raf proteins stabilised by interaction with Hsp90 were more sensitive to inhibition with 17-AAG, ERK activation could be affected by treatment with this compound. Celastrol, on the other hand, as a less specific inhibitor targeting a few other cellular pathways, could promote ERK activation *via* a Hsp90-independent mechanism.

To resolve the riddle of what role Hsp90 plays in extrusion, we decided to use a different approach. A dominant negative form of this chaperone cotransfected with Ras^{V12} into MDCK cells, enhanced their extrusion from normal monolayers comparing to either Ras^{V12} transfected alone or together with a wild type form of *Hsp90β*. Importantly, the latter also resulted in higher extrusion rates comparing to cells expressing only Ras^{V12}. This finding opens a possibility that increased extrusion could be an effect of lower fitness of doubly transfected cells, further amplified by partial inhibition of an important cellular chaperone.

Since Hsp90 was identified as a protein forming an altered molecular complex or differentially modified in mixed cultures of Ras^{V12} and MDCK cells, one of the aims of my project was clarifying what the change was. The first attempt to immunoprecipitate interactors of Hsp90 from single cell type and mixed cultures of normal and transformed cells, failed. Neither of three commercially available antibodies, some of which were previously used for immunoprecipitation of this protein in mammalian cells, efficiently bound the endogenous form of this chaperone in our system. The reason for our failure could have been a large size of the Hsp90 complex, and multiple binding partners possibly preventing the antibodies from accessing particular epitopes within this molecule. In a second attempt, a stable cell line of Ras^{V12} cells expressing wild type form of Hsp90β with an HA tag was established. These cells were subsequently mixed with normal cells and an efficient anti-HA antibody was used to immunoprecipitate their Hsp90 complexes. Ras^{V12} cells stably expressing Hsp90β mixed with Ras^{V12} cells were used as a control. Unfortunately, despite identification of a few proteins that were immunoprecipitated to a greater extend with Hsp90β-HA from Ras^{V12} cells in mixed cultures with normal cells, neither result was validated using specific antibodies.

The combined results from the study with the dominant negative Hsp90 and the lack of success in immunoprecipitation of different interactors of Hsp90

in mixed cultures point towards a more general role of this chaperone in maintaining fitness of tumour cells in their battle against normal epithelium. In this scenario, Hsp90 could be overexpressed as an element of a non-specific stress response in about-to-be-extruded Ras^{V12} cells, possibly playing a similar protective part to another chaperone, Sparc, known from cell competition in *Drosophila*, but also found upregulated in some cancer cells (section 1.3.5). Although attractive, this theory does not account for the results of the 2D gel screen and further studies are required to elucidate what changes occur in Hsp90β from Ras^{V12} cells grown in the presence of normal cells.

In the view of Hsp90 as a target for cancer treatment, it is important to address the question of the fate of Ras^{V12} cells after extrusion upon exposure to the inhibitors of this chaperone. Although Ras^{V12} cells treated with celastrol died in both mixed and single cell type cultures on glass (data not shown), neither of the two compounds we used for Hsp90 inhibition resulted in apoptosis or even cytostasis of Ras^{V12} cells on collagen type I matrix up to 48 hours from inducing oncogene expression. These findings highlight the importance of further studies on the effect of Hsp90 inhibition in living organisms. It is possible that higher concentrations of celastrol should be used on collagen or *in vivo* to kill cancer cells; however, the anti-tumour effect of Hsp90 could well be more complex than our current understanding of this problem. Perhaps inhibition of Hsp90 leaves cancer cells more prone not only to attacks of the immune system (Annamalai et al., 2009), but also to recognition by the epithelium itself. Whether extrusion is a part of this epithelial immune response and if it, at least partially, underlies the sensitivity of tumours to Hsp90 inhibition *in vivo*, remains to be elucidated.

CHAPTER 4:

SCREEN FOR TYROSINE-PHOSPHORYLATED PROTEINS

CHAPTER 4: SCREEN FOR TYROSINE-PHOSPHORYLATED PROTEINS

4.1 INTRODUCTION

During my PhD I performed a number of biochemical screens in order to identify molecules selectively regulated by interactions between normal and transformed cells. Many signalling pathways controlling cellular behaviour (e.g. changes of cell shape, migration, response to growth factors, etc.) are activated *via* alterations in phosphorylation status of participating proteins. Therefore I decided to focus on identification of differences in the level of phosphoryalation of isolated proteins. In a first attempt, I concentrated on tyrosine phosphorylation, as proteins carrying this modification can specifically and easily be isolated and analysed.

4.2 RESULTS

Firstly, MDCK and Ras^{V12} cells were plated separately or in a coculture with a mixing ratio of 1 to 1 (Figure 17). After an incubation of 6 to 8 hours allowing the cells to attach and form a monolayer, tetracycline (2 µg ml^{-1}) was added to the medium. Following an overnight incubation, cells were lysed and phosphorylated proteins were immunoprecipitated using a mixture of two different antibodies against phosphorylated tyrosine residues conjugated to either agarose or sepharose beads. Immunoprecipitated fractions were subsequently separated by SDS-polyacrylamide gel electrophoresis and bands were visualized by staining with SYPRO Ruby dye.

Figure 17. Schematic representation of an immunoprecipitation experiment of tyrosine-phosphorylated proteins. Phosphorylated proteins were isolated using a cocktail of anti-phospho-tyrosine antibodies from lysates of homotypic cultures of Ras^{V12} and MDCK cells as well as both of these cell types mixed in a 1 to 1 ratio. Immunoprecipitated fractions were then separated using SDS-polyacrylamide gels followed by protein staining and analysis.

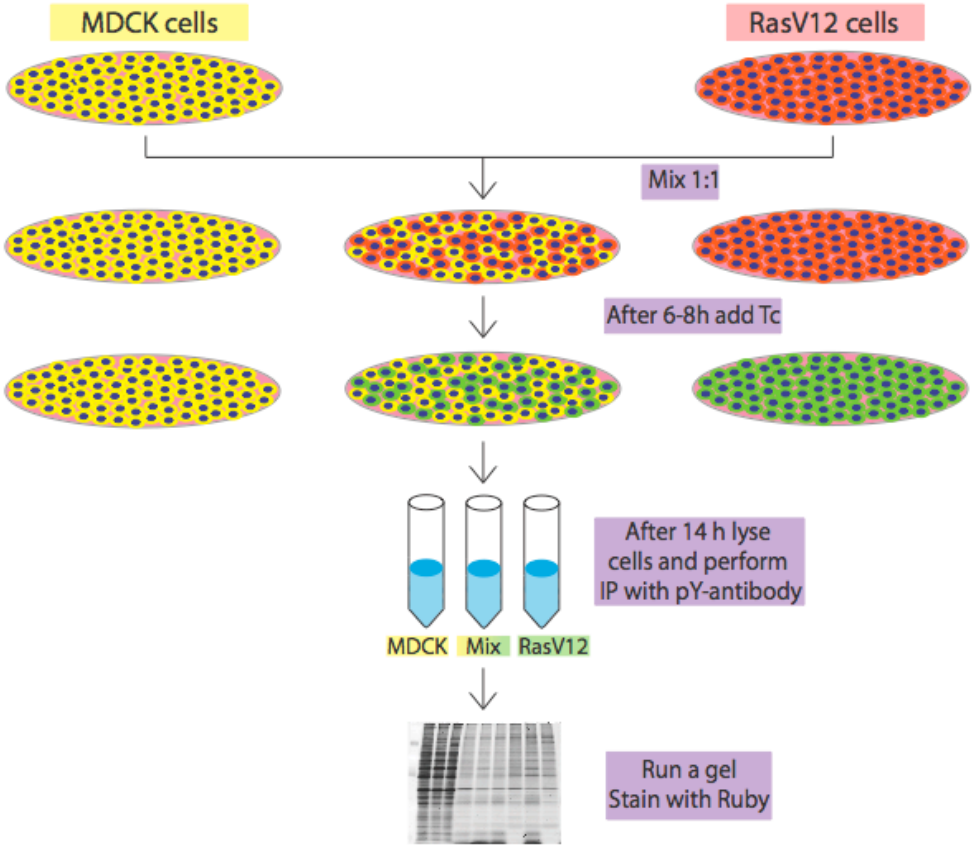

Banding patterns from several independent experiments were examined. Bands that were visibly enhanced in immunoprecipitated fractions from mixed cultures comparing to fractions from MDCK and Ras^{V12} cells alone, were chosen for further analysis. Bands of two proteins that were found to be reproducibly enriched in at least three independent experiments were cut out from the gels and identified by mass spectrometry (Figure 18).

Figure 18. Immunoprecipitation of tyrosine-phosphorylated proteins using anti-phospho-tyrosine antibodies from single cell type cultures of Ras^{V12} and MDCK cells and both cell types mixed in a 1 to 1 ratio. (A, B, C) Comparison of immunoprecipitated fractions from normal MDCK cells alone (MM), Ras^{V12} cells alone (RR) and a mixed in a 1 to 1 ratio population (RM). Fractions were separated on SDS-polyacrylamide gels and stained with SYPRO Ruby dye. Data from three independent experiments are shown (A, B, C). In red – proteins enriched in mixed population and isolated for mass spectrometry anaysis. (a, b, c) Enlargement of boxed areas in (A, B, C).

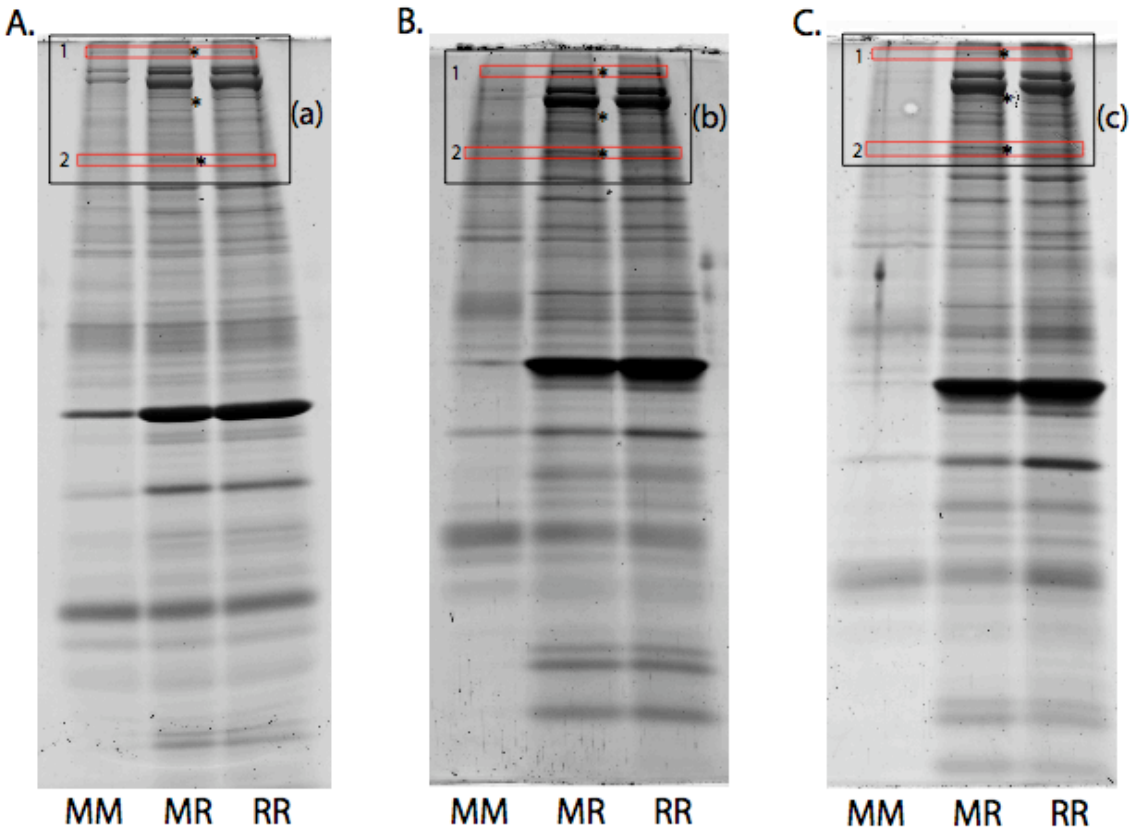

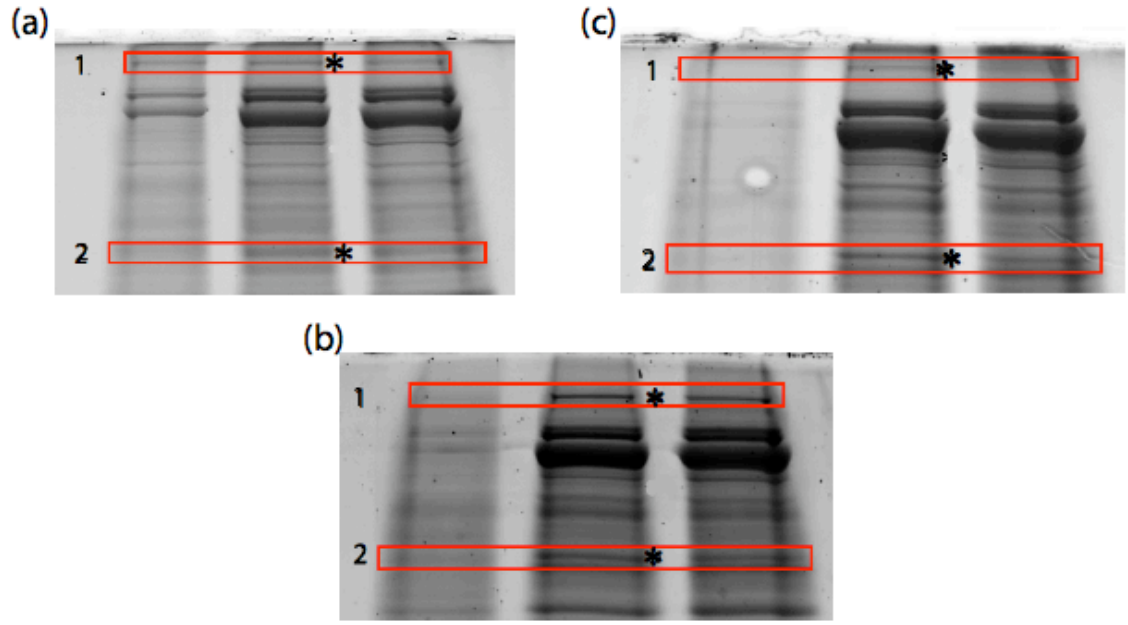

The higher molecular weight band (considerably higher than 220 kDa) was identified as plectin (actual size: 500 kDa), whereas the smaller one (± 130 kDa), as myosin IE (actual size: 127 kDa).

In order to validate the results of the screen we have purchased several commercially available antibodies as well as two custom antibodies against plectin, neither of which recognised this protein in lysates of MDCK cells by immunoblotting. Eventually, we confirmed the result of our screen using an anti-plectin antibody from Santa Cruz Biotechnology (Figure 19). Although the last antibody recognised canine plectin in immunoblotting, there was still quite a lot of non-specific background staining present. This antibody was also suitable for immunofluorescence after methanol fixation; however, initially promising results suggesting that plectin localized in a perinuclear region in Ras^{V12} cells just before their extrusion were unfortunately difficult to reproduce.

Figure 19. Plectin is enriched in fraction immunoprecipitated on anti-phospho-tyrosine beads from mixed cultures of normal and transformed cells. Immunoprecipitated fractions from experiment (B) in figure 18 were separated on SDS-polyacrylamide gels and analysed by immunoblotting using anti-plectin antibody.

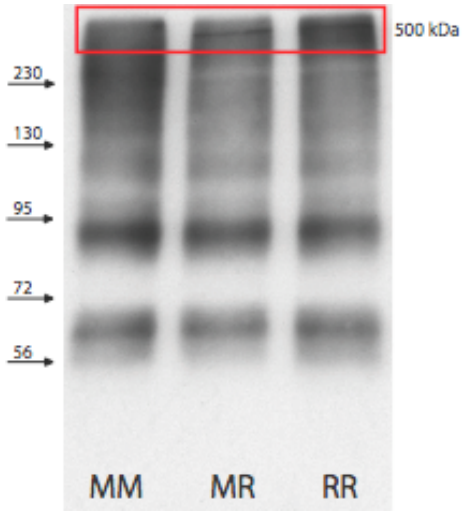

The other molecule identified in the screen, myosin IE, had not been extensively studied before, hence not much was known about its function and very few antibodies against this protein were commercially available. The antibody we bought was unfortunately not specific in immunoblotting.

4.4 DISCUSSION

As a result of the screen two proteins were identified, both preferentially phosphorylated (or interacting with preferentially phosphorylated proteins) upon interaction of normal and transformed cells. One of them, plectin, is a widely expressed, large protein scaffold mediating interactions of major cytoskeletal components: microfilaments, microtubules and intermediate filaments (reviewed in (Allen and Shah, 1999)). Particularly important for organisation of intermediate filaments, pectin anchors them to junctional complexes, the nuclear envelope and cytoplasmic organelles (reviewed in (Wiche and Winter, 2011)). Lately plectin was implicated in proliferation and migration of cancer cells (McInroy and Maatta, 2011); consequently, high levels of this protein were found to correlate with poor prognosis for patients with head and neck squamous carcinoma (Katada et al., 2012).

Interestingly, plectin was found enriched in the phosphorylated fraction in a corresponding screen performed in the Src system, as well as later on in the Scribble system (unpublished data from the Fujita laboratory), pointing towards a more universal role of this protein in interactions of normal and transformed cells. Although plectin was a potentially interesting target to study, due to problems with validation and immunostaining, we decided not to continue research on this protein during my PhD.

The other proteins identified in the screen, myosin IE, is a single-headed fast motor protein, participating in the phagocytic uptake of solid particles and cells in *Dictyostelium discoideum* (Durrwang et al., 2006). Since nearly all studies on myosin IE up to date were performed in this organism, we lacked resources to validate the result of the screen or to examine the role of this protein in extrusion.

CHAPTER 5:

SILAC SCREEN

CHAPTER 5: SILAC SCREEN

5.1 INTRODUCTION

In all proteomic screens described so far, aiming to identify changes in Ras^{V12} and normal MDCK cells upon their interaction, we were unable to distinguish between proteins isolated from these two cell types in lysates or immunoprecipitated fractions of the mixed cultures. Moreover, an important issue was the inability to quantitatively assess the identified changes. Additionally, in visual comparisons of banding patterns in SYPRO Ruby stained gels, proteins modified or upregulated in one cell type, while downregulated in the other, could have been easily missed.

In order to avoid the problems listed above, we established a collaboration with Dr Claus Jørgensen's laboratory at the Institute of Cancer Research to use a phosphoproteomic approach developed by Dr Jørgensen (Jorgensen et al., 2009). This strategy was based on a cell type-specific labelling technique with stable isotopomeric versions of amino acids (SILAC), combined with mass spectrometric identification and relative quantification of phosphorylated peptides. Once again we chose to analyse signalling pathways employing phosphorylation to transmit information and evoke cellular responses. This time, however, we decided to focus on changes in Ras^{V12} cells that occur only upon their interaction with normal cells. Moreover, we expanded our search of modifications to three most common types of naturally occurring eukaryotic phosphorylations: serine, threonine and tyrosine phosphorylation, bearing in mind that the latter, although extensively studied, is quite rare compared to the others (from: www.uniprot.org).

5.2 SETUP OF THE SCREEN

In order to differentially label proteins with stable isotopomeric arginine and lysine, Ras^{V12} and MDCK cells were grown for five generations in the SILAC medium. Three different labels were used: 'heavy' and 'medium' for Ras^{V12} cells, and 'light' for normal MDCK cells (details in section 2.4.1). A gradual decline in growth and proliferation rates of both cell types was observed along with the incorporation of the label, as a consequence of prolonged incubation in media supplemented with dialysed FCS. Thus, conditions of labelling required optimisation, as cells could not be plated too sparsely, particularly at later stages of the labelling process. Incorporation of isotopomeric amino acids into cellular proteins was confirmed by mass spectrometry and reached 98% for each type of label after five generations of labelling.

Taking into account that the planned experiment required incubation of differentially labelled MDCK and Ras^{V12} cells in mixed cultures, which can eventually lead to an exchange of isotopomeric amino acids, we were compelled to shorten the standard seeding protocol. Preliminary tests revealed that MDCK cells plated in highly confluent conditions formed a monolayer nearly instantly after attaching to the dish. Moreover, when *GFP-Ras^{V12}* expression was induced only 2 hours after plating the cells, 8 hours later Ras^{V12} cells surrounded by normal cells became taller than their neighbours and began to accumulate actin on the junctions between each other. Importantly, in line with our previous observations, Hsp90β was upregulated in these cells and localized to their apical domain (Figure 20). Eventually Ras^{V12} cells underwent extrusion from normal monolayers indicating that this experimental setup could be used to study extrusion.

Figure 20. Hsp90β is increased in Ras^{V12} cells surrounded by normal cells, but not in Ras^{V12} cells alone 8 hours from addition of tetracycline and 10 hours from plating. Confocal images of xz sections of Ras^{V12} cells surrounded by normal cells and Ras^{V12} cells alone on collagen. Cells were plated in confluent conditions (2 x 10^6 cells / well in a 6-well plate), left for 2 hours to attach, fixed after 8 hours of incubation with tetracycline (2 μg ml^{-1}) and stained with anti-Hsp90β antibody (red) and phalloidin (purple).

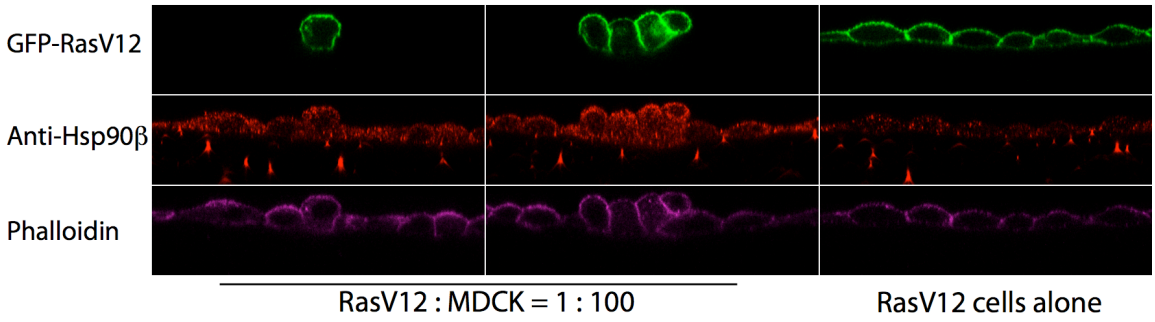

For the main experiment, fully labelled cells were plated confluently in 15-cm plates in two conditions: 'heavy'-labelled Ras^{V12} cells mixed with 'light'-labelled MDCK cells (in four plates) and 'medium'-labelled Ras^{V12} cells alone (in two plates) (Figure 21). After seeding, all types of cultures were incubated in 'light' medium to minimise the effects of the exchange of isotopomeric amino acids on subsequent quantification of 'heavy'- and 'medium'-labelled peptides (in the experiment we focused on changes in Ras^{V12} cells). Two hours after plating, tetracycline was added to the culture medium. At this point, highly confluent cells appeared to form monolayers and reestablished cell contacts. Following a further 6 hour-incubation, lysis buffer was added to the plates, cells were collected and sonicated. Only the soluble fraction obtained after sonication underwent further biochemical analyses. After trypsinisation of isolated proteins, obtained peptides were purified. Precipitation of phosphorylated peptides was achieved using an immobilized metal ion affinity chromatography (IMAC) approach. Eventually, fractionation with hydrophilic interaction liquid chromatography (HILIC) was performed, and phosphorylated peptides were identified by mass spectrometry and quantified.

Figure 21. Schematic representation of the SILAC screen for phosphorylated peptides. Proteins in Ras^{V12} and MDCK cells were labelled for 5 generations and plated at confluence in two conditions: Ras^{V12} cells alone or in a coculture with MDCK cells. After 2 hours, tetracycline (2 µg ml^{-1}) was added. Following a subsequent incubation for further 6 hours, cells were lysed, lysates were combined, and indicated biochemical steps were performed leading to isolation and identification of phosphorylated peptides (for details check section 2.4).

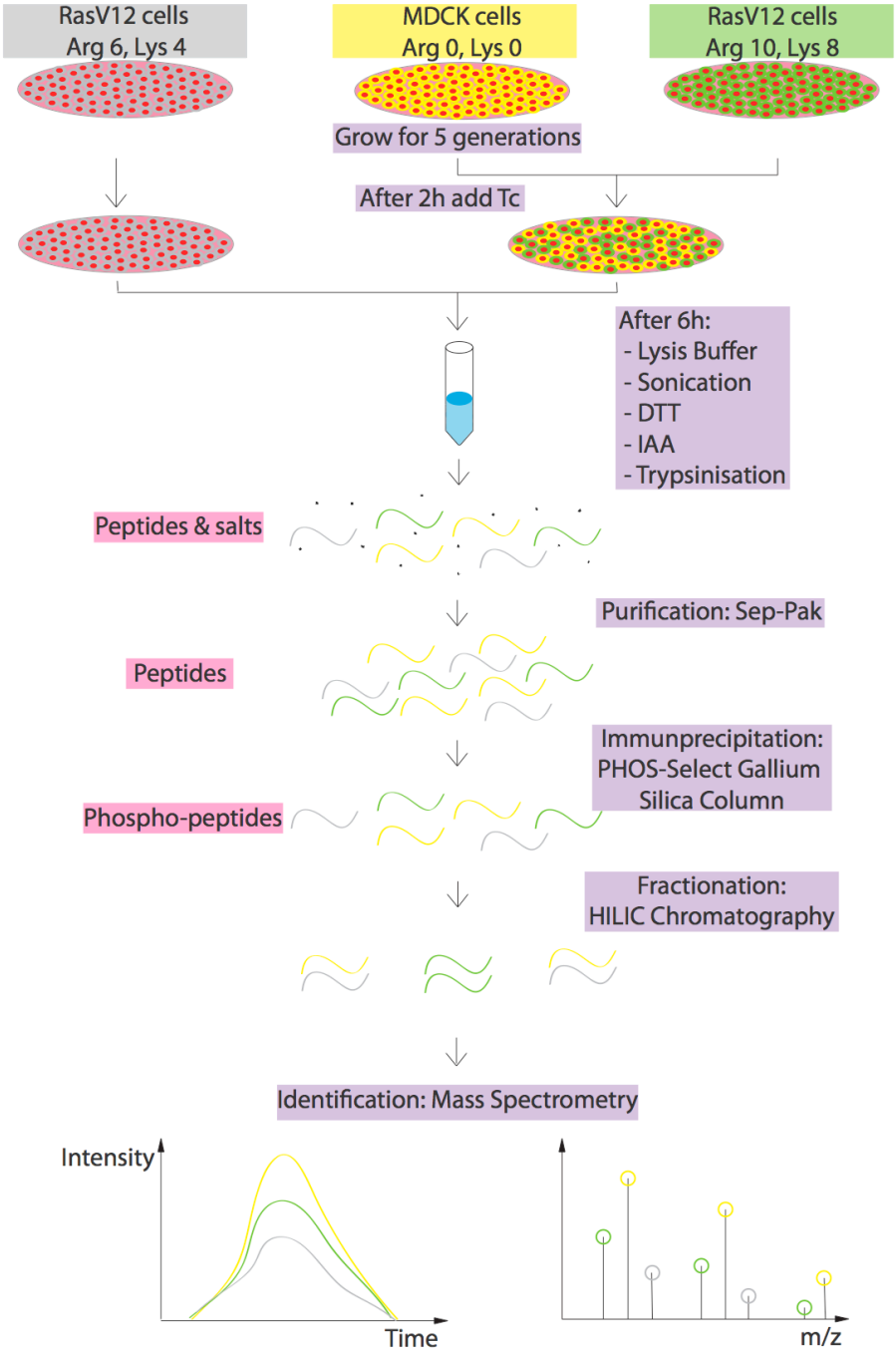

5.3 RESULTS

Three successful experiments were performed: the first (referred to as 'Exp 1' in Tables 5, 6, 7; coloured in yellow) was done without the HILIC fractionation step; the second (referred to as 'Exp 2' in Table 5, 6, 7; coloured in orange) included HILIC and was performed on the same biological samples as the first experiment; the third (referred to as ' Exp3' in Tables 5, 6, 7; coloured in pink) was performed on newly obtained biological samples according to the same protocol as Exp 2. For each peptide, a ratio of labels 'heavy' to 'medium' was calculated (hereafter called H/M ratio). In biological terms this ratio reflected a change in phosphorylation levels occurring in Ras^{V12} cells upon their interaction with normal cells ('heavy' label) compared to Ras^{V12} cells grown alone ('medium' label). Peptides with the H/M ratio higher than 2 or lower than 0.5 in either attempt were compared among different experiments. Peptides for which the identified ratio was reproduced biologically (in Exp 1 or Exp 2, and in Exp 3) were chosen for further analysis. Importantly, in each attempt the H/M ratio for most of the peptides identified was close to 1 (Table 5).

Table 5. Combined statistical analysis of three successful SILAC experiments. Presented numbers apply to already filtered results (for details check section 2.4.8).

	Exp 1	Exp 2	Exp 3	Combined results
All identified peptides	4,432	12,913	11,570	28,915
Different peptides	1,285	3,087	2,504	4,285
Peptides with H/M score	512	892	677	
Peptides with H/M x > 2	**20**	**45**	**12**	**18 (17 proteins)**
Peptides with H/M 2 > x > 0.5	481	821	631	
Peptides with H/M x < 0.5	**11**	**26**	**34**	**16 (15 proteins)**
All identified proteins	460	882	784	1084

Of note, in Exp 3 the identified H/M ratios were shifted towards lower values (over twice as many downregulated than upregulated phosphopeptides were identified), suggesting that more 'medium'- than 'heavy'-labelled Ras^{V12} cells were used in this experiment. Therefore, H/M values for upregulated peptides in this experiment (Table 6) are generally lower; this was taken into account in the analysis of these results.

Due to stringent parameters applied in the search concerning the quality of the analysed spectra, H/M ratios were not quantified for all identified peptides by the Proteome Discover v1.3 software (details of the search in section 2.4.8). For some of these peptides, it was possible to analyse their spectra manually and assess H/M ratios from the raw data (described as not quantified, N/Q, in Tables 6, 7). A few peptides were not repeatedly identified between experiments (described as N/I in Tables 6, 7).

Altogether, among 4,285 different phosphorylated peptides identified in all three experiments, we found 18 of them reproducibly upregulated (Table 6), and 16 of them reproducibly downregulated (Table 7) in Ras^{V12} cells upon their interaction with normal cells. A comparison against Ensembl dog database as well as further confirmation using Basic Local Alignment Search Tool (BLAST from NCBI website) revealed that these peptides were obtained from triptic digestion of 17 and 15 different proteins, respectively. In total, 31 proteins of very diverse functions, potentially important for interactions between normal and transformed cells, were identified in this screen (Tables 8, 9 list the most prominent known cellular functions performed by these proteins according to combined data from Gene NCBI, UniProt and PhosphoSitePlus databases; Figure 22 is a graphical representation of these functional data).

Table 6. Modified peptides found reproducibly upregulated in Ras^{V12} cells from mixed cultures in the SILAC screen. Exp – experiment. Exp 1 and 2 were performed on the same biological samples, but with an independent repeat of peptide isolation and MS identification. Exp 3 was a full biological repeat. H/M ratio – a ratio of a number of 'heavy'-labelled peptides to a number of 'medium'-labelled peptides identified. N/I – peptide was not identified in this experiment. N/Q – peptide was identified, but H/M ratio was not quantified, in brackets values of estimated H/M ratio from the raw data. Abbreviations of protein names are in agreement with the Gene NCBI database and are explained in table 8.

Protein	Peptide Sequence	Modification within the peptide (protein)	Analogous modifi-cation in human	Found in Exp	H/M ratio	Other Exp 1	H/M Ratio	Other Exp 2	H/M Ratio
SRP14	KG**s**VEGFEP SDNK	S3 (S45)	T45	1	12.6	2	N/Q (±6)	3	1.6
SF3B1	RWDQTADQ**t** PGA**t**PK	T9 (T208), T13 (T212)	T207, T211	3	3.5	1	N/I	2	N/Q (±4)
CDK1	IGEG**ty**GVV YK	T5 (T14), Y6 (Y15)	T14, Y15	2	4.2	1	N/I	3	1.7
PLEC	GYY**s**PYSVS GSG**s**AAGSR	S4 (S4206), S13 (S4215)	S4613, S4622	1	3.4	2	2.1	3	1.7
ZO1	**s**VA**s**SQPPK PTK	S1 (S166), S4 (S169)	S175; S178	2	3.2	1	N/I	3	1.5
VASP	KV**s**KQEEAS GGPPVPK	S3 (S242)	S239	1	3.2	2	3.3	3	1.3
CAMK2D	KPDGVKES**t** ESSNT**t**IED EDVK	T9 (T331), T15 (T337)	S395, T401	2	3.1	1	N/I	3	1.7
FUNDC2	KS**s**QIPTEV K	S3 (S181)	S151	1	3.0	2	3.1	3	N/Q (±2)
Hnrnpc	NDK**s**EEEQS SSSLK	S4 (S221)	S233	2	2.8	1	N/I	3	2.5
STRN	FLESAAADF **s**DEDEDDDI DGREK	S10 (S164)	S245	3	2.0	1	N/I	2	1.7
MCM2	**s**DPLTS**s**PG R	S1 (S20), S7 (S26)	(-), S27	2	2.6	1	N/I	3	1.5
VIM	ETNLD**s**LPL VDTHSKR	S6 (S430)	S430	2	2.5	1	N/I	3	2.5
BAIAP2L1	SI**s**TVDLTE K	S3 (S382)	S422	1	2.4	2	2.4	3	N/Q (±2)
NPM1	**s**APG**s**GSKV PQKK	S1 (S143), S5 (S147)	S143	2	2.1	1	N/I	3	2.0
PLEC	GYY**s**PYSV**s** GSGSAAGSR	S4 (S4206), S9 (S4211)	S4613, S4616	2	2.1	1	N/I	3	1.5
SERBP1	SK**s**EEAHAE DSVMDHHFR	S3 (S308)	S328	2	2.1	1	1.7	3	N/Q (±2.3)
LMO7	RK**s**YTSDLQ K	S3 (S260)	S751	2	2.1	1	N/I	3	2.0
EF-2	AGETRF**t**DT R	T7 (T57)	S57	2	2.1	1	N/I	3	1.4

Table 7. Modified peptides found reproducibly downregulated in Ras^{V12} cells from mixed cultures in the SILAC screen. Exp – experiment. Exp 1 and 2 were performed on the same biological samples, but with an independent repeat of peptide isolation and MS identification. Exp 3 is a full biological repeat. H/M ratio – a ratio of a number of 'heavy' labelled peptides to a number of 'medium' labelled peptides identified. N/I – peptide was not identified in this experiment. N/Q – peptide was identified, but H/M ratio was not quantified, in brackets values of estimated H/M ratio from the raw data. Abbreviations of protein names are in agreement with the Gene NCBI database and are explained in table 9.

Protein	Peptide Sequence	Modification within the peptide (protein)	Analogous modification in human	Found in Exp	H/M ratio	Other Exp 1	H/M Ratio	Other Exp 2	H/M Ratio
TNS1	RM**s**VGDR	S3 (S1370)	S1393	2	0.14	1	N/Q (±0.5)	3	0.23
JUNB	DA**t**PPV**s**PI NMEDQER	T3 (T247), S7 (S251)	S255, S259	2	0.18	1	N/Q	3	N/Q (±0.3)
COL17A1	AH**s**PASTLP N**s**PGSTFER	S3 (S85), S11 (S93)	S85, S93	1	0.24	2	0.12	3	0.22
MCT1	**s**KE**s**LQEAE K	S1 (S200), S4 (S203)	S210, S213	2	0.24	1	N/I	3	0.13
PDXDC1	VQGTGV**t**PP Q**t**PSGTR	T7 (T721), T11 (T725)	T687, T691	3	0.19	1	N/I	2	N/Q (±0.3)
ZC3HC1	SQDA**t**CSPG SEQAER**s**PG PIVSR	T5 (T336), S16 (S347)	T333, S344	2	0.29	1	N/I	3	0.36
MRCKβ	HSTPSNSSN PSGPP**s**PN**s** PHR	S15 (S1693), S18 (S1696)	S1690, S1693	1	0.33	2	N/Q (±0.5)	3	N/Q (±0.3)
SQSTM1	LTPV**s**PGG**s** STEDR	S5 (S245), S9 (S249)	S272, S276	2	0.34	1	0.79	3	0.31
SPEN	HS**s**FHEEDD PVG**s**PR	S3 (S1209), S13 (S1219)	S1268, S1278	2	0.37	1	N/I	3	0.24
EML4	A**s**P**s**PQPSS QPLQIHR	S2 (S144), S4 (S146)	S144, S146	3	0.30	1	N/I	2	0.60
TXLNA	EQGCEGPGA QSPG**s**PR	S14 (S530)	S515	2	0.41	1	0.69	3	0.32
FOSL2	**s**PPASGLQP LR	S1 (S115)	S200	1	0.42	2	N/Q (±0.5)	3	N/Q (±0.4)
SRP72	TVSSPPTSP RPG**s**AA**t**AS ASTSNIIPP R	S13 (S630), T16 (T633)	S630, S633	2	0.44	1	N/I	3	0.29
Foxk1	SAPA**s**PTHP GLM**s**PR	S5 (S234), S13 (S242)	S420, S428	3	0.35	1	N/I	2	0.50
SQSTM1	LTPV**s**PGGS STEDR	S5 (S245)	S272	2	0.48	1	0.73	3	0.43
LARP1	SLPTTVPE**s** PNYR	S9 (S657)	S774	2	0.49	1	N/I	3	0.27

Table 8. Well-established functions of proteins found phosphorylated in Ras^{V12} cells upon interaction with normal cells in the SILAC screen. Full names of proteins as well as their functional role in cellular processes based on Gene (NCBI), UniProt and PhosphoSitePlus databases.

Protein	FULL NAME	MAIN KNOWN FUNCTION
SRP14	**Signal Recognition Particle 14kDa**	Targeting secretory proteins to the membrane of rough endoplasmic reticulum
SF3B1	**Splicing Factor 3b subunit 1**	Splicing; SF3B1 is a part of the U2 small nuclear ribonucleoproteins complex, known also as complex A
CDK1	**Cyclin-Dependent Kinase 1**	Enabling cell cycle progression: transitions between phases G1 to S and G2 to M; CDK1 is a catalytic subunit of M-phase promoting factor
PLEC	**Plectin**	Interlinking intermediate filaments with microtubules and microfilaments, anchoring intermediate filaments to desmosomes or hemidesmosomes, scaffolding proteins involved in cellular signalling
ZO1	**Zonula Occludens 1**	Regulating tight junction assembly and determining some of their properties
VASP	**Vasodilator-Stimulated Phosphoprotein**	Promoting formation of filamentous actin, localizing to focal adhesions and playing a role in cell adhesion and motility
CAMK2D	**Calcium/Calmodulin -Dependent Protein Kinase II Delta**	Regulating plasticity at glutamatergic synapses (e.g. exocytosis, calcium-dependent oscillations, and ion-channel activation)
FUNDC2	**FUN14 Domain Containing 2**	Unknown function
Hnrnpc	**Heterogeneous Nuclear Ribonucleoprotein C (C1/C2)**	Binding pre-mRNA and nucleating the assembly of 40S hnRNP particles, sorting RNA into: mRNA and small nuclear RNA (U snRNA) prior to their transportation
STRN	**Striatin, Calmodulin Binding Protein**	Scaffolding of mediators of vesicular trafficking in neurons
MCM2	**Minichromosome Maintenance Complex Component 2**	Initiating eukaryotic genome replication, preventing DNA from undergoing more than a single round of replication per cell cycle
VIM	**Vimentin**	Maintaining cell shape, integrity of the cytoplasm, and stabilizing cytoskeletal interactions, organising a number of critical proteins involved in attachment, migration, and cell signaling
BAIAP2L1	**BAI1-Associated Protein 2-like 1**	Clustering actin bundles, playing a role in signal transduction pathways that link deformation of the plasma membrane and remodelling of the actin cytoskeleton (through interactions with RAC1)
NPM1	**Nucleophosmin 1**	Controlling centrosome duplication, DNA repair and ribosome biogenesis; NPM1 is a nucleolar chaperone
PLEC	**Plectin**	Details above
SERBP1	**SERPINE1 mRNA Binding Protein 1**	Regulating mRNA stability
LMO7	**LIM Domain 7**	Regulating transcription of many genes, playing a role in migration, possibly transmitting mechanical signals from focal adhesions
EF-2	**Elongation Factor 2**	Enabling protein synthesis, promoting translocation of the nascent protein chain from the A-site to the P-site on the ribosome

Table 9. Well established functions of proteins found dephosphorylated in Ras^{V12} cells upon interaction with normal cells in the SILAC screen. Full names of proteins as well as their functional role in cellular processes based on Gene (NCBI), UniProt and PhosphoSitePlus databases.

Protein	FULL NAME	MAIN KNOWN FUNCTION
TNS1	**Tensin 1**	Crosslinking actin filaments, localizing to focal adhesions, playing a role in cell migration, cartilage development and in linking signal transduction pathways to the cytoskeleton
JUNB	**Jun B Proto-Oncogene**	Regulating gene activity following the primary growth factor response
COL17A1	**Collagen type XVII alpha 1**	Playing a role in the integrity of hemidesmosome and the attachment of basal keratinocytes to the underlying basement membrane
MCT1	**Monocarboxylate Transporter 1 Fragment**	Catalyzing transport across the plasma membrane of many monocarboxylates such as lactate, pyruvate
PDXDC1	**Pyridoxal-Dependent Decarboxylase Domain Containing 1**	Unknown function
ZC3HC1	**Zinc Finger C3HC-Type Containing 1**	Controlling mitotic entry by mediating ubiquitination and subsequent degradation of cyclin B1; ZC3HC1 is a part of SCF(NIPA) complex
MRCKβ	**CDC42 Binding Protein Kinase Beta (DMPK-like)**	Mediating the effect of CDC42 in cytoskeletal reorganization, contributing to actomyosin contractility required for cell invasion through MLC2 phosphorylation
SQSTM1	**Sequestosome 1**	Shuttling proteins to the proteasome after binding to ubiquitin, playing a role in cell differentiation, apoptosis, immune response and regulation of potassium channels
SPEN	**Spen Homolog Transcriptional Regulator (Drosophila)**	Acting as a hormone inducible transcriptional activator or repressor, regulating Notch pathway
EML4	**Echinoderm Microtubule Associated Protein Like 4**	Regulating microtubule dynamics and mitosis
TXLNA	**Taxilin Alpha**	Playing a role in intracellular vesicle trafficking
FOSL2	**Fos-Related Antigen 2 Fragment**	Promoting gene expression; the only known downstream target up to now is gene encoding leptin
SRP72	**Signal Recognition Particle 72 kDa Protein**	Targeting secretory proteins to the membrane of rough endoplasmic reticulum
Foxk1	**Forkhead Box K1**	Playing a role in the regulation of myogeneic progenitor cells and skeletal muscle regeneration
SQSTM1	**Sequestosome 1**	Details above
LARP1	**La Ribonucleoprotein Domain Family Member 1**	Regulating mitosis, playing a role in cell survival and migration

Figure 22. Known key functions and most common cellular localization of proteins identified in the SILAC screen. Pathways and processes that particular proteins regulate are specified in colour-coded frames within the figure. Phosphorylation status of regulated sites is indicated with a red star, if upregulated, and a blue star, if downregulated. PM – plasma membrane, NE – nuclear envelope. Abbreviations of proteins are in agreement with the Gene NCBI database and are explained in tables 8 and 9.

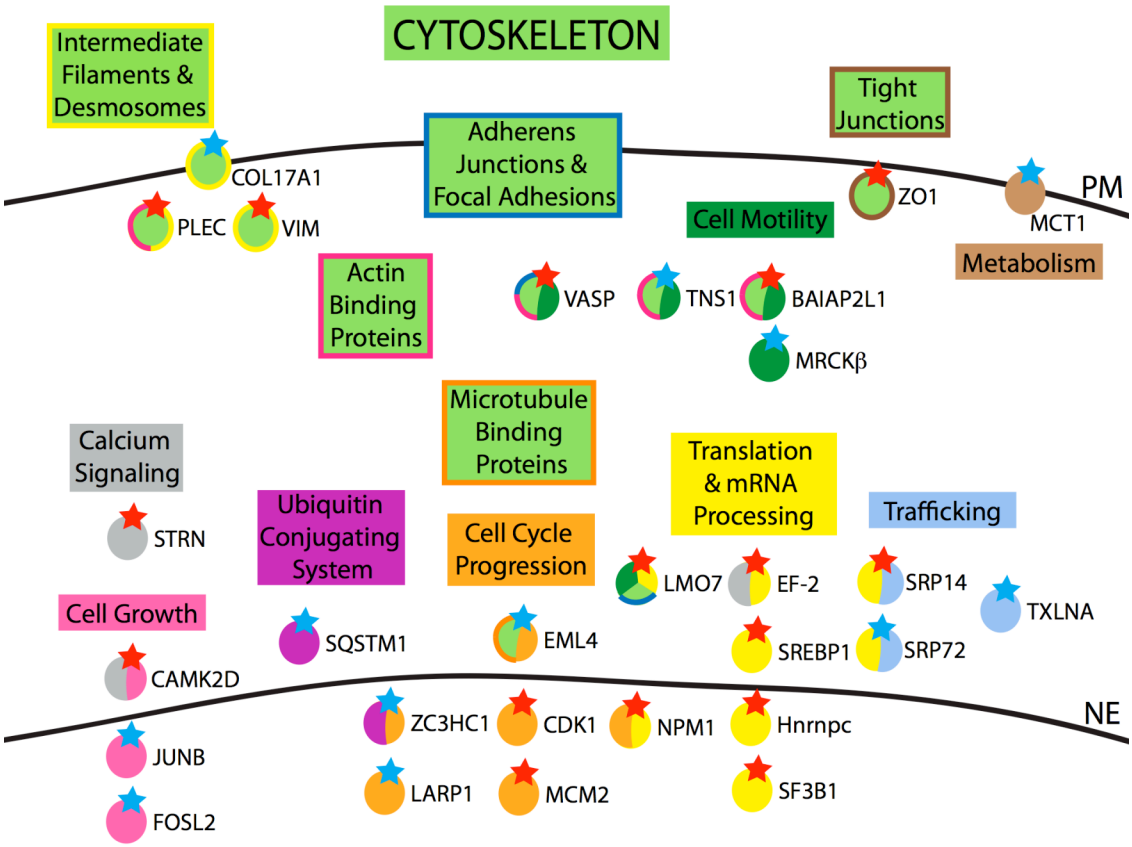

Identified peptides were subsequently aligned with homologous human proteins and equivalent phosphorylation sites of interest were localized using the PhosphoSitePlus database (Table 6, 7). All but one modifications had a corresponding phosphorylation site within human proteins. Moreover, all of them had been identified before, most commonly exclusively in mass spectrometric studies (PhosphoSitePlus database). Five of the sites had been extensively studied before and have a known cellular function.

5.4 DISCUSSION

The proteins regulated in Ras^{V12} cells upon their interaction with normal cells identified in the SILAC screen belong to a number of different groups and participate in multiple cellular processes. Several modified molecules regulate cytoskeletal rearrangements (for example, VASP, plectin, vimentin), modify cell-cell interactions and cell attachment (for expample, ZO-1, COL17A1) or play a role in cell motility (for example, MRCKβ, TNS1). Other identified proteins control vesicular trafficking (for example, TXLNA, SRP14), cell growth (for example, JUNB), protein translation (for example, EF-2) or cell cycle progression (for example, CDK1, MCM2).

Among the modifications with a previously identified cellular function were phosphorylations within two cell cycle proteins, CDK1 and MCM2, cell cycle-regulated SQSTM1, actin-binding cytoskeletal VASP, and the regulator of translation EF-1.

Phosphorylation of threonine 14 and tyrosine 15 in CDK1 inhibits enzymatic activity of this kinase leading to cell cycle arrest between phases G2 and M (Krek and Nigg, 1991; Norbury et al., 1991). Inhibited CDK1 is not able to phosphorylate its etablished target protein SQSTM1 on serine 272, a site found downregulated in our screen. As a result of phosphorylation by CDK1, SQSTM1 is believed to stabilize cyclin B1 and active CDK1 ensuring correct entry and exit from mitosis (Linares et al., 2011). It is unclear, however, how lack of this phosphorylation along with inhibited CDK1 would affect proliferation of transformed cells. It is possible that this mechanism is transiently activated to prevent proliferation during extrusion, as complex morphological processes and cell migration are not normally compatible with mitosis and usually require cell cycle arrest.

Another cell cycle protein with upregulated phosphorylation on a serine site is MCM2. This phosphorylation was shown in mammalian cells to be necessary for activation of MCM2, permitting its interaction with DNA and initiation of DNA replication. Taken together with data on other proteins identified in the screen known to have a role in the cell cycle, these results suggest that upon interaction with normal cells proliferation of Ras^{V12} cells is affected. In order to verify this hypothesis, we performed BrdU labelling of Ras^{V12}

cells interacting with normal cells (different mixing ratios were used) and Ras^{V12} cells alone. Since proliferation is tightly linked to contact inhibition, which is still observed in Ras^{V12}-transformed cells, incorporation of BrdU into dividing nuclei was normalized to cell density. Unfortunately, after normalisation we could not see any differences between proliferation of Ras^{V12} cells in mixed cultures and Ras^{V12} cells alone (data not shown). We noticed however, that Ras^{V12} cells plated alone were repeatedly less confluent despite counting the cells prior to each experiment. It is possible that migratory phenotypes of Ras^{V12} cells after oncogene induction allows them to spread and, providing that they are grown alone, to balance cell density on the plates. In contrast, Ras^{V12} cells mixed with normal MDCK cells are trapped between immobile neighbours and locally experience greater contact inhibition, possibly leading to phosphorylation and inhibition of CDK1 in these conditions.

Nevertheless, dismissing the cell cycle related results of the SILAC screen could be a mistake. Inhibition of proliferation of transformed cells within a monolayer of normal cells was reported in the 1960s (Borek and Sachs, 1966; Stoker, 1964) as well as more recently (Alexander et al., 2004; Leung and Brugge, 2012). It is likely then that within an established epithelium, where divisions occur mainly to replace dying or extruded cells, Ras^{V12} cells experience inhibitory signals, which overcome their transformed phenotype. In this scenario extrusion would be a way to release this epithelial block and allow uncontrolled divisions (a similar hypothesis was suggested in (Leung and Brugge, 2012); however, no quantitative data were presented to support the existence of this block).

Apart from proteins implicated in the cell cycle, we identified modifications within many other types of proteins, including molecules regulating cytoskeletal rearrangements and cell motility. Knowing that modifications affecting cytoskeletal organisation and cellular shape are often relatively simple to follow by immunofluorescence or time-lapse imaging, we decided to choose two proteins from this functional group for validation. Our first candidate was VASP, an actin-binding member of Ena/VASP family, which drew our attention due to the known inhibitory role of the identified phosphorylated site on VASP-dependent actin polymerisation. The other protein was a serine-threonine protein kinase MRCKβ, a protein studied by other members of the Matter laboratory, for which many required reagents were already available.

In the SILAC screen, plectin was also identified as a protein with several different sites modified in Ras^{V12} cells upon their interaction with normal cells. As mentioned previously, plectin was independently found in the screen for tyrosine-phosphorylated proteins (Chapter 4). Although neither of the modifications sequenced in the SILAC approach was on a tyrosine residue, this protein appears to play a role in extrusion and should be studied in greater details with appropriate resources in the future.

CHAPTER 6:

VALIDATION OF THE SILAC SCREEN

- VASP

CHAPTER 6: VALIDATION OF THE SILAC SCREEN – VASP

6.1 INTRODUCTION

The vasodilator-stimulated phosphoprotein (VASP) was originally purified from platelets in 1989 as a molecule phosphorylated by protein kinases dependent on both cAMP and cGMP (Halbrugge and Walter, 1989). Only three years later, VASP was found to interact with actin and localize along microfilament bundles (stress fibres and junctional actin) as well as to focal adhesions (Reinhard et al., 1992). During the past 20 years of extensive studies on VASP, this protein was shown to be implicated in many processes, including regulation of platelet activation (Aszodi et al., 1999; Massberg et al., 2004), maintenance of endothelial barrier (Furman et al., 2007; Rentsendorj et al., 2008), phagocytosis (Coppolino et al., 2001), lamellipodia formation and cell motility (Bear et al., 2002; Lindsay et al., 2007), metastasis and invasion of cancer cells (Zuzga et al., 2011), and even cellular growth and proliferation (Chen et al., 2004). A common denominator for all these functions is the interaction of VASP with actin and, in particular, promoting elongation and bundling of growing microfilaments (reviewed in (Bear and Gertler, 2009; Trichet et al., 2008)). Despite controversy surrounding VASP since its discovery (reviewed in (Trichet et al., 2008)), there is general agreement in the field that through association with barbed ends of microfilaments, VASP acts as an anti-capping protein (reviewed in (Bear and Gertler, 2009)).

Apart from direct interactions with actin, VASP facilitates cytoskeletal remodelling by binding to other molecules, e.g. components of focal adhesions, vinculin and zyxin (Brindle et al., 1996; Reinhard et al., 1995). Three different domains within VASP mediate formation of all these complexes: (1) an N-terminal Ena/VASP homology 1 domain (EVH1) that binds specific poly-proline motifs in, for example, vinculin and zyxin; (2) a central proline-rich region (PRR) with affinity to proteins containing SH3 and WW domains as well as to profilin, which complexes with G-actin; (3) a C-terminal Ena/VASP homology 2 domain (EVH2) interacting with G- and F-actin and mediating VASP oligomerisation (Figure 23) (reviewed in (Bear and Gertler, 2009; Chesarone and Goode, 2009)).

There are three well characterised phosphorylation sites within human VASP that are known to regulate its activity: serine 157 (S157), serine 239 (S239) and threonine 278 (T278). *In vivo* they are targeted by three different nucleotide-dependent kinases: (1) cAMP-dependent proteins kinase A (PKA), which phosphorylates S157 and with lower affinity S239, (2) cGMP-dependent protein kinase G (PKG) with preference for S239 over S157 (Butt et al., 1994), and (3) AMP-activated protein kinase (AMPK) known to target T278 (Blume et al., 2007). Recently protein kinase C (PKC) was also implicated in phosphorylation of VASP (Chitaley et al., 2004).

Figure 23. Structure, binding partners and major regulators of VASP.

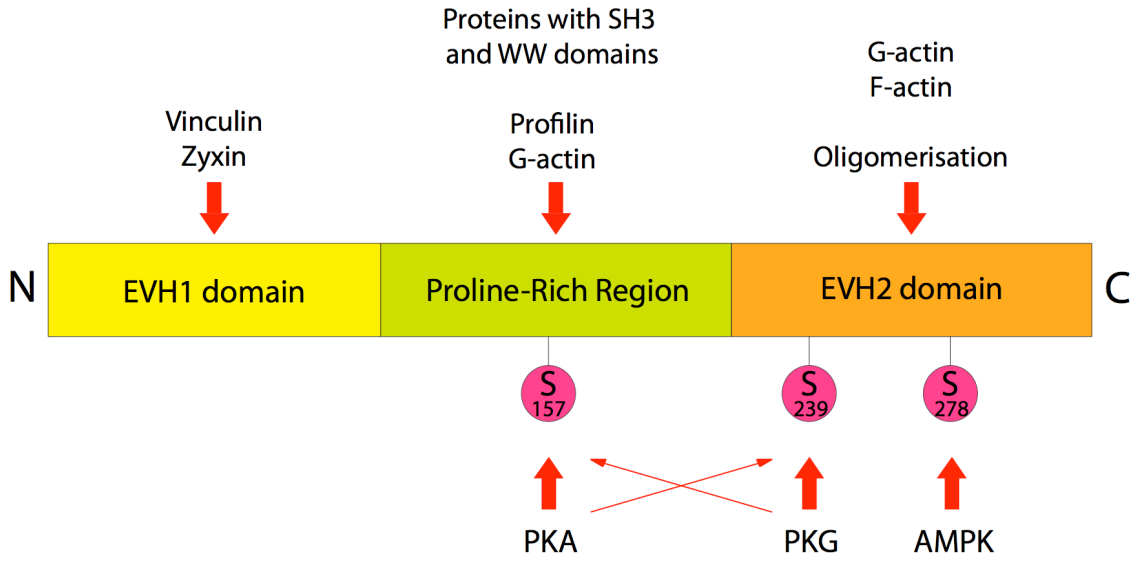

Detailed functional characterization of these three major phosphorylation sites in VASP using phosphomimetic substitutions, revealed that while modification of S157 abrogates interaction of this protein with several SH3 domain-containing partners, e.g. Abl (Lambrechts et al., 2000), and, to some extent, affects its localization (Benz et al., 2008; Benz et al., 2009), it has no effect on actin polymerisation. Conversely, phosphorylation of either S239 or T278 within the EVH2 domain results in inhibition of the anti-capping and filament-bundling activities towards actin (Benz et al., 2009), and consequently affects formation of membrane protrusions (Lindsay et al., 2007; Zuzga et al., 2011). In platelets, modification of S239 occurs downstream of nitric oxide (NO) release from the endothelium, which in turn activates PKG and ultimately leads to inhibition of

platelet activation by promoting their round phenotype (Becker et al., 2000). Phosphorylation of S239 has a similar effect on invasion of cancer cells, preventing them from forming invadopodia and again resulting in a round cellular shape (Benz et al., 2009).

In the SILAC screen, modification on S239 in VASP was found upregulated 6 hours after inducing *GFP-Ras^{V12}* expression. If the effect of this phosphorylation in our cells is similar to what was previously reported for fibroblasts, platelets or colon carcinoma cell lines, Ras^{V12} cells should round up at this point. Indeed, prior to their extrusion from normal monolayers Ras^{V12} cells become taller, and adopt a more roundish cellular shape. This observation further encouraged us to study modification of VASP on S239, which could be a necessary step in extrusion, leading to detachment and release of a transformed cell.

6.2 RESULTS

6.2.1 VASP DEPLETION ENHANCES EXTRUSION OF RAS CELLS FROM A MONOLAYER OF NORMAL EPITHELIAL CELLS

To study if VASP is important for extrusion and what role it plays, we used an siRNA-based technique to deplete this protein in Ras^{V12} cells prior to mixing them with normal cells. Since phosphorylation on the site identified in the SILAC screen inhibits VASP activity towards actin, we hoped that depletion of the whole protein would mimic this phosphorylation in our system and give us some indication of its contribution to extrusion.

Firstly, the conditions for depleting VASP in normal MDCK cells using an Interferin-based transfection system were optimised. While the protein content of VASP was reduced in MDCK cells after treatment with each of the three oligonucleotides (in fact, treatment with O3 resulted in increased toxicity indicated by the lower tubulin content), a similar effect was not observed in Ras^{V12} cells (Figure 24 A). To deplete VASP in transformed cells, we decided to use a modified protocol, in which instead of allowing the cells to attach over night before treating them with the transfection reagents, we added oligonucleotides immediately after plating. Under these conditions, more cellular membrane was supposed to be exposed to Interferin and siRNA complexes, resulting in a better uptake of the siRNA and depletion of the targeted protein. In fact, depletion of VASP in Ras^{V12} cells was so efficient that cells treated with nucleotides O2 and O3 died and detached from the plates within 2 days of transfection. Hence, in all subsequent experiments we decided to use oligonucleotide O1 only (Figure 24 B).

Downregulation of VASP in Ras^{V12} cells cocultured with normal cells was further confirmed by immunofluorescence on glass (Figure 24 C), as well as on collagen (Figure 24 D, E). Interestingly, while on glass VASP localized to cell-cell junctions and the cytoplasm (Figure 24 C), on collagen the signal was mostly cytoplasmic, and only rarely seen at the junctions (Figure 24 D, E). Even so, the differences between intensity or localization of VASP in Ras^{V12} cells cocultured with normal cells in comparison to Ras^{V12} cells alone were negligible.

Figure 24. Treatment with siRNA reagents targeting VASP mRNA results in efficient depletion of VASP proteins in MDCK as well as Ras^{V12} cells. (A, B) Total cell lysates of MDCK cells and Ras^{V12} cells transfected with siRNA reagents, cultured for 4 days from transfection and analysed by immunoblotting using anti-VASP antibody. Transfection conditions were optimized for MDCK cells (A) and Ras^{V12} cells (B) by shortening the time between plating and transfection for Ras^{V12} cells. (C, D, E) Confocal images of xy (C, D) and xz (E) sections of Ras^{V12} cells with depleted VASP surrounded by normal cells on glass (C) and on collagen (D, E). Cells were fixed after 8 hours of incubation with tetracycline (2 µg ml^{-1}) and stained with anti-VASP antibody (red in C, E and purple in D) as well as phalloidin (purple in C). Ctrl – control siRNA, O1, O2, O3 – three different oligonucleotides designed and used to deplete VASP in MDCK cells. O1 – O3 – a pool of all three oligonucleotides mixed in a ratio 1:1:1.

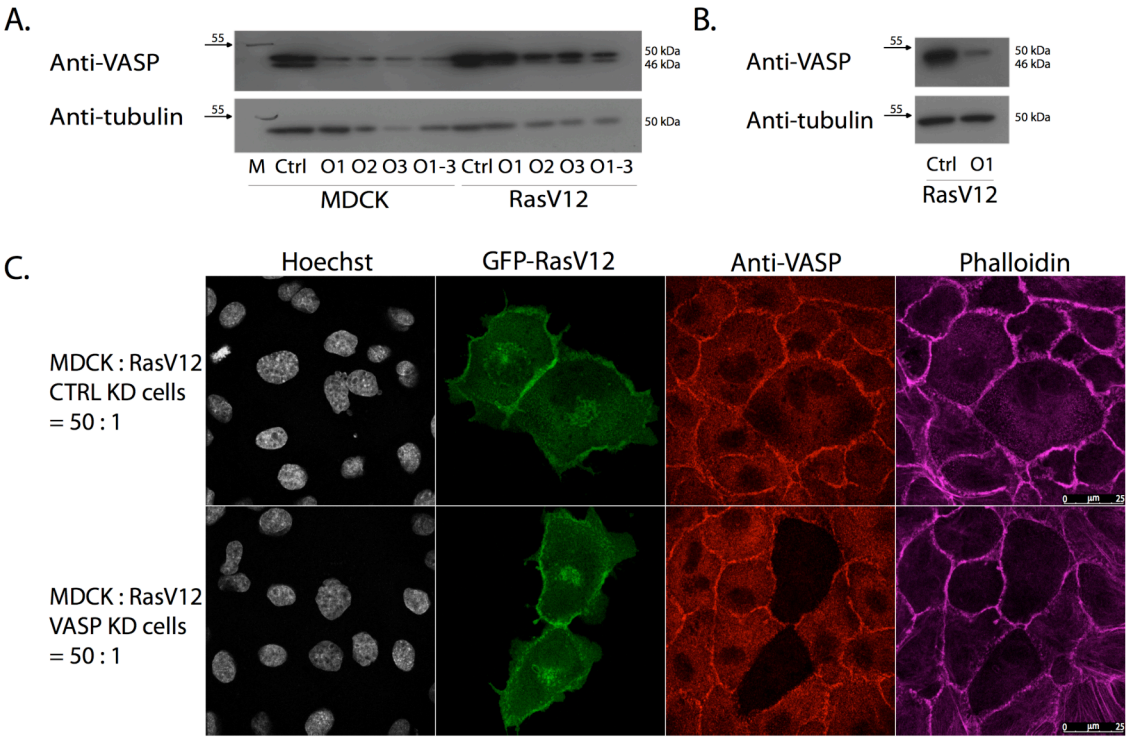

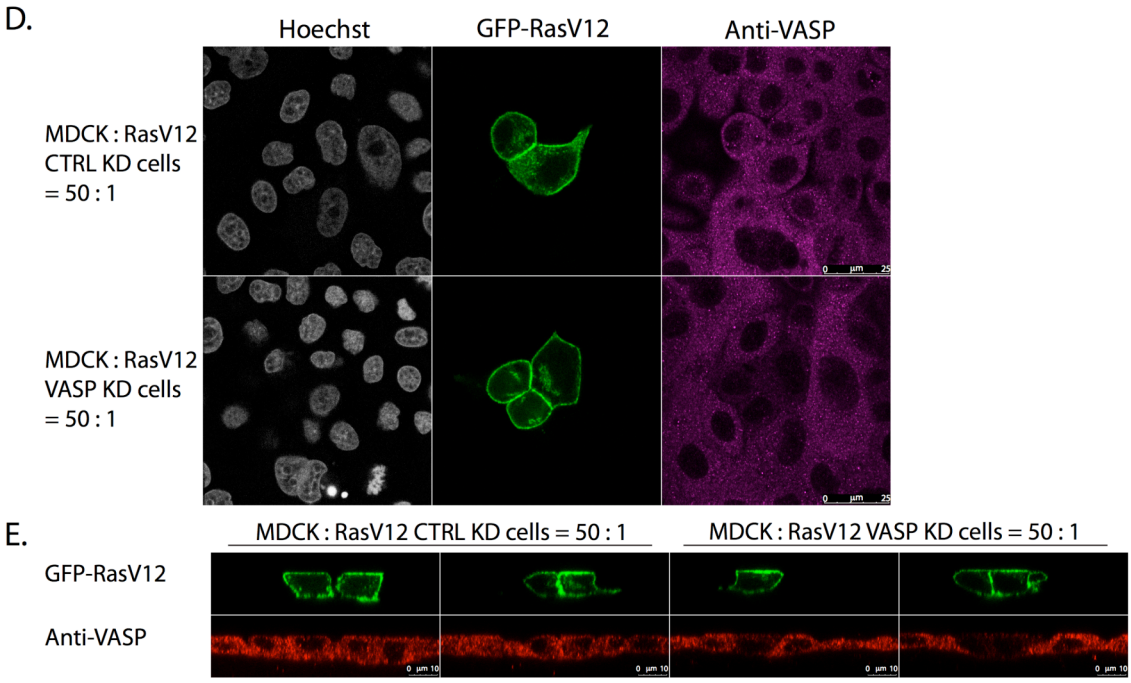

Since an antibody against VASP phosphorylated on S239 was commercially available (Cell Signaling), we tested it for immunofluorescence. Unfortunately, the signal obtained by immunostaining with this antibody was non-specific as no differences were seen in staining of VASP-depleted cells compared to the control cells (data not shown).

Having established conditions for depletion of VASP in Ras^{V12} cells, we examined the effect of the VASP knockdown on extrusion. Ras^{V12} cells were treated with the transfection reagents, and, after a 2 day-incubation, plated on collagen together with normal MDCK cells in a ratio 1 to 50. Following an overnight incubation, GFP-Ras^{V12} expression was induced. Four hours later, small groups of Ras^{V12} cells (size 1 to 4 cells) were randomly chosen and followed for 21 hours (25 hours from addition of tetracycline) by time-lapse microscopy (Figure 25 A).

While the average time at which single Ras^{V12} cells underwent extrusion during the imaging did not significantly differ between VASP-depleted and control cells (Table 10), over twice as many VASP-depleted cells escaped from the monolayer throughout the experiment (Figure 25 B, Table 10).

Figure 25. Depletion of VASP in Ras^{V12} cells enhances their extrusion from a monolayer of normal cells. (A) Ras^{V12} cells depleted in VASP (VASP KD) were extruded more efficiently than Ras^{V12} cells transfected with control siRNA (CTRL KD). Ras^{V12} cells were combined with normal cells at a ratio of 1 to 50 and cultured on type-I collagen gels, followed by tetracycline treatment. Images were extracted from representative time-lapse analysis. (B) Quantification of time-lapse analysis of Ras^{V12} cells extruded from a monolayer of MDCK cells 25 hours after tetracycline addition (21 hours from the beginning of the recording). Data are mean ± s.d. of two independent experiments (n = 174 CTRL KD cells, n = 163 VASP KD cells); *$P < 0.05$. Arrows indicate extruded Ras^{V12} cells.

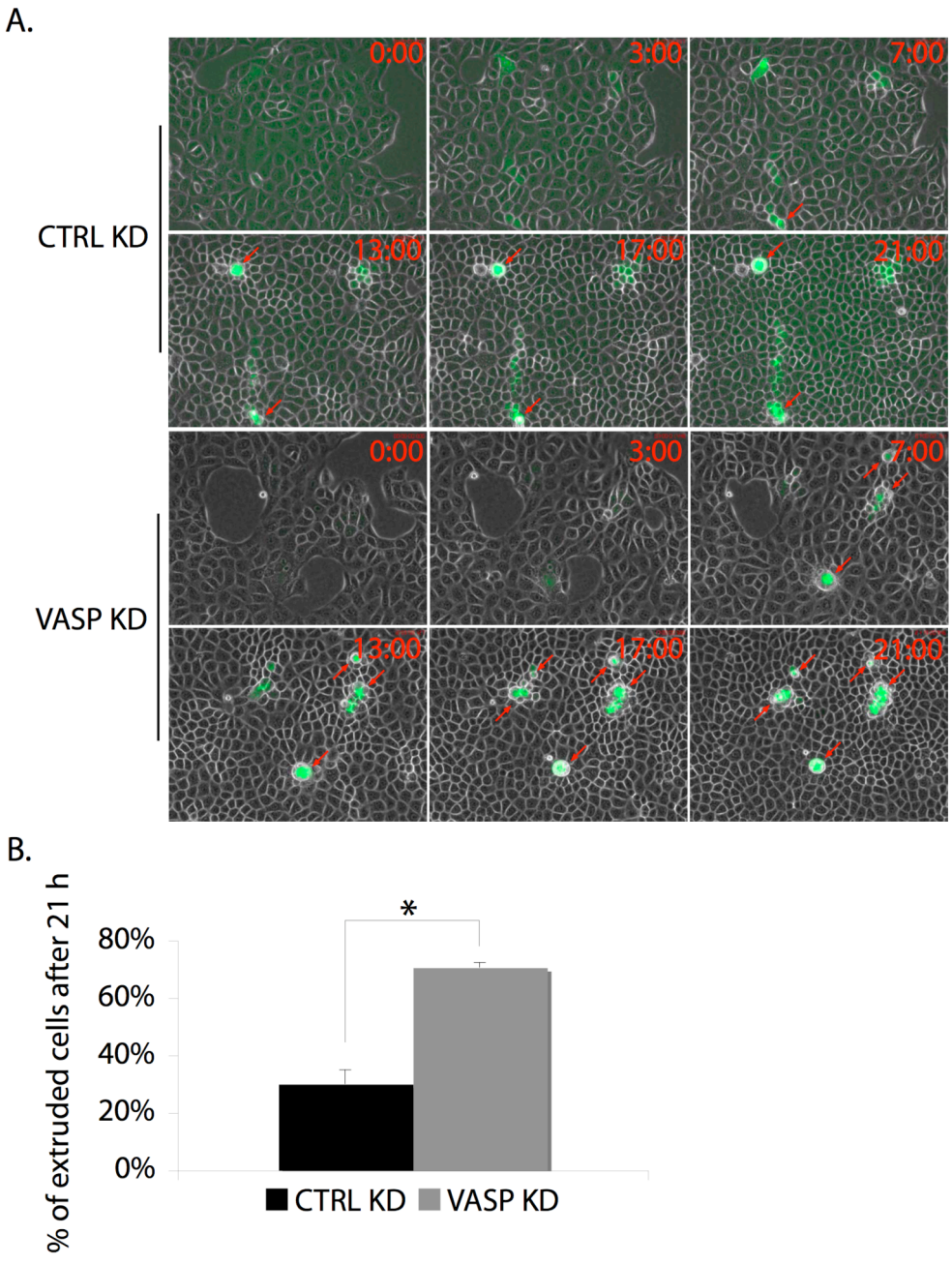

Table 10. Depletion of VASP in Ras^{V12} cells enhances their extrusion from a monolayer of normal cells. Details of quantification of time-lapse analysis from figure 25. Proliferation rate was assessed by dividing total cell number at 21 hours by total cell number at 0 hours. Extrusion rate was assessed by dividing the number of all extruded cells up to 21 hours by total cell number at 21 hours.

	Proliferation rate	Average group size at 21 hours	Extrusion rate	Average extrusion time [hours]
CTRL KD	2.5 ± 0.5	5.1 ± 0.1	30% ± 5%	14 ± 2
VASP KD	2.2 ± 0.0	6.5 ± 0.1	71% ± 2%	13 ± 0

Importantly, depletion of VASP in non-transformed GFP cells (stable cells lines created by transfection of the original construct into which *Ras^{V12}* was cloned) did not result in extrusion of these cells from a normal monolayer even after 24 hours from tetracycline addition (Figure 26).

Figure 26. Depletion of VASP in GFP cells does not result in their extrusion from a monolayer of normal cells. Confocal images of xz and xy sections of GFP cells with depleted VASP surrounded by normal cells. Cells were fixed after 24-hour incubation with tetracycline (2 µg ml^{-1}), and stained with Hoechst (grey) and phalloidin (purple).

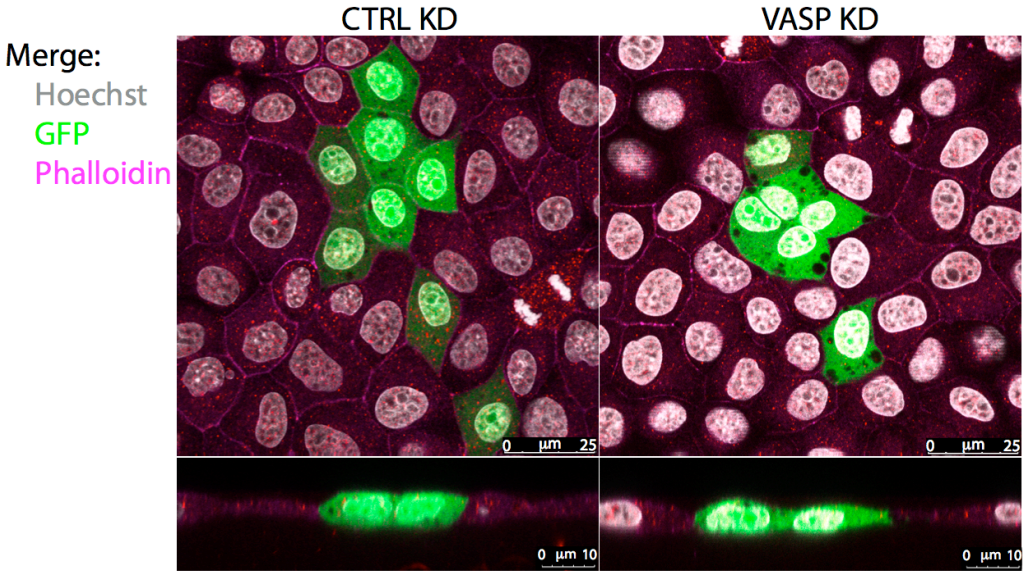

6.2.2 VASP DEPLETION DOES NOT AFFECT ACTIN ACCUMULATION AT THE RAS-RAS JUNCTIONS IN NORMAL MONOLAYERS

Searching for differences in phenotype that would account for more efficient extrusion of Ras^{V12} cells depleted in VASP comparing to the control Ras^{V12} cells, we firstly looked at junctional actin accumulation. According to the previous studies carried out in the Fujita laboratory, Ras^{V12} cells accumulate F-actin on the junctions between each other when they are plated among normal cells, comparing to a situation in which they are grown alone (Hogan et al., 2009). Knowing of the actin anti-capping activity attributed to VASP, leading to microfilament polymerisation, as well as of its junctional localization in MDCK cells, we examined whether depletion in VASP affected accumulation of F-actin in Ras^{V12} cells surrounded by normal cells. Ras^{V12} cells transfected earlier with oligonucleotides targeting VASP mRNA were plated together with normal cells on collagen. Following an 8 hour-long incubation with tetracycline, cells were fixed, stained with phalloidin and examined by confocal microscopy. Junctional actin accumulation was quantified as an average pixel intensity of phalloidin staining along the junction multiplied by the junctional length. To avoid deviation coming from differences in immunostaining, we normalised the intensity of junctional staining in Ras^{V12} cells to an average pixel intensity along the junctions between normal MDCK cells (M-M).

No significant differences were observed in accumulation of actin on junctions between Ras^{V12} cells themselves (R-R) surrounded by normal cells or junctions between Ras^{V12} cells and normal cells (R-M) upon deletion of VASP comparing to the control (Figure 27 A, B). Moreover, upon examination of actin content in cocultures incubated with tetracycline for 24 hours, no visible differences between actin accumulated at junctions in Ras^{V12} cells depleted in VASP to the control were observed (data not shown).

Figure 27. Depletion of VASP in Ras^{V12} cells does not affect junctional actin accumulation between Ras^{V12} cells in a monolayer of normal cells. (A) Confocal images of xz sections of Ras^{V12} cells with depleted VASP surrounded by normal cells. Cells were fixed after 8 hours of incubation with tetracycline (2 µg ml^{-1}) and stained with phalloidin (purple). (B) Quantification of accumulation of actin at junctions between neighbouring Ras^{V12} cells (R-R) and between Ras^{V12} cells and MDCK cells (R-M) after 8 hours of incubation with tetracycline. The final actin accumulation values were obtained by multiplying average intensity of phalloidin staining at the junctions (normalised to average junctional intensity of phalloidin staining between MDCK cells) by the average junctional length. Data are average of three independent experiments ± s.d. Altogether, 84, 92, 68 (in control Ras^{V12} cells) and 49, 91, 59 (in VASP depleted Ras^{V12} cells) R-R, R-M, and M-M junctions, respectively, were analysed. JA – junctional actin accumulation.

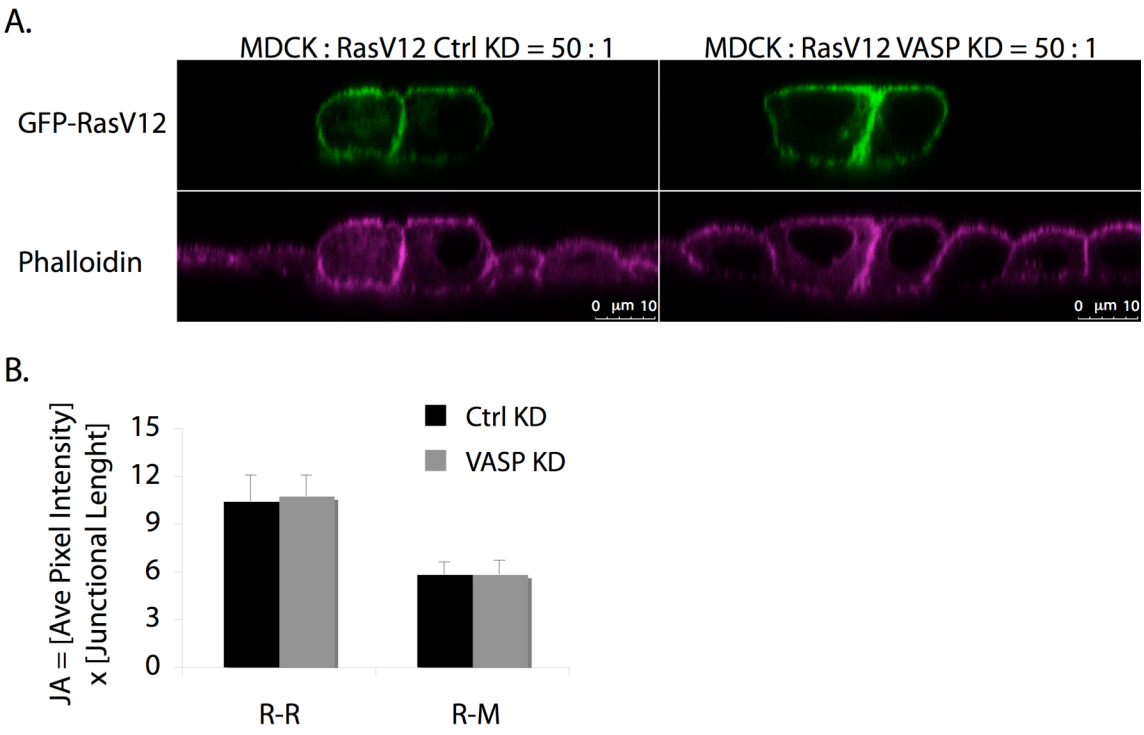

6.2.3 VASP DEPLETION MILDLY DECEASES NUCLEAR LIFT IN RAS CELLS TO THE APICAL DOMAIN DURING EXTRUSION

During extrusion Ras^{V12} cells become taller than the rest of the epithelium and adopt a "mushroom-like" shape with the nucleus close to the apical membrane (Hogan et al., 2009). At 8 hours from inducing GFP-Ras^{V12} expression, approximately 50% of the nuclei are relocated apically in Ras^{V12} cells, while in MDCK cells surrounding them as well as in transformed cells plated alone, this change is not observed. The nuclear relocation is inhibited by treatment with blebbistatin (Figure 28) suggesting that this process, similarly to extrusion itself, is dependent on myosin activity and actomyosin contractility.

Figure 28. Inhibition of myosin II with blebbistatin compromises nuclear movement to the apical domain in Ras^{V12} cells during their extrusion from a monolayer of normal cells. Quantification of the number of Ras^{V12} cells with nuclei lifted to the apical domain after 8 hours of incubation with tetracycline and 60 μM blebbistatin. The values are percentage of lifted nuclei to total quantified nuclei in Ras^{V12} cells. Data are mean of two independent experiments ± s.d. (n = 62 cells per condition per experiment); $*P < 0.05$.

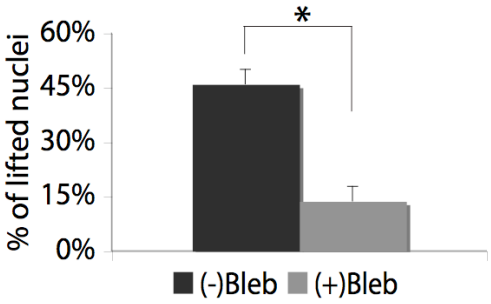

To determine whether the lift of the nucleus in a transformed epithelial cell during its extrusion was dependent on actin polymerisation downstream of VASP, we examined how VASP depletion affected nuclear positioning at 8 hours after tetracycline induction. Indeed, in VASP-depleted Ras^{V12} cells, apical relocation of the nuclei was suppressed by approximately 10% comparing to the control Ras^{V12} cells (Figure 29 A, B). As mentioned earlier, in contrast to treatment with blebbistatin, this moderate inhibition or delay of nuclear positioning did not

result in preventing extrusion. We concluded that although VASP might be partially responsible for actin polymerisation leading to the nuclear lift during extrusion, it is not essential for the escape to occur.

Figure 29. Depletion of VASP in Ras^{V12} cells compromises nuclear movement to the apical domain in Ras^{V12} cells during their extrusion from a monolayer of normal cells. (A) Confocal images of xz sections of Ras^{V12} cells with depleted VASP surrounded by normal cells and Ras^{V12} cells alone on collagen. Cells were fixed after 8 hours of incubation with tetracycline (2 µg ml^{-1}) and stained with Hoechst (grey), anti-VASP antibody (red) and phalloidin (purple). (B) Quantification of the number of Ras^{V12} cells with lifted to the apical domain nuclei after 8 hours of incubation with tetracycline. The values are percentage of lifted nuclei to total quantified nuclei in Ras^{V12} cells. Data are mean of three independent experiments ± s.d. (n = 125 CTRL KD cells, n = 112 VASP KD cells); *$P < 0.05$.

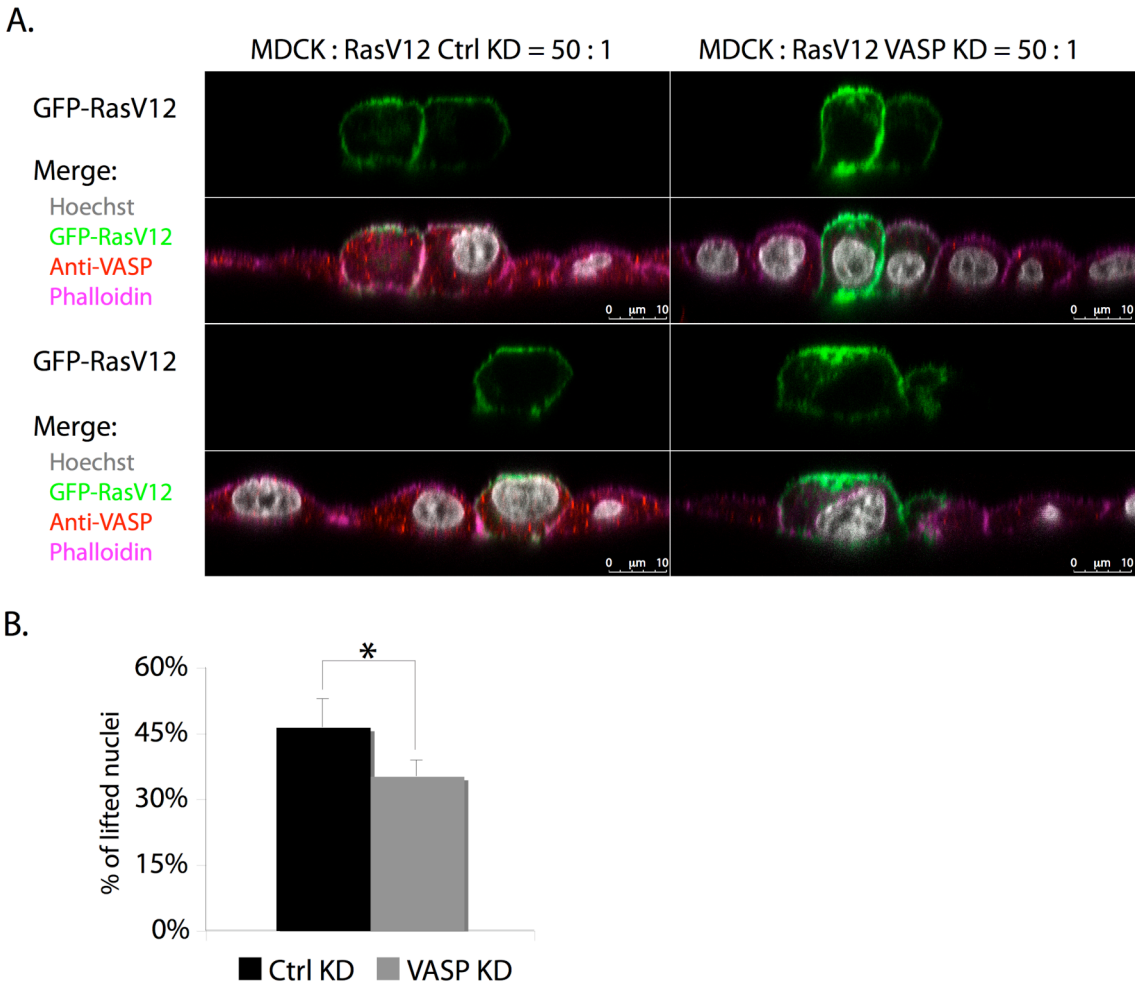

6.2.4 VASP DEPLETION AFFECTS APPREARENCE OF STRESS FIBERS AND LOCALIZATION OF VINCULIN TO FOCAL ADHESIONS IN RAS CELLS

Since neither of the processes involving actin in Ras^{V12} cells we examined thus far was profoundly affected by depletion of VASP, we turned towards focal adhesions, the basal structures at which VASP is known to localize. To look at focal adhesions, we plated cocultures of Ras^{V12} and normal cells on glass, knowing that these cellular components are not well defined (or visible) in epithelial cells grown on softer types of matrix, e.g. collagen or matrigel. Consistent with our previous data obtained for cells plated on collagen type I, on glass Ras^{V12} cells depleted in VASP underwent extrusion within 24 hours from inducing GFP-Ras^{V12} expression in far greater numbers comparing to the control Ras^{V12} cells (data not shown).

Firstly, we checked whether VASP localized to the basal part of the cells in our system. Indeed, immunostaining with anti-VASP antibody on glass revealed the presence of a signal specific for VASP in this area (Figure 30).

Figure 30. A pool of VASP localizes basally in Ras^{V12} cells surrounded by normal cells. Confocal images of xy basal sections of Ras^{V12} cells with depleted VASP surrounded by normal cells on glass. Cells were fixed after 8 hours of incubation with tetracycline (2 µg ml^{-1}) and stained with anti-VASP antibody (purple). (a, b) Enlargement of boxed areas in the main figure.

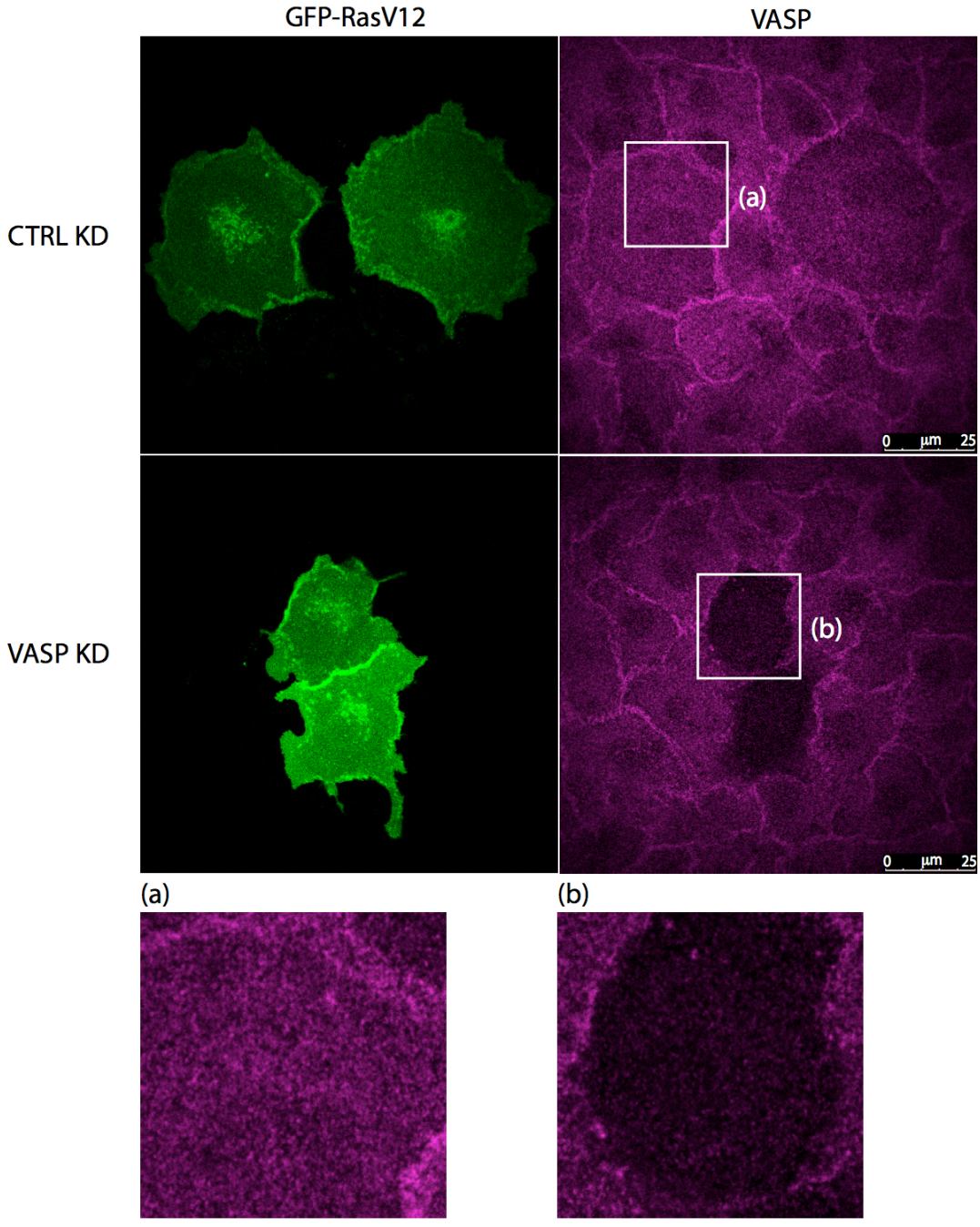

Next, we examined the appearance of focal adhesions and stress fibres in Ras^{V12} cells with depleted VASP compared to the control by staining for vinculin and F-actin. Cells treated with siRNA reagents were plated on glass coverslips and grown in cocultures with normal MDCK cells for 8 hours after inducing GFP-Ras^{V12}

expression. Immunostaining with an anti-vinculin antibody revealed that localization of this protein to the basal part of Ras^{V12} cells was suppressed compared to vinculin in the surrounding normal neighbours (Figure 31 A). This effect was further enhanced by depletion of VASP in Ras^{V12} cells from mixed cultures (Figure 31 A). Likewise, far fewer stress fibres were observed in Ras^{V12} cells compared to normal cells and, in particular, in VASP-depleted Ras^{V12} cells (Figure 31 B).

Figure 31. Stress fibres formation and localization of vinculin to focal adhesions are affected by depletion of VASP in Ras^{V12} cells surrounded by normal cells. (A, B) Confocal images of xy basal sections of Ras^{V12} cells with depleted VASP surrounded by normal cells on glass. Cells were fixed after 8 hours of incubation with tetracycline (2 µg ml^{-1}) and stained with anti-VASP antibody (red in A), anti-vinculin antibody (purple in A), and phalloidin (red in B). (a, b) Enlargement of boxed areas in A.

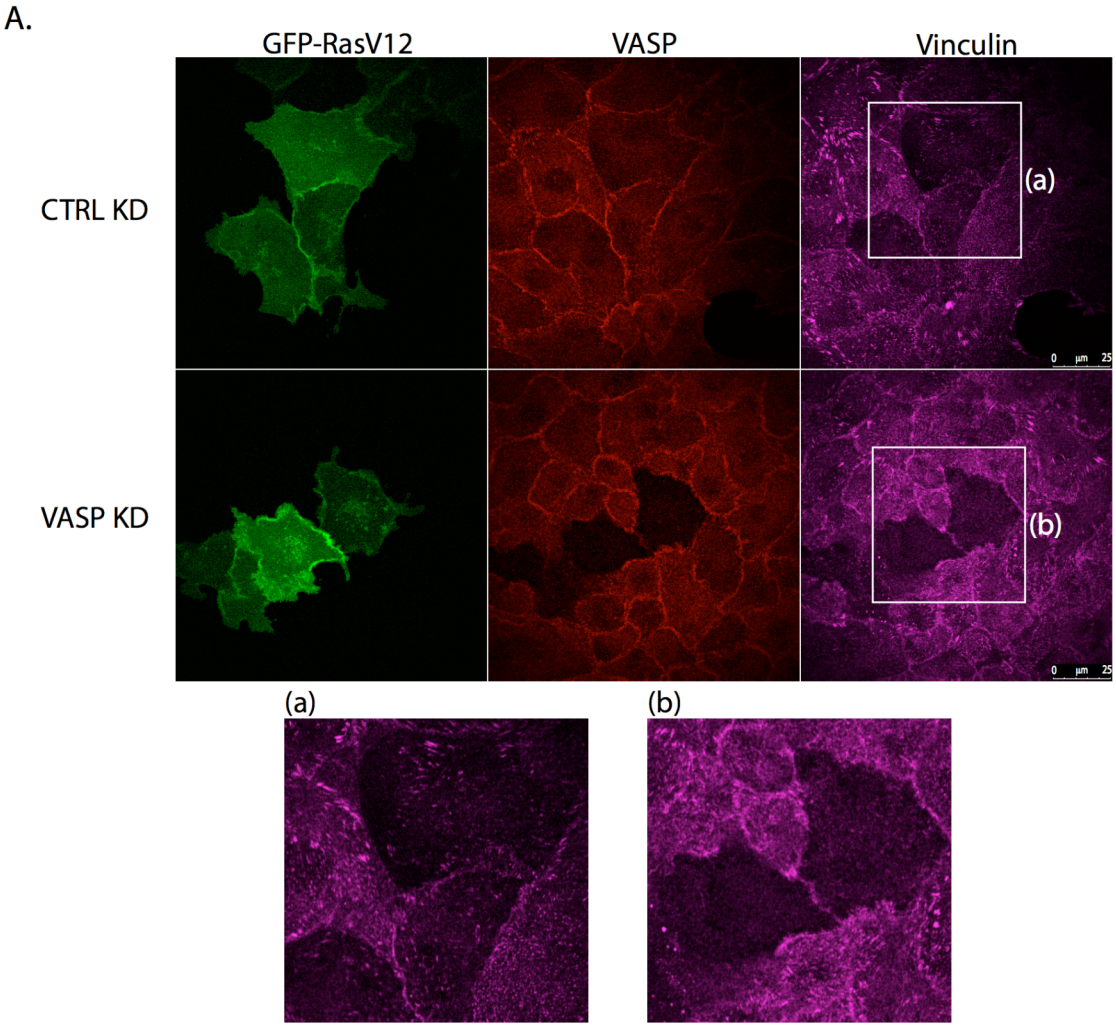

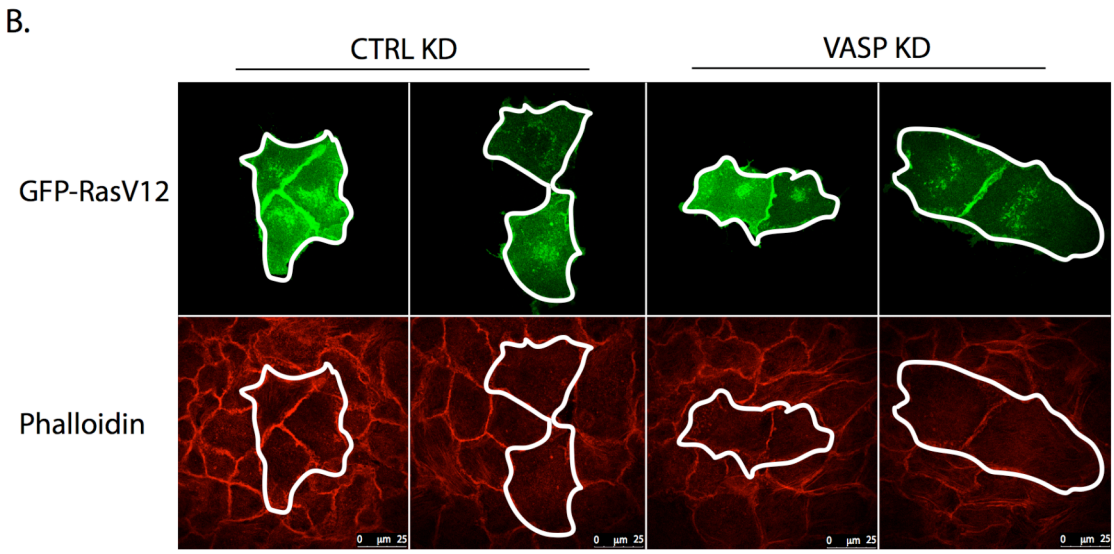

Considering the possibility that depletion of VASP might affect stability of focal contacts and stress fibres leading to compromised attachment and quicker extrusion of Ras^{V12} cells from normal monolayers, we examined the effect of VASP depletion on these structures in Ras^{V12} cells plated alone. In Ras^{V12} cells treated with siRNA targeting VASP transcripts after 8 hours of GFP-Ras^{V12} induction, both localization of vinculin to focal adhesions as well as formation of stress fibres along the cell base were heavily impaired compared to control Ras^{V12} cells (Figure 32 A, B). This finding is consistent with our hypothesis of compromised attachment resulting in enhanced extrusion of Ras^{V12} cells upon depletion of VASP. Moreover, in many VASP-depleted cells F-actin formed large globular structures along the cell base, suggesting an imbalance between actin branching and actin elongation factors in these cells (Figure 32 B).

Intrigued by the particularly striking appearance of vinculin in basal confocal sections of Ras^{V12} cells surrounded by normal MDCK cells, we examined localization of this protein to the focal contacts formed by transformed cells grown in cocultures compared to these cells grown alone. Indeed, 8 hours after GFP-Ras^{V12} induction, vinculin was not adopting the normal basal dashed pattern in Ras^{V12} cells plated with normal neighbours, but remained occasionally present at their cell periphery (Figure 33). Importantly, in tranformed cells plated alone, this phenomenon was not observed, and vinculin formed a clear dashed basal pattern (Figure 33).

Figure 32. Stress fibre formation and localization of vinculin to focal adhesions are affected by depletion of VASP in Ras^{V12} cells plated alone. (A, B) Confocal images of xy basal sections of Ras^{V12} cells with depleted VASP on glass. Cells were fixed after 8 hours of incubation with tetracycline (2 µg ml^{-1}) and stained with anti-VASP antibody (red in A), anti-vinculin antibody (purple in A, red in B), and phalloidin (purple in B).

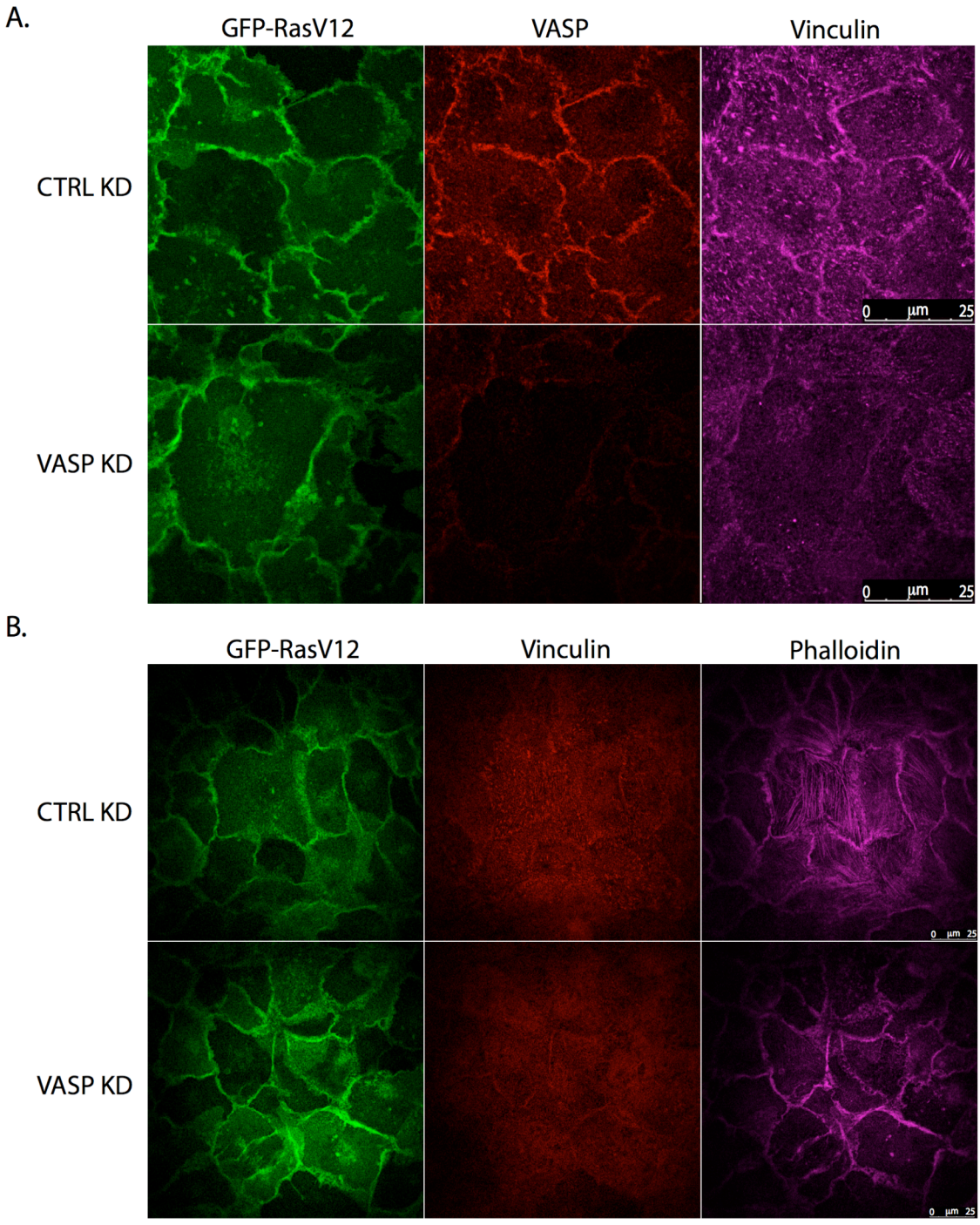

Figure 33. Vinculin localization to focal adhesions is reduced in Ras^{V12} cells surrounded by normal cells compared to Ras^{V12} cells alone. Confocal images of xy basal sections of Ras^{V12} cells surrounded by normal cells and Ras^{V12} cells alone on glass. Cells were fixed after 8 hours of incubation with tetracycline (2 μg ml^{-1}) and stained with anti-vinculin antibody (red) and anti-VASP antibody (purple). (a, b, c) Enlargement of boxed areas in the main figure.

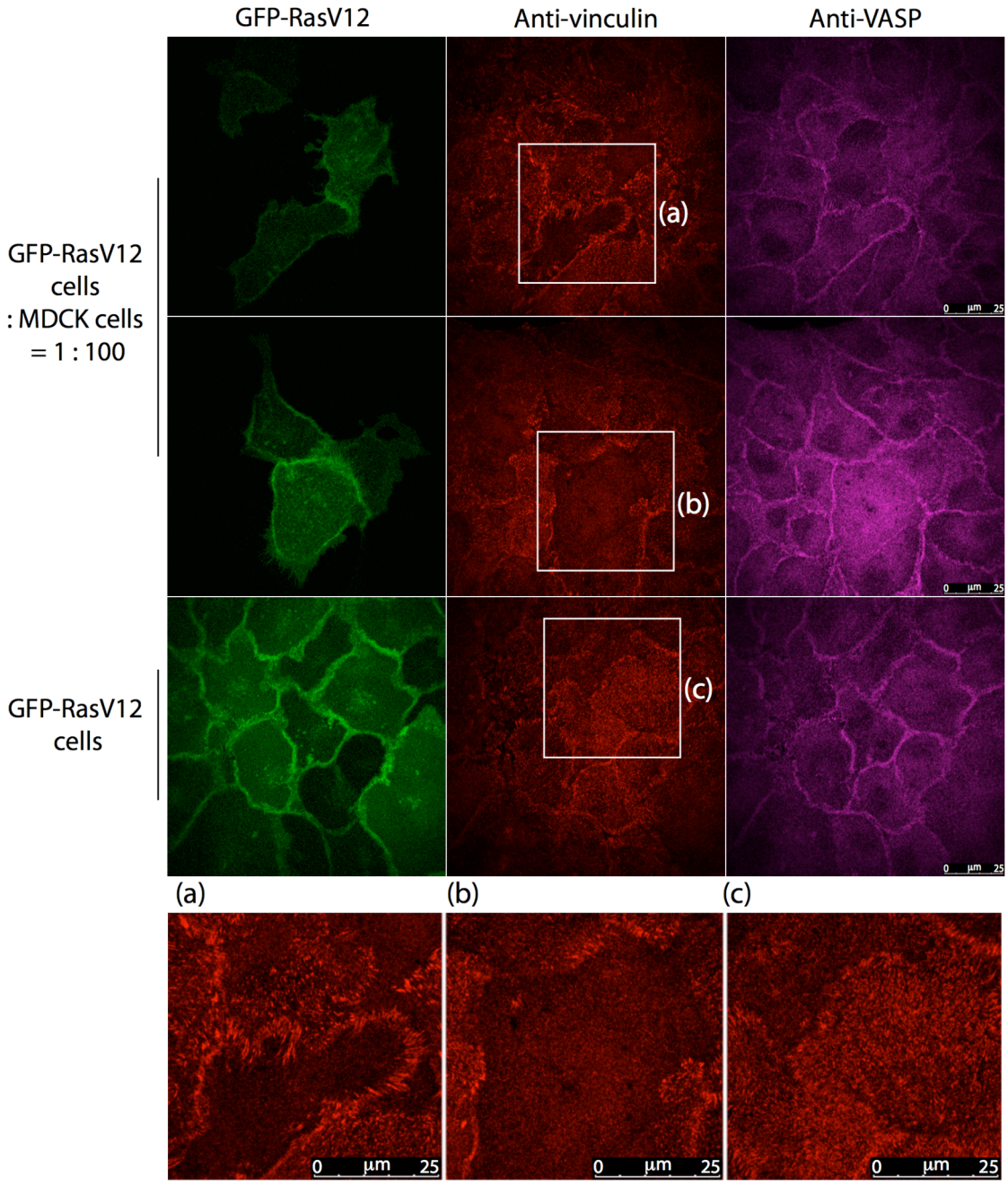

6.3 DISCUSSION

For validation of the SILAC screen performed earlier, we chose a protein previously implicated in remodelling of the cytoskeleton. Having an anti-capping activity towards actin inhibited by the very phosphorylation on S239 that we found upregulated in Ras^{V12} cells surrounded by normal cells, VASP was an attractive candidate for our study.

We began with depletion of VASP in Ras^{V12} cells, which was expected to mimic the phosphorylation on S239 in our system, at least in respect to its regulation of actin polymerisation. The depletion of VASP in transformed cells resulted in more efficient extrusion of these cells from a monolayer of normal cells. Importantly, these cells remained viable after extrusion and proliferated on the top of the monolayer similarly to control Ras^{V12} cells. This observation indicates that it was not induction of cell death that stimulated enhanced extrusion. Importantly, constitutive Ras signalling was required for the VASP depletion effect, as control GFP cells were not extruded upon depletion.

Searching for the role that VASP plays in extrusion, we examined several possible cellular locations and processes related to actin polymerisation in VASP-depleted cells. While downregulation of VASP in Ras^{V12} cells did not affect accumulation of junctional actin in these cells plated within a normal monolayer, it mildly impaired the process of nuclear relocation to the apical membrane occurring in transformed cells during their extrusion. Therefore, VASP-dependent actin polymerisation contributes, but is not essential for the nuclear lift to occur.

Knowing that VASP is often localized to focal contacts where it interacts with zyxin and vinculin, we examined these structures in transformed cells with endogenous and lower levels of VASP. Indeed, depletion of VASP resulted in apparently less vinculin localized to focal adhesions and less prominent stress fibres in Ras^{V12} cells grown in cocultures with normal cells as well as in Ras^{V12} cells grown alone. In conclusion, the depletion of VASP in Ras^{V12} cells, having an autonomous effect on stability of focal contacts and stress fibres, resulted in more efficient extrusion of these cells when grown within normal monolayers. Although the role of VASP in maintenance and elongation of stress fibres is still debated (reviewed in (Ciobanasu et al., 2012)) and conflicting functions were

assigned to this protein in different cell types (Bear et al., 2002; Schlegel and Waschke, 2009), our data from Ras^{V12}-transformed epithelial cells feed into this discussion and suggest that, at least in our system, VASP is important for cell attachment. Reassuringly, our findings are in agreement with some previous studies on endothelial cells and mouse fibroblasts, in which downregulation of VASP and vinculin, respectively, was shown to promote cell migration often linked to instability and increased dynamics of focal adhesions (Bear et al., 2002; Saunders et al., 2006).

Another burning question is why depletion of VASP resulted in mislocalisation or instability of vinculin at focal contacts? There are two possible explanations: the lack of direct interaction of vinculin with VASP or lower tension at focal sites due to compromised actin polymerisation rates, either of which could potentially result in quicker turnover of vinculin. Indeed, the latter option is supported by a study in which a mechanosensor inserted into vinculin proved that high tension across this protein was associated with maturation of focal adhesions, whereas less force applied on vinculin led to their disassembly (Grashoff et al., 2010).

During the study of focal contacts in transformed cells, we noticed that the basal localization of vinculin in control Ras^{V12} cells was already quite low relative to either surrounding normal cells or transformed cells grown on their own. Quite likely, at 8 hours from addition of tetracycline, focal contacts started to undergo disassembly, which is necessary for transformed cells to escape from the epithelium. At this time point, the talin content in focal adhesions was unaffected in the control cells (data not shown), suggesting that disassembly of these structures during extrusion occurs gradually (talin interacts with integrins directly and is recruited relatively early to nascent adhesions (Zaidel-Bar et al., 2003)). A close assessment of stress fibres at 8 hours from inducing GFP-Ras^{V12} expression in transformed cells surrounded by normal neighbours was not conclusive. Although in many of these cells far fewer stress fibres were observed; in others these structures were still quite prominent. Perhaps a more striking effect on stress fibres could be seen at a later time point after addition of tetracycline.

Of course, a crucial question to our study remains unanswered. In order to fully validate the screen as well as understand how reducing cell attachment is executed in Ras^{V12} cells during their extrusion, we need to examine the effect of

phosphorylation of VASP on S239 in this process. According to our current hypothesis, this modification is a necessary step in disassembly of focal contacts in transformed cells. This theory is supported by previous observations in fibroblasts, endothelial cells, platelets as well as cancer cells, all of which were demonstrated to retract their lamellipodia and round up upon phosphorylation of VASP on S239 (details in section 6.1). Encouraging data were obtained in a study showing changes in actin cytoskeleton in the presence of phosphomimetic mutants of VASP. The presence of VASP in which S239 was replaced with aspartic acid (D) in microvascular endothelial cells resulted in formation of large actin aggregates at the basal membrane of these cells (Figure 3 G in (Benz et al., 2009)), resembling structures observed in VASP-depleted Ras^{V12} cells (Figure 33 B).

To confirm our hypothesis, we will perform rescue experiments with transiently expressed wild type and mutants of VASP carrying mutations mimicking permanent phosphorylation (S239 replaced with D) as well as lack of phosporylation (S239 replaced with A) in VASP-depleted Ras^{V12} cells. We will examine the effect of the rescue on extrusion as well as the appearance of focal adhesions and stress fibres.

Since a conserved pathway downstream of NO release and PKG activation was frequently shown to regulate phosphorylation of VASP on S239 in various cell types, including MDCK cells (Jaeger et al., 2010), we will investigate its role in extrusion. If PKG activated by NO indeed phosphorylates S239 of VASP in Ras^{V12} cells before their extrusion, it would be interesting to know what the source of NO is in our system. Is it produced by Ras^{V12} cells themselves in order to escape from the monolayer of normal cells or is it a part of an intrinsic epithelial defence mechanism leading to elimination of a transformed cell through apical extrusion? Further studies beyond the scope of this thesis are required to address all the issues listed above.

CHAPTER 7:

VALIDATION OF THE SILAC SCREEN

- MRCK BETA

CHAPTER 7: VALIDATION OF THE SILAC SCREEN – MRCK BETA

7.1 INTRODUCTION

In the SILAC screen we have found that phosphorylation on two sites within myotonic dystrophy kinase-related Cdc42-binding kinase β (MRCKβ) are non-cell-autonomously downregulated in Ras^{V12} cells interacting with normal MDCK cells. Modification of these sites has been reported before (in the PosphoSitePlus database), but not studied in depth. Knowing that MRCK can be activated by Cdc42, a Rho GTPase which was previously implicated in extrusion (Hogan et al., 2009), we became interested in this molecule.

Cdc42 is a member of the Rho family of small GTPases conserved from yeast to mammals. In cells it exists in two states: GTP-bound active form or GDP-bound inactive form. Transitions between these two states are facilitated by a large group of GEFs, GAPs and GDIs. Upon activation by a variety of surface receptors, Cdc42 binds and stimulates multiple proteins, including kinases such as p21-activated kinases (PAKs), mixed-lineage kinases (MLKs), MRCKs as well as scaffolding proteins such as Par6, WASP, and IQGAP (reviewed in (Stengel and Zheng, 2011)). Through modulation of its effectors Cdc42 is implicated in a number of cellular processes primarily related to reorganisation of actin cytoskeleton, e.g. formation of actin-rich membrane protrusions called filopodia, establishment of cell polarity, and migration (reviewed in (Etienne-Manneville and Hall, 2002)).

Downstream of Cdc42, its effect on migration is mediated in part by MRCK kinases. The two conserved isoforms of MRCKs, α and β, alongside ROCK, belong to the AGC kinase family (reviewed in (Pearce et al., 2010)). MRCKs are large 190 kDa proteins with kinase domains highly homologous to that of ROCK. Consequently, they also share a similar set of substrates, among them myosin light chain (MLC) and a myosin binding subunit of the myosin light chain phosphatase complex, MYPT1 (Tan et al., 2001). In contrast to ROCK, which was demonstrated to phosphorylate MLC on both serine 19 (S19) and threonine 18

(T18), MRCKs appear to regulate this molecule only on S19 (Tan et al., 2011). At a cellular level, activation of the Cdc42-MRCK pathway can complement Rho-ROCK signalling in migration. While MRCKs regulate actomyosin contractility necessarily for invasion of cells with elongated mesenchymal morphology, ROCK is important for migration in three-dimensional environments characterised by rounded blebbing morphology (Wilkinson et al., 2005). Rho- and Cdc42-dependent pathways were also found to collaborate in collective cell migration in which leading fibroblasts rely on signalling downstream of Rho, whereas the movement of the following carcinoma cells is dependent on MRCK (Gaggioli et al., 2007). Additionally, MRCK was implicated in the maintenance of focal adhesions (Dong et al., 2002) as well as nuclear positioning and reorientation of the microtubule organising centre (MTOC) in migrating fibroblasts through activation of actin retrograde flow (Gomes et al., 2005).

7.2 RESULTS

7.2.1 MRCK DEPLETION ENHANCES EXTRUSION OF RAS CELLS FROM A MONOLAYER OF NORMAL EPITHELIAL CELLS

To study the role of MRCKβ in extrusion of Ras^{V12} cells from normal monolayers we depleted this protein using the Interferin-based siRNA method. Similarly to our previous observations concerning depletion of VASP, MRCK could only be downregulated in Ras^{V12} cells, if the transfection reagents were added immediately after plating the cells. Since MRCKβ depletion using an isoform-specific oligonucleotide was relatively inefficient, we decided to target both MRCK isoforms using the pool of all three siRNA molecules tested (Figure 34). MRCKα isoform is less abundant in MDCK cells and, in our hands, could not be detected by immunoblotting.

Unfortunately, we were unable to obtain specific immunostaining of MRCKβ in MDCK cells with several tested commercially available antibodies; hence, each depletion experiment was confirmed by immunoblotting.

Figure 34. Treatment with siRNA reagents targeting MRCK mRNA results in efficient depletion of MRCKβ protein in Ras^{V12} cells. Total cell lysates of Ras^{V12} cells transfected with siRNA reagents, cultured for 4 days from transfection and analysed by immunoblotting using anti-MRCKβ antibody. Ctrl – control siRNA, Pan – siRNA designed to deplete both isoforms of MRCK, α – MRCKα, β – MRCKβ, Pool – the three oligonucleotides mixed in a ratio 1 : 1 : 1.

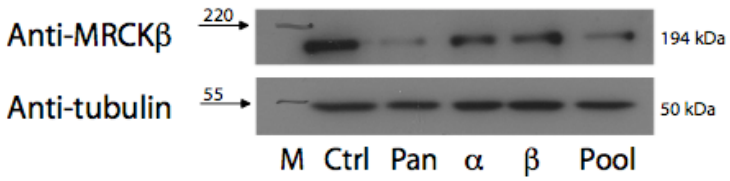

To determine whether MRCK was important for extrusion, we cocultured MRCK-depleted Ras^{V12} cells with normal cells in a ratio 1 to 50 on collagen and followed their fate using time-lapse imaging. Twenty five hours after inducing GFP-Ras^{V12} expression (21 hours from the beginning of imaging), 74% of MRCK-

depleted Ras^{V12} cells had left the monolayer, comparing to only 30% of control Ras^{V12} cells (Figure 35 A, B; Table 11). This result corresponded to data obtained for cells cocultured on glass coverslips instead of the collagen matrix (data not shown).

Figure 35. Depletion of MRCK in Ras^{V12} cells enhances their extrusion from a monolayer of normal cells. (A) Ras^{V12} cells depleted in MRCK (MRCK KD cells) were extruded from a monolayer of normal cells more efficiently than Ras^{V12} cells transfected with control siRNA (CTRL KD cells). Ras^{V12} cells were combined with normal MDCK cells at a ratio of 1 to 50 and cultured on type-I collagen gels, followed by tetracycline treatment. Images were extracted from a representative time-lapse analysis. (B) Quantification of time-lapse analyses of Ras^{V12} cells extruded from a monolayer of MDCK cells 25 hours after tetracycline addition (21 hours after the beginning of the recording). Data are mean ± s.d. of two independent experiments (n = 174 CTRL KD cells, n = 159 MRCK KD cells); $*P < 0.05$. Arrows indicate extruded Ras^{V12} cells.

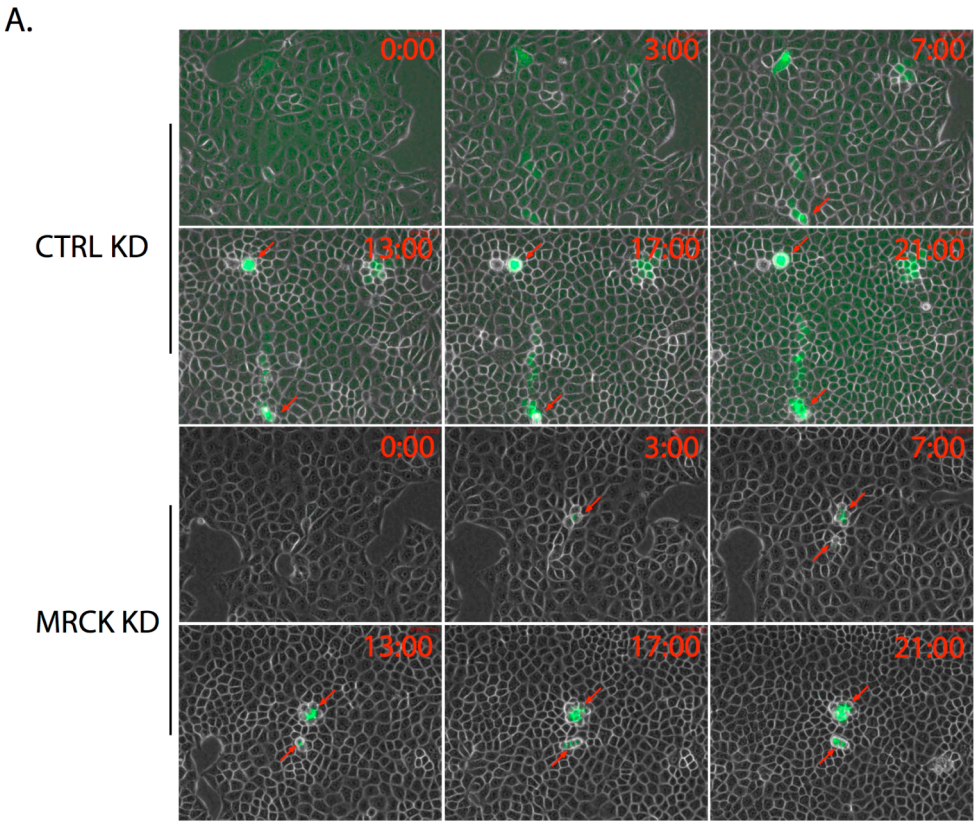

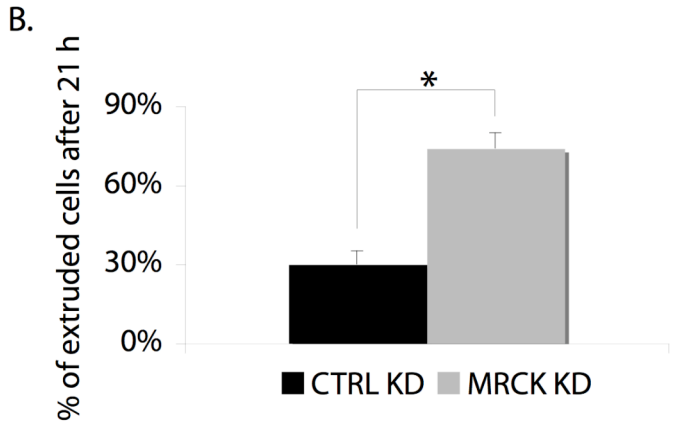

Table 11. Depletion of MRCK in Ras^{V12} cells enhances their extrusion from a monolayer of normal cells. Details of quantification of time-lapse analyses from figure 35. Proliferation rates were assessed by dividing total cell number at 21 hours (25 hours of incubation with tetracycline) by total cell number at 0 hours (4 hours of incubation with tetracycline). Extrusion rate was assessed by dividing the number of all extruded cells up to 21 hours by total cell number at 21 hours.

	Proliferation rate	**Average group size at 21 h**	**Extrusion rate**	**Average extrusion time [hours]**
CTRL KD	2.5 ± 0.5	5.1 ± 0.1	30% ± 5%	14 ± 2
MRCK KD	2.3 ± 0.6	5.3 ± 0.3	74% ± 6%	13 ± 1

Importantly, when MRCK was depleted in GFP cells (a cell line stably expressing the original GFP construct into which Ras^{V12} was cloned) plated among normal neighbours, these cells did not undergo extrusion or present any apparent phenotypical changes up to 24 hours from inducing GFP expression (Figure 36).

Figure 36. Depletion of MRCK in GFP cells does not result in their extrusion from a monolayer of normal cells. Confocal images of xz and xy sections of GFP cells with depleted MRCK surrounded by normal cells. Cells were fixed after 24-hour incubation with tetracycline (2 µg ml^{-1}), and stained with Hoechst (grey) and phalloidin (purple).

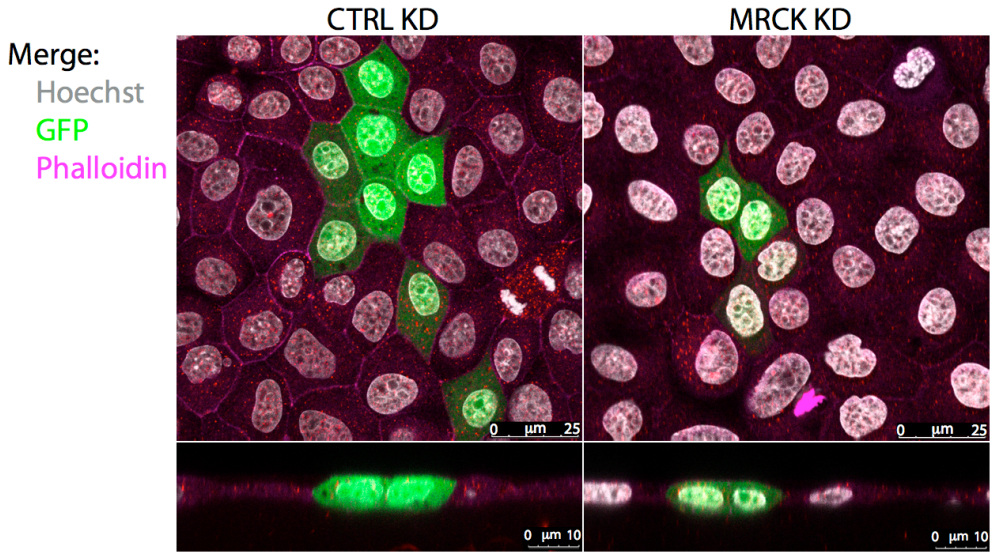

7.2.2 MRCK DEPLETION DOES NOT AFFECT ACTIN ACCUMULATION AT RAS-RAS JUNCTIONS IN NORMAL MONOLAYERS

Next, we decided to assess whether downregulation of MRCK, an important regulator of myosin II activity, had any effect on F-actin in transformed cells during their extrusion. Considering the possibility that high extrusion rates of MRCK-depleted Ras^{V12} cells could be correlated with actin localization, we determined accumulation of F-actin at junctions between transformed and normal cells (R-M) as well as transformed cells themselves (R-R) plated among normal neighbours.

After 8 hours of induction of oncogenic Ras, cocultures of MRCK-depleted Ras^{V12} cells and normal cells were fixed with 4% PFA and immunostained with phalloidin (Figure 37 A). F-actin present at cellular junctions was quantified in the same manner as described previously for VASP-depleted cells (section 6.2.2). No

significant changes in accumulation of junctional F-actin were observed at this time point in Ras^{V12} cells upon depletion of MRCK (Figure 37 B).

Figure 37. Depletion of MRCK in Ras^{V12} cells does not affect junctional F-actin accumulation between neighbouring Ras^{V12} cells in a monolayer of normal cells. (A) Confocal images of xz sections of Ras^{V12} cells with depleted MRCK surrounded by normal cells and Ras^{V12} cells alone on collagen. Cells were fixed after 8 hours of incubation with tetracycline (2 µg ml^{-1}) and stained with phalloidin (purple). (B) Quantification of accumulation of actin at junctions between neighbouring Ras^{V12} cells (R-R) and between Ras^{V12} cells and MDCK cells (R-M) after 8 hours of incubation with tetracycline. The final F-actin accumulation values were obtained by multiplying average intensity of phalloidin staining at the junctions (normalised to average junctional intensity of phalloidin staining between MDCK cells) by the average junctional length. Data are mean of two independent experiments ± s.d. Altogether, 67, 67, 43 (in control Ras^{V12} cells) and 44, 45, 47 (in MRCK depleted Ras^{V12} cells) R-R, R-M, and M-M junctions, respectively, were analysed.

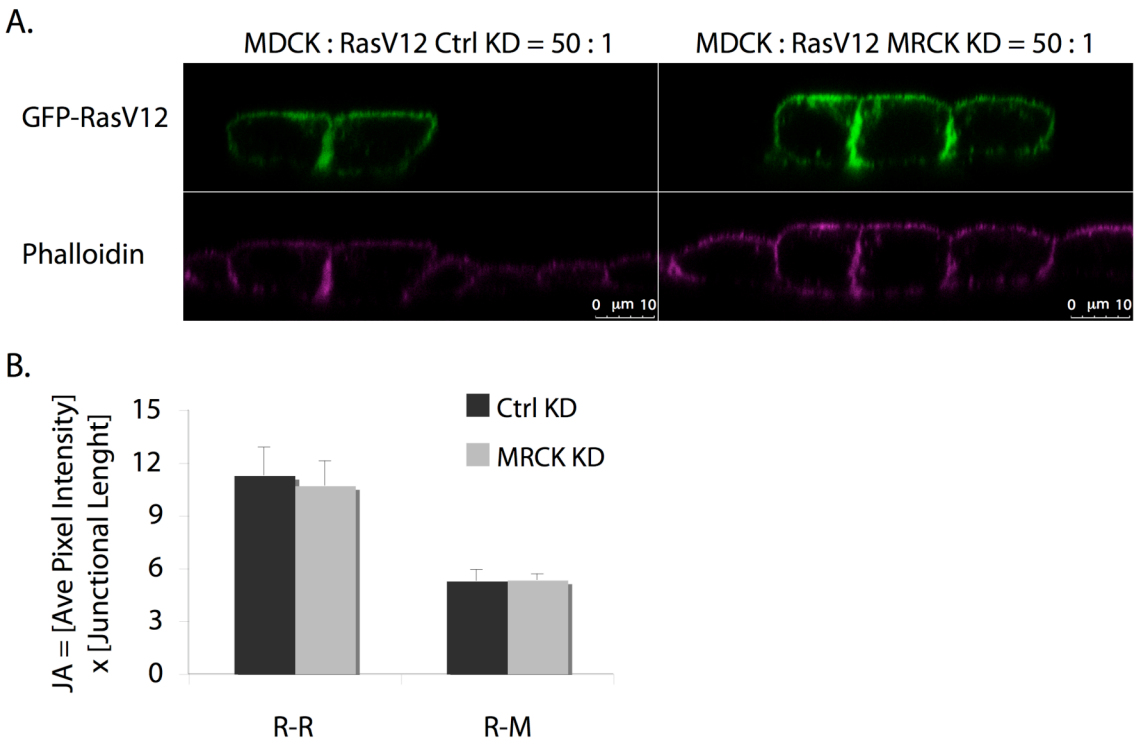

7.2.3 MRCK DEPLETION PROMOTES NUCLEAR LIFT IN RAS CELLS TO THE APICAL DOMAIN DURING EXTRUSION

Since blebbistain, an inhibitor of myosin II activity, was shown to prevent relocation of the nuclei in Ras^{V12} cells prior to their extrusion (Figure 28), we examined whether depletion of MRCK had any effect on this process. At 8 hours from tetracycline addition over 60% of nuclei in MRCK-depleted Ras^{V12} cells plated among normal neighbours were localized apically, comparing to 45% relocated nuclei in the control Ras^{V12} cells (Figure 38 A, B). This significant promotion of the nuclear lift indicates that MRCK activity is not required for this process in Ras^{V12} cells prior to their extrusion. On the contrary, downregulation of this kinase appears to enhance both extrusion and the accompanying apical translocation of the nucleus. In other words, MRCK promotes the differentiated phenotype with the nucleus positioned close to the basal membrane.

Figure 38. Depletion of MRCK in Ras^{V12} cells promotes apical nuclear movement in Ras^{V12} cells during their extrusion from a monolayer of normal cells. (A) Confocal images of xz sections of Ras^{V12} cells with depleted MRCK surrounded by normal cells and Ras^{V12} cells alone on collagen. Cells were fixed after 8 hours of incubation with tetracycline (2 µg ml^{-1}) and stained with Hoechst (grey), and phalloidin (purple). (B) Quantification of Ras^{V12} cells with apically located nuclei after 8 hours of incubation with tetracycline. The values are a percentage of apically lifted nuclei to total quantified nuclei in Ras^{V12} cells. Data are mean of three independent experiments ± s.d. (n = 134 CTRL KD cells, n = 90 MRCK KD cells); *$P < 0.05$.

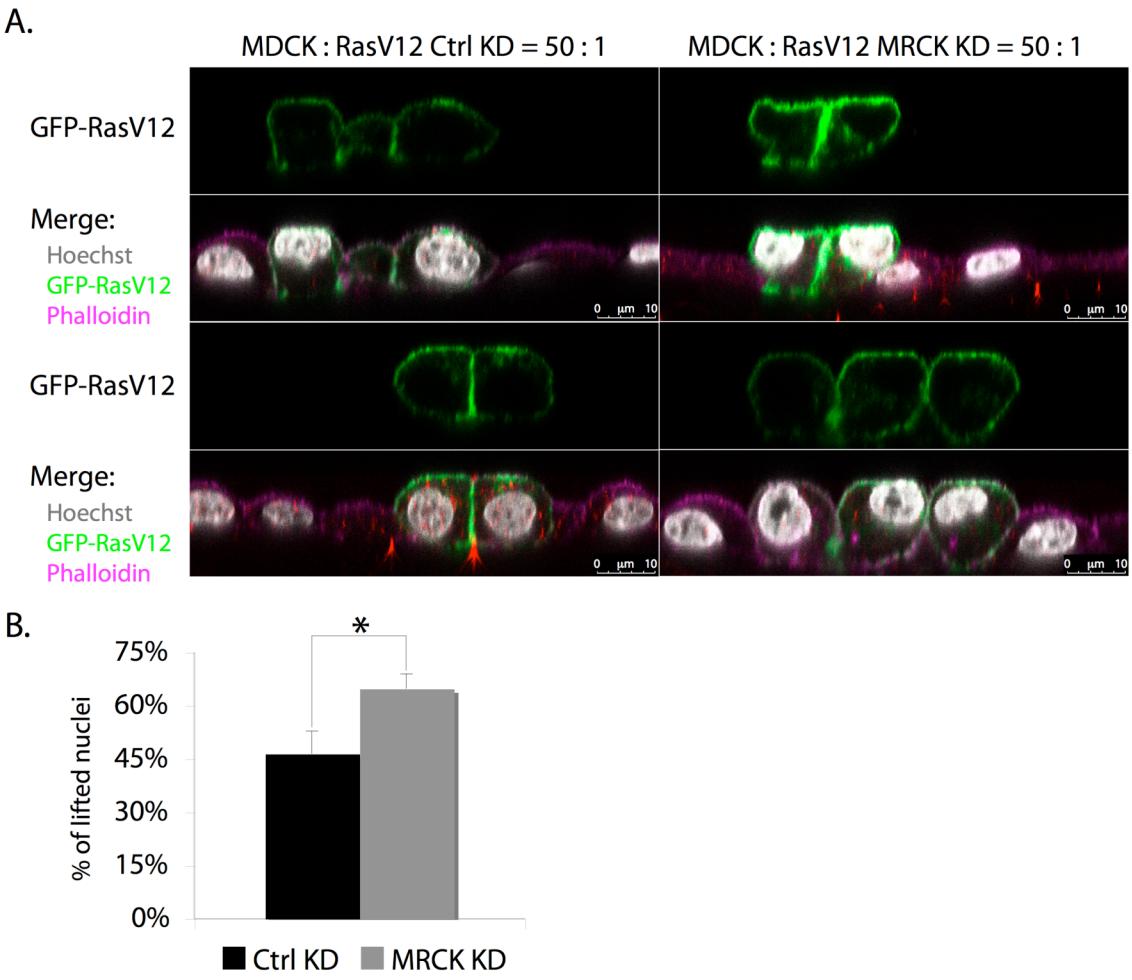

7.3 DISCUSSION

Knowing that Cdc42 activity in Ras^{V12} cells is necessary for their extrusion from normal monolayers (Hogan et al.), we became interested in MRCK, a kinase activated downstream of Cdc42. Since MRCK is a known regulator of myosin II, which is essential for extrusion, we hoped that this kinase found modified in the SILAC screen could be the missing link between Cdc42 and myosin II in our system. To our surprise, however, depletion of MRCK in Ras^{V12} cells resulted in enhanced extrusion. Extruded MRCK-depleted transformed cells, similarly to the control cells, remained loosely attached to the monolayer and proliferated at least for 50 hours after induction of GFP-Ras^{V12} expression.

In the SILAC screen phosphorylation of two sites within the tail domain of MRCK was decreased. Since depletion of the whole protein results in enhanced extrusion of transformed cells, it is likely that decreased phosphorylation of these sites inhibits MRCK activity, but this has not been tested yet. We can speculate that downstream of Cdc42 other targets are required for extrusion, while activation of MRCK needs to be suppressed. In this scenario, inhibition of MRCK may act as a switch between two different states of MLC phosphorylation: from single phsophorylated MLC (pMLC; regulated by MRCK) to double phosphorylated MLC (ppMLC; regulated by ROCK). Previous data from the Fujita laboratory support this hypothesis. Active ROCK was indeed shown to be necessary for extrusion and to regulate double phosphorylation of MLC in our system (Hogan et al., 2009). Unfortunately, due to problems with immunostaining for pMLC, we are currently unable to confirm our predictions. In fact, according to our latest preliminary data, there is some basal accumulation of pMLC in Ras^{V12} cells prior to their extrusion, and this seems to be reduced in MRCK-depleted cells. It is possible that active myosin II located basally promotes cell attachment to the matrix; hence, inactivation of MRCK leads to more efficient extrusion. Indeed, MRCK has been previously implicated in the maintenance of focal adhesions (Dong et al., 2002). Moreover, myosin contractility is an established functional switch between accumulation of maturation factors at focal contacts and their disassembly (Kuo et al., 2011).

To verify our theory of MRCK modulating the attachment of Ras^{V12} cells and contributing to their extrusion, we will assess the appearance of focal adhesions and stress fibres in MRCK depleted cells and optimise pMLC immunostaining. Finally, we will construct phosphomimetic mutant versions of MRCKβ in which the sites of interest are replaced with D (to mimic permanent phosporylation) or A (to mimic the lack of phosphorylation). We will transfect these constructs into MRCK-depeted Ras^{V12} cells to assess the involvement of identified phosphorylation sites in regulation of the kinase activity as well as their role in extrusion.

CHAPTER 8:

FINAL DISCUSSION

CHAPTER 8: FINAL DISCUSSION

8.1 SUMMARY OF DATA PRESENTED

In this thesis, I present data that contribute to a better understanding of interactions between normal and transformed cells at early stages of extrusion. By performing different unbiased biochemical screens, I identified many molecules that may be important for these interactions. I also confirmed that three of the identified proteins have a role in extrusion and that inhibiting their functions results in changing the dynamics this process.

8.2 IS EXTRUSION STRESSFUL?

The first important finding described in this thesis is the upregulation of the molecular chaperone Hsp90 in transformed cells surrounded by normal neighbours. Decreasing Hsp90 activity either by treatment with the inhibitor celastrol or using a dominant negative form of this protein in our system resulted in enhanced extrusion of Ras^{V12} cells. Since the change in the amount of Hsp90 was non-cell-autonomous, it appears that transformed cells undergo some form of stress during extrusion possibly caused by the necessary changes in the protein expression programme, in an analogous manner to upregulation of certain heat shock proteins in cells entering the cell cycle. The mechanism that leads to upregulation of this chaperone is not known. Alternatively, Hsp90 could also be overexpressed in order to perform a more specific function and serve as a chaperone for a particular client. The results from the 2D gel screen indeed indicated that Hsp90 forms an altered complex, suggesting that interaction between normal and transformed cells changes its client(s). During this study, however, we were unable to identify a specific binding partner of Hsp90 in cocultures.

Involvement of another chaperone was demonstrated in cell competition in *Drosophila*. dSparc, also known as osteonectin, is upregulated in 'loser' cells at early stages of several different types of cell competition (details in section 1.3.5).

The role attributed to dSparc is to transiently protect these cells from activation of caspases and to delay their apoptosis (Portela et al., 2010). Moreover, human SPARC was found to be overexpressed at the boundaries between tumour mass and surrounding normal tissues, suggesting that its expression is also affected by contacts between normal and altered cells (Petrova et al., 2011). Similarly, Hsp90α was found upregulated in different types of cancer (Kang et al., ; Ogata et al., 2000). High expression levels of both chaperones were correlated with poor prognosis for patients, and often with increased metastasis (Chen et al., 2011; Derosa et al., 2012; Pick et al., 2007; Zhao et al., 2010). Our data suggest that during Ras-mediated extrusion Hsp90 could play a corresponding protective role as dSparc in cell competition. Taken a step further, the analogy with dSparc places Ras^{V12} cells in the position of 'losers'. Following the hypothesis of an intrinsic epithelial immune response leading to clearance of transformed 'intruders', perhaps the theory behind the role of Hsp90 in cancer should be revisited. Apart from managing proteolytic stress triggered by transformation itself, this central cellular chaperone could also buffer competition-related signalling from normal epithelium to tumours.

8.3 ATTACHMENT MUST BE MODIFIED DURING EXTRUSION

The results of the SILAC screen performed in this study brought to our attention a large group of proteins modified in transformed cells upon interaction with normal cells. While most of the proteins will be left for future analyses due to the limited time available, here we concentrated on molecules previously implicated in cytoskeleton rearrangements: VASP and MRCKβ. Depletion of either VASP or MRCKβ in Ras^{V12} cells led to increased extrusion rates of these cells from normal monolayers. My data show that VASP is important for formation of stress fibres and maturation of focal adhesions in Ras^{V12} cells. The lack of well-defined basal adhesion structures in VASP-depleted transformed cells is most likely the cause for their loosened attachment and more efficient extrusion from normal monolayers. In the near future, we will aim to confirm that phosphorylation of VASP, which we found upregulated in the screen, has a corresponding effect on attachment of Ras^{V12} cells to VASP depletion, and is an

actual step in extrusion. Preliminary data we obtained suggest that MRCKβ could also be involved in altering attachment of transformed cells.

Identification of proteins regulating mechanical aspects of extrusion is an important progress in understanding this process. Until now, we have been unable to pinpoint pathways involved in disassembly of focal contacts. Our current findings can be related to the recent analysis of clonal outgrowth of single transformed cells carried out in acinar structures (Leung and Brugge, 2012). In this study, sole depletion of talin led to luminal translocation of otherwise normal epithelial cells. Although in our system loosening attachment is not sufficient for extrusion to occur and the presence of an active oncoprotein is necessary, we began to dissect the complex process of extrusion into separate stages, which eventually will lead us to a full understanding of this phenomenon.

8.4 OTHER CYTOSKELETAL ISSUES – HOW DOES THE NUCLEUS TRAVEL?

During extrusion not only attachment is modified in Ras^{V12} cells. Their whole cellular shape is changed from columnar into droplet-like with the nucleus localized apically. It does not come as a surprise that apart from VASP and MRCKβ other cytoskeletal proteins were identified in the SILAC screen, e.g. tensin, vimentin and plectin. In particular, plectin drew our attention since it had previously been identified in an independent screen for tyrosine-phosphorylated proteins as increased in cocultures of Ras^{V12} and MDCK cells (chapter 4) as well as in mixed populations of Src- and Scribble-transformed cells with normal neighbours (unpublished data from the Fujita laboratory). This enormous scaffold protein ties the three major types of filaments together: microfilaments, microtubules and intermediate filaments. Therefore, it seems very plausible that plectin function is regulated during a process that requires major alterations of cell shape as does extrusion.

The nuclear lift occurring during extrusion is one of the likely candidate events dependent on the interplay between vimentin filaments, plectin and actin cytoskeleton. Intriguingly, although blebbistatin was shown to inhibit the nuclear relocation, no actin accumulation around the nucleus was ever observed. It is

possible that this process is mediated by intermediate filaments present in the cytoplasm of Ras^{V12} transformed cells. Both plectin and vimentin appear to form nuclear rings in Ras^{V12} cells (data not shown), and in case of vimentin, we found it accumulated in already extruded Ras^{V12} cells (data not shown). Perhaps similarly to a process of actin-dependent positioning of the nucleus in migrating as well as immobile astrocytes, intermediate filaments are the missing link that transmits the tension from peripheral actin to the nucleus (Dupin et al., 2011). Further studies are necessary to shed some light on the process of nuclear relocation and its consequences for extrusion.

8.5 IMPLICATIONS OF THE NITRIC OXIDE HYPOTHESIS

The finding of upregulated phosphorylation of S239 in VASP in Ras^{V12} cells cocultured with normal cells brought up an entirely new question. PKG, a kinase that is nearly exclusively responsible for phosphorylation of S239 *in vivo* across different cell types, is often regulated by NO. If this pathway participates in modification of VASP in our system, it would be crucial to know which cells produce NO. Synthesis of this molecule could well be a part of the hypothesised epithelial immune response leading to the removal of transformed cells from a monolayer. Additionally, NO present in Ras^{V12} cells would also affect metabolism of these cells. Incidentally, during this study a non-cell-autonomous decrease of mitochondrial membrane potential in Ras^{V12} cells surrounded by normal cells was discovered (data not shown), supporting the notion of disturbed metabolism.

Interestingly, activation of p38 MAPK, which drives apoptosis of outcompeted Scribble cells (Norman et al., 2012), has not only often been shown to correlate with increases in NO levels in endothelial cells (Sanchez et al., 2012), but also to mediate NO-induced apoptosis in mouse embryonic stem cells (mES) (Lee et al., 2012). It would be exciting to know if p38 is activated during extrusion of Ras^{V12} cells and whether NO could be a common denominator between the Scribble and the Ras systems.

8.6 ARE TRANSFORMED CELLS ACTIVE OR PASSIVE IN EXTRUSION?

Another intriguing question arises with the appealing hypothesis of an innate immune response of the epithelium against transformed cells: why are Ras^{V12} cells not killed in a similar fashion to Scribble cells? Perhaps extrusion of this particular type of transformed cells is not passive. They might be using collective migration to escape from aggressive neighbours before the threshold of the proapoptotic epithelial signals is achieved. There are several lines of evidence supporting the hypothesis of active rather than passive extrusion.

Firstly, before extrusion Ras^{V12} cells repolarise: the nucleus is translocated from a basal to an apical position, while the Golgi apparatus (GA) as well as the endoplasmic reticulum (ER) are moved in the opposite direction and in tall cells localize below the nucleus (data not shown). This change in polarisation is accompanied by the disassembly of focal adhesions (vinculin is nearly completely lost from these structures once cells become taller) as well as by relocation of basolateral polarity marker, Scribble, from the predominantly lateral to the basal area (data not shown). At this point, however, adherence junctions are preserved. In fact, both E-cadherin as well as F-actin accumulate gradually between the neighbouring Ras^{V12} cells within normal monolayers prior to and after extrusion. This accumulation might contribute to creating tension between transformed cells, which allows them later to collectively push themselves out of the monolayer. According to our unquantified observation, if a single transformed cell surrounded only by normal neighbours undergoes extrusion, it does not proliferate but remains in a cytostatic state on the top of the monolayer without incorporating ethidium dye for at least 50 hours. Hence, it is possible that for evading apoptotic/cytostatic signals, Ras^{V12} cells need to emigrate in groups.

Secondly, vimentin, a marker of epithelial to mesenchymal transition (EMT) is upregulated in Ras^{V12} cells prior to their extrusion and further accumulates in already extruded cells (data not shown).

Finally, active Rho and Cdc42 present in Ras^{V12} cells are required for extrusion to occur (Hogan et al., 2009). As mentioned earlier, these two major small GTP-ases are well known regulators of cytoskeletal rearrangements implicated in cell migration. Since depletion of MRCK in our system results in

quicker extrusion, it is possible that a switch from Cdc42-MRCK-dependent mesenchymal movement to Rho-ROCK-mediated migration is required for extrusion.

Active involvement of normal cells in extrusion was also studied in the Fujita laboratory, particularly in the Src system. Vimentin and filamin were found to accumulate in MDCK cells in contact with transformed cells and to form a ring or a 'hugging' protrusion. Furthermore, depletion of filamin prevented extrusion of Src cells [under submission]. These findings clearly show that normal cells dynamically pursue elimination of their neighbours either by squeezing them out of the monolayer or transducing signals in a filamin-dependent manner to their transformed neighbours.

From all the gathered data and observations, it appears that both sides, normal and transformed, could play an active role during extrusion and the final result most likely depends on an interplay between these two cell types.

8.7 QUESTIONS FOR THE FUTURE

Currently a lot of questions as to extrusion and its significance lack answers. Most importantly, we have still not determined how normal and transformed cells recognise each other. Although this thesis marks out a few new directions that could be taken to shed more light on the pathways activated upon recognition, we cannot be sure, what the actual role of extrusion is. It might be a part of an immune response: extruded cells could be eliminated directly by the immune system or through exposure to harsh conditions in the lumen of urinal tacks, intestines, etc. Alternatively, extrusion could play a role in tumour formation, for example in growth of glandular tumours (breat, pancrease, etc) that often fill the apical lumen of an organ. On the other hand, extrusion could be a prelude to early metastasis. Perhaps extruded cells migrate to a more supportive environment to develop into tumours. It is also possible that the directionality of extrusion is biased *in vitro*. Perhaps, *in vivo* in vertebrates transformed cells at this early stage of cancerogenesis migrate underneath the epithelium to metastasise in a previously described for advanced tumours fashion.

Considerable amount of support could come from the latest research in *Drosophila*, which prove that cell competition, similar in many aspects to the phenomena studied in mammalian systems, is not only a developmental process. Competition has recently been observed also in epithelia of adult flies (de Navascues et al., 2012). It is likely that parallels drawn between the two models will lead to a better understanding of extrusion and its role in tumuorigenesis.

ACKNOWLEDGEMENTS

Firstly, I would like to thank both my PIs: Prof Yasu Fujita and Prof Karl Matter. Thank you, Yasu, for infecting me with the extrusion bug, for inspiring and encouraging me every step of the way. Karl, I am most grateful to you for adopting me and my project, for extending a helping hand during a difficult time and for your guidance.

This thesis would not come into existence without help and input from Dr Claus Jorgensen and Dr John Sinclair, who have collaborated with me on the SILAC project. Claus, thank you for your enthusiasm and generosity. Your lab in the ICR was, for a while, the only place where I could hide from all the changes and storms that happened around me. I will always appreciate your support.

I would like to thank Dr Catherine Hogan for introducing me to the project, for showing me how science works and for helping along the way with all scientific and non-scientific issues. Catherine, Mihoko and Mark, thank you for creating a great atmosphere in the lab. I will always remember our journal clubs, lab meetings, dinners and hikes.

I would also like to show my appreciation to the Matter lab, who welcomed me over a year ago, particularly to Elisa and Ahmed. Thank you, guys, for all your moral and scientific support, for listening patiently about all the disasters and cheering me up with coffee, sweets and activities. I could not have wished for better friends than you.

Going through my PhD would have been much more difficult without the help and support of my year group: Liz, Sinead, Catia and Justynka. There is nothing more comforting than knowing that you are not alone in your struggle. A special thank you to you, Liz, for always finding time to grab a cup of coffee, to listen, and to go back in time to our UCSF days, and for simply being a wonderful friend.

Finally, I would like to thank my family, and in particular my parents. Dziekuje Wam, ze zawsze stoicie obok mnie, za wsparcie, za pomoc, za troske. Dziekuje, ze pozwoliscie mi rozwinac skrzydla i ze ufacie moim wyborom. Bez Was,

ta praca nigdy by nie powstala. I am also grateful to my newly acquired in-laws, for all their warmth and love. It is a privilege to become a part of your family.

Most of all, I would like to thank my wonderful husband. You are the most precious result I got from my PhD. Thank you for your patience and understanding, accepting all the spoilt weekends, cold meals, tragedies and tears. Thank you for your smile and hugs, for your persistence and support. Without you, I would never have been able to finish.

REFERENCES

Ahearn, I.M., K. Haigis, D. Bar-Sagi, and M.R. Philips. 2012. Regulating the regulator: post-translational modification of RAS. *Nat Rev Mol Cell Biol*. 13:39-51.

Alexander, D.B., H. Ichikawa, J.F. Bechberger, V. Valiunas, M. Ohki, C.C. Naus, T. Kunimoto, H. Tsuda, W.T. Miller, and G.S. Goldberg. 2004. Normal cells control the growth of neighboring transformed cells independent of gap junctional communication and SRC activity. *Cancer Res*. 64:1347-58.

Allen, P.G., and J.V. Shah. 1999. Brains and brawn: plectin as regulator and reinforcer of the cytoskeleton. *Bioessays*. 21:451-4.

Annamalai, B., X. Liu, U. Gopal, and J.S. Isaacs. 2009. Hsp90 is an essential regulator of EphA2 receptor stability and signaling: implications for cancer cell migration and metastasis. *Mol Cancer Res*. 7:1021-32.

Aszodi, A., A. Pfeifer, M. Ahmad, M. Glauner, X.H. Zhou, L. Ny, K.E. Andersson, B. Kehrel, S. Offermanns, and R. Fassler. 1999. The vasodilator-stimulated phosphoprotein (VASP) is involved in cGMP- and cAMP-mediated inhibition of agonist-induced platelet aggregation, but is dispensable for smooth muscle function. *Embo J*. 18:37-48.

Bai, Y., H. Edamatsu, S. Maeda, H. Saito, N. Suzuki, T. Satoh, and T. Kataoka. 2004. Crucial role of phospholipase Cepsilon in chemical carcinogen-induced skin tumor development. *Cancer Res*. 64:8808-10.

Baines, A.T., D. Xu, and C.J. Der. 2011. Inhibition of Ras for cancer treatment: the search continues. *Future Med Chem*. 3:1787-808.

Bandyopadhyay, S., C.Y. Chiang, J. Srivastava, M. Gersten, S. White, R. Bell, C. Kurschner, C.H. Martin, M. Smoot, S. Sahasrabudhe, D.L. Barber, S.K. Chanda, and T. Ideker. 2010. A human MAP kinase interactome. *Nat Methods*. 7:801-5.

Bear, J.E., and F.B. Gertler. 2009. Ena/VASP: towards resolving a pointed controversy at the barbed end. *J Cell Sci*. 122:1947-53.

Bear, J.E., T.M. Svitkina, M. Krause, D.A. Schafer, J.J. Loureiro, G.A. Strasser, I.V. Maly, O.Y. Chaga, J.A. Cooper, G.G. Borisy, and F.B. Gertler. 2002. Antagonism between Ena/VASP proteins and actin filament capping regulates fibroblast motility. *Cell*. 109:509-21.

Becker, E.M., P. Schmidt, M. Schramm, H. Schroder, U. Walter, M. Hoenicka, R. Gerzer, and J.P. Stasch. 2000. The vasodilator-stimulated phosphoprotein (VASP): target of YC-1 and nitric oxide effects in human and rat platelets. *J Cardiovasc Pharmacol*. 35:390-7.

Benz, P.M., C. Blume, J. Moebius, C. Oschatz, K. Schuh, A. Sickmann, U. Walter, S.M. Feller, and T. Renne. 2008. Cytoskeleton assembly at endothelial cell-cell contacts is regulated by alphaII-spectrin-VASP complexes. *J Cell Biol*. 180:205-19.

Benz, P.M., C. Blume, S. Seifert, S. Wilhelm, J. Waschke, K. Schuh, F. Gertler, T. Munzel, and T. Renne. 2009. Differential VASP phosphorylation controls remodeling of the actin cytoskeleton. *J Cell Sci*. 122:3954-65.

Bergerat, A., B. de Massy, D. Gadelle, P.C. Varoutas, A. Nicolas, and P. Forterre. 1997. An atypical topoisomerase II from Archaea with implications for meiotic recombination. *Nature*. 386:414-7.

Bignami, M., S. Rosa, G. Falcone, F. Tato, F. Katoh, and H. Yamasaki. 1988. Specific viral oncogenes cause differential effects on cell-to-cell communication, relevant to the suppression of the transformed phenotype by normal cells. *Mol Carcinog*. 1:67-75.

Blume, C., P.M. Benz, U. Walter, J. Ha, B.E. Kemp, and T. Renne. 2007. AMP-activated protein kinase impairs endothelial actin cytoskeleton assembly by phosphorylating vasodilator-stimulated phosphoprotein. *J Biol Chem*. 282:4601-12.

Bondar, T., and R. Medzhitov. 2010. p53-mediated hematopoietic stem and progenitor cell competition. *Cell Stem Cell*. 6:309-22.

Borek, C., and L. Sachs. 1966. The difference in contact inhibition of cell replication between normal cells and cells transformed by different carcinogens. *Proc Natl Acad Sci U S A*. 56:1705-11.

Brindle, N.P., M.R. Holt, J.E. Davies, C.J. Price, and D.R. Critchley. 1996. The focal-adhesion vasodilator-stimulated phosphoprotein (VASP) binds to the proline-rich domain in vinculin. *Biochem J*. 318 (Pt 3):753-7.

Brumby, A.M., and H.E. Richardson. 2003. scribble mutants cooperate with oncogenic Ras or Notch to cause neoplastic overgrowth in Drosophila. *Embo J*. 22:5769-79.

Butt, E., K. Abel, M. Krieger, D. Palm, V. Hoppe, J. Hoppe, and U. Walter. 1994. cAMP- and cGMP-dependent protein kinase phosphorylation sites of the focal adhesion vasodilator-stimulated phosphoprotein (VASP) in vitro and in intact human platelets. *J Biol Chem*. 269:14509-17.

Chadli, A., S.J. Felts, Q. Wang, W.P. Sullivan, M.V. Botuyan, A. Fauq, M. Ramirez-Alvarado, and G. Mer. 2010. Celastrol inhibits Hsp90 chaperoning of steroid receptors by inducing fibrillization of the Co-chaperone p23. *J Biol Chem*. 285:4224-31.

Chen, C.L., M.C. Schroeder, M. Kango-Singh, C. Tao, and G. Halder. 2012. Tumor suppression by cell competition through regulation of the Hippo pathway. *Proc Natl Acad Sci U S A*. 109:484-9.

Chen, L., G. Daum, K. Chitaley, S.A. Coats, D.F. Bowen-Pope, M. Eigenthaler, N.R. Thumati, U. Walter, and A.W. Clowes. 2004. Vasodilator-stimulated phosphoprotein regulates proliferation and growth inhibition by nitric oxide in vascular smooth muscle cells. *Arterioscler Thromb Vasc Biol*. 24:1403-8.

Chen, W.S., C.C. Lee, Y.M. Hsu, C.C. Chen, and T.S. Huang. 2011. Identification of heat shock protein 90alpha as an IMH-2 epitope-associated protein and correlation of its mRNA overexpression with colorectal cancer metastasis and poor prognosis. *Int J Colorectal Dis*. 26:1009-17.

Chesarone, M.A., and B.L. Goode. 2009. Actin nucleation and elongation factors: mechanisms and interplay. *Curr Opin Cell Biol*. 21:28-37.

Chitaley, K., L. Chen, A. Galler, U. Walter, G. Daum, and A.W. Clowes. 2004. Vasodilator-stimulated phosphoprotein is a substrate for protein kinase C. *FEBS Lett*. 556:211-5.

Ciobanasu, C., B. Faivre, and C. Le Clainche. 2012. Actin dynamics associated with focal adhesions. *Int J Cell Biol*. 2012:941292.

Coppolino, M.G., M. Krause, P. Hagendorff, D.A. Monner, W. Trimble, S. Grinstein, J. Wehland, and A.S. Sechi. 2001. Evidence for a molecular complex consisting of Fyb/SLAP, SLP-76, Nck, VASP and WASP that links the actin cytoskeleton to Fcgamma receptor signalling during phagocytosis. *J Cell Sci*. 114:4307-18.

Cordero, J.B., J.P. Macagno, R.K. Stefanatos, K.E. Strathdee, R.L. Cagan, and M. Vidal. 2010. Oncogenic Ras diverts a host TNF tumor suppressor activity into tumor promoter. *Dev Cell*. 18:999-1011.

Cox, A.D., and C.J. Der. 2010. Ras history: The saga continues. *Small GTPases*. 1:2-27.

de la Cova, C., M. Abril, P. Bellosta, P. Gallant, and L.A. Johnston. 2004. Drosophila myc regulates organ size by inducing cell competition. *Cell*. 117:107-16.

de Navascues, J., C.N. Perdigoto, Y. Bian, M.H. Schneider, A.J. Bardin, A. Martinez-Arias, and B.D. Simons. 2012. Drosophila midgut homeostasis involves neutral competition between symmetrically dividing intestinal stem cells. *Embo J*. 31:2473-85.

DeBoer, C., P.A. Meulman, R.J. Wnuk, and D.H. Peterson. 1970. Geldanamycin, a new antibiotic. *J Antibiot (Tokyo)*. 23:442-7.

Derosa, C.A., B. Furusato, S. Shaheduzzaman, V. Srikantan, Z. Wang, Y. Chen, M. Seifert, L. Ravindranath, D. Young, M. Nau, A. Dobi, T. Werner, D.G. McLeod, M.T.

Vahey, I.A. Sesterhenn, S. Srivastava, and G. Petrovics. 2012. Elevated osteonectin/SPARC expression in primary prostate cancer predicts metastatic progression. *Prostate Cancer Prostatic Dis*. 15:150-6.

Dong, J.M., T. Leung, E. Manser, and L. Lim. 2002. Cdc42 antagonizes inductive action of cAMP on cell shape, via effects of the myotonic dystrophy kinase-related Cdc42-binding kinase (MRCK) on myosin light chain phosphorylation. *Eur J Cell Biol*. 81:231-42.

Dupin, I., Y. Sakamoto, and S. Etienne-Manneville. 2011. Cytoplasmic intermediate filaments mediate actin-driven positioning of the nucleus. *J Cell Sci*. 124:865-72.

Dupre-Crochet, S., A. Figueroa, C. Hogan, E.C. Ferber, C.U. Bialucha, J. Adams, E.C. Richardson, and Y. Fujita. 2007. Casein kinase 1 is a novel negative regulator of E-cadherin-based cell-cell contacts. *Mol Cell Biol*. 27:3804-16.

Durrwang, U., S. Fujita-Becker, M. Erent, F.J. Kull, G. Tsiavaliaris, M.A. Geeves, and D.J. Manstein. 2006. Dictyostelium myosin-IE is a fast molecular motor involved in phagocytosis. *J Cell Sci*. 119:550-8.

Duval, M., F. Le Boeuf, J. Huot, and J.P. Gratton. 2007. Src-mediated phosphorylation of Hsp90 in response to vascular endothelial growth factor (VEGF) is required for VEGF receptor-2 signaling to endothelial NO synthase. *Mol Biol Cell*. 18:4659-68.

Ellis, C.A., and G. Clark. 2000. The importance of being K-Ras. *Cell Signal*. 12:425-34.

Etienne-Manneville, S., and A. Hall. 2002. Rho GTPases in cell biology. *Nature*. 420:629-35.

Fasolo, A., and C. Sessa. 2012. Targeting mTOR pathways in human malignancies. *Curr Pharm Des*. 18:2766-77.

Ferro, E., and L. Trabalzini. 2010. RalGDS family members couple Ras to Ral signalling and that's not all. *Cell Signal*. 22:1804-10.

Flaherty, K.T., I. Puzanov, K.B. Kim, A. Ribas, G.A. McArthur, J.A. Sosman, P.J. O'Dwyer, R.J. Lee, J.F. Grippo, K. Nolop, and P.B. Chapman. 2010. Inhibition of mutated, activated BRAF in metastatic melanoma. *N Engl J Med*. 363:809-19.

Froldi, F., M. Ziosi, F. Garoia, A. Pession, N.A. Grzeschik, P. Bellosta, D. Strand, H.E. Richardson, A. Pession, and D. Grifoni. 2010. The lethal giant larvae tumour suppressor mutation requires dMyc oncoprotein to promote clonal malignancy. *BMC Biol*. 8:33.

Furman, C., A.L. Sieminski, A.V. Kwiatkowski, D.A. Rubinson, E. Vasile, R.T. Bronson, R. Fassler, and F.B. Gertler. 2007. Ena/VASP is required for endothelial barrier function in vivo. *J Cell Biol*. 179:761-75.

Gaggioli, C., S. Hooper, C. Hidalgo-Carcedo, R. Grosse, J.F. Marshall, K. Harrington, and E. Sahai. 2007. Fibroblast-led collective invasion of carcinoma cells with differing roles for RhoGTPases in leading and following cells. *Nat Cell Biol*. 9:1392-400.

Gomes, E.R., S. Jani, and G.G. Gundersen. 2005. Nuclear movement regulated by Cdc42, MRCK, myosin, and actin flow establishes MTOC polarization in migrating cells. *Cell*. 121:451-63.

Gordon, M., and S. Baksh. 2011. RASSF1A: Not a prototypical Ras effector. *Small GTPases*. 2:148-157.

Grashoff, C., B.D. Hoffman, M.D. Brenner, R. Zhou, M. Parsons, M.T. Yang, M.A. McLean, S.G. Sligar, C.S. Chen, T. Ha, and M.A. Schwartz. 2010. Measuring mechanical tension across vinculin reveals regulation of focal adhesion dynamics. *Nature*. 466:263-6.

Green, D.R. 2010. Cell competition: pirates on the tangled bank. *Cell Stem Cell*. 6:287-8.

Grenert, J.P., W.P. Sullivan, P. Fadden, T.A. Haystead, J. Clark, E. Mimnaugh, H. Krutzsch, H.J. Ochel, T.W. Schulte, E. Sausville, L.M. Neckers, and D.O. Toft. 1997. The amino-terminal domain of heat shock protein 90 (hsp90) that binds geldanamycin is an ATP/ADP switch domain that regulates hsp90 conformation. *J Biol Chem*. 272:23843-50.

Grzeschik, N.A., N. Amin, J. Secombe, A.M. Brumby, and H.E. Richardson. 2007. Abnormalities in cell proliferation and apico-basal cell polarity are separable in Drosophila lgl mutant clones in the developing eye. *Dev Biol*. 311:106-23.

Haigis, K.M., K.R. Kendall, Y. Wang, A. Cheung, M.C. Haigis, J.N. Glickman, M. Niwa-Kawakita, A. Sweet-Cordero, J. Sebolt-Leopold, K.M. Shannon, J. Settleman, M. Giovannini, and T. Jacks. 2008. Differential effects of oncogenic K-Ras and N-Ras on proliferation, differentiation and tumor progression in the colon. *Nat Genet*. 40:600-8.

Halbrugge, M., and U. Walter. 1989. Purification of a vasodilator-regulated phosphoprotein from human platelets. *Eur J Biochem*. 185:41-50.

Hanahan, D., and R.A. Weinberg. 2000. The hallmarks of cancer. *Cell*. 100:57-70.

Hanahan, D., and R.A. Weinberg. 2011. Hallmarks of cancer: the next generation. *Cell*. 144:646-74.

Heidorn, S.J., C. Milagre, S. Whittaker, A. Nourry, I. Niculescu-Duvas, N. Dhomen, J. Hussain, J.S. Reis-Filho, C.J. Springer, C. Pritchard, and R. Marais. 2010. Kinase-dead BRAF and oncogenic RAS cooperate to drive tumor progression through CRAF. *Cell*. 140:209-21.

Hieronymus, H., J. Lamb, K.N. Ross, X.P. Peng, C. Clement, A. Rodina, M. Nieto, J. Du, K. Stegmaier, S.M. Raj, K.N. Maloney, J. Clardy, W.C. Hahn, G. Chiosis, and T.R. Golub. 2006. Gene expression signature-based chemical genomic prediction identifies a novel class of HSP90 pathway modulators. *Cancer Cell*. 10:321-30.

Hogan, C., S. Dupre-Crochet, M. Norman, M. Kajita, C. Zimmermann, A.E. Pelling, E. Piddini, L.A. Baena-Lopez, J.P. Vincent, Y. Itoh, H. Hosoya, F. Pichaud, and Y. Fujita. 2009. Characterization of the interface between normal and transformed epithelial cells. *Nat Cell Biol*. 11:460-7.

Hu, H., J.M. Bliss, Y. Wang, and J. Colicelli. 2005. RIN1 is an ABL tyrosine kinase activator and a regulator of epithelial-cell adhesion and migration. *Curr Biol*. 15:815-23.

Hunter, T. 1980. Protein phosphorylated by the RSV transforming function. *Cell*. 22:647-8.

Igaki, T., J.C. Pastor-Pareja, H. Aonuma, M. Miura, and T. Xu. 2009. Intrinsic tumor suppression and epithelial maintenance by endocytic activation of Eiger/TNF signaling in Drosophila. *Dev Cell*. 16:458-65.

Jaeger, V., S. Hoppe, P. Petermann, T. Liebig, M.K. Jansen, T. Renne, and D. Knebel-Morsdorf. 2010. Herpes simplex virus type 1 entry into epithelial MDCKII cells: role of VASP activities. *J Gen Virol*. 91:2152-7.

Jarosz, D.F., and S. Lindquist. 2010. Hsp90 and environmental stress transform the adaptive value of natural genetic variation. *Science*. 330:1820-4.

Jorgensen, C., A. Sherman, G.I. Chen, A. Pasculescu, A. Poliakov, M. Hsiung, B. Larsen, D.G. Wilkinson, R. Linding, and T. Pawson. 2009. Cell-specific information processing in segregating populations of Eph receptor ephrin-expressing cells. *Science*. 326:1502-9.

Kajiho, H., K. Sakurai, T. Minoda, M. Yoshikawa, S. Nakagawa, S. Fukushima, K. Kontani, and T. Katada. 2011. Characterization of RIN3 as a guanine nucleotide exchange factor for the Rab5 subfamily GTPase Rab31. *J Biol Chem*. 286:24364-73.

Kajita, M., C. Hogan, A.R. Harris, S. Dupre-Crochet, N. Itasaki, K. Kawakami, G. Charras, M. Tada, and Y. Fujita. 2010. Interaction with surrounding normal epithelial cells influences signalling pathways and behaviour of Src-transformed cells. *J Cell Sci*. 123:171-80.

Kamal, A., L. Thao, J. Sensintaffar, L. Zhang, M.F. Boehm, L.C. Fritz, and F.J. Burrows. 2003. A high-affinity conformation of Hsp90 confers tumour selectivity on Hsp90 inhibitors. *Nature*. 425:407-10.

Kang, G.H., E.J. Lee, K.T. Jang, K.M. Kim, C.K. Park, C.S. Lee, D.Y. Kang, S.H. Lee, T.S. Sohn, and S. Kim. Expression of HSP90 in gastrointestinal stromal tumours and mesenchymal tumours. *Histopathology*. 56:694-701.

Karnoub, A.E., and R.A. Weinberg. 2008. Ras oncogenes: split personalities. *Nat Rev Mol Cell Biol*. 9:517-31.

Katada, K., T. Tomonaga, M. Satoh, K. Matsushita, Y. Tonoike, Y. Kodera, T. Hanazawa, F. Nomura, and Y. Okamoto. 2012. Plectin promotes migration and invasion of cancer cells and is a novel prognostic marker for head and neck squamous cell carcinoma. *J Proteomics*. 75:1803-15.

Khokhlatchev, A., S. Rabizadeh, R. Xavier, M. Nedwidek, T. Chen, X.F. Zhang, B. Seed, and J. Avruch. 2002. Identification of a novel Ras-regulated proapoptotic pathway. *Curr Biol*. 12:253-65.

Kimura, T., T. Sakisaka, T. Baba, T. Yamada, and Y. Takai. 2006. Involvement of the Ras-Ras-activated Rab5 guanine nucleotide exchange factor RIN2-Rab5 pathway in the hepatocyte growth factor-induced endocytosis of E-cadherin. *J Biol Chem*. 281:10598-609.

Kongsuwan, K., Q. Yu, A. Vincent, M.C. Frisardi, M. Rosbash, J.A. Lengyel, and J. Merriam. 1985. A Drosophila Minute gene encodes a ribosomal protein. *Nature*. 317:555-8.

Kovacs, J.J., P.J. Murphy, S. Gaillard, X. Zhao, J.T. Wu, C.V. Nicchitta, M. Yoshida, D.O. Toft, W.B. Pratt, and T.P. Yao. 2005. HDAC6 regulates Hsp90 acetylation and chaperone-dependent activation of glucocorticoid receptor. *Mol Cell*. 18:601-7.

Krek, W., and E.A. Nigg. 1991. Differential phosphorylation of vertebrate p34cdc2 kinase at the G1/S and G2/M transitions of the cell cycle: identification of major phosphorylation sites. *Embo J*. 10:305-16.

Kubota, H., S. Yamamoto, E. Itoh, Y. Abe, A. Nakamura, Y. Izumi, H. Okada, M. Iida, H. Nanjo, H. Itoh, and Y. Yamamoto. 2010. Increased expression of co-chaperone HOP with HSP90 and HSC70 and complex formation in human colonic carcinoma. *Cell Stress Chaperones*. 15:1003-11.

Kundrat, L., and L. Regan. 2010. Balance between folding and degradation for Hsp90-dependent client proteins: a key role for CHIP. *Biochemistry*. 49:7428-38.

Kuo, J.C., X. Han, C.T. Hsiao, J.R. Yates, 3rd, and C.M. Waterman. 2011. Analysis of the myosin-II-responsive focal adhesion proteome reveals a role for beta-Pix in negative regulation of focal adhesion maturation. *Nat Cell Biol*. 13:383-93.

Kyriakis, J.M. 2009. Thinking outside the box about Ras. *J Biol Chem*. 284:10993-4.

Lai, B.T., N.W. Chin, A.E. Stanek, W. Keh, and K.W. Lanks. 1984. Quantitation and intracellular localization of the 85K heat shock protein by using monoclonal and polyclonal antibodies. *Mol Cell Biol*. 4:2802-10.

Lambrechts, A., A.V. Kwiatkowski, L.M. Lanier, J.E. Bear, J. Vandekerckhove, C. Ampe, and F.B. Gertler. 2000. cAMP-dependent protein kinase phosphorylation of EVL, a Mena/VASP relative, regulates its interaction with actin and SH3 domains. *J Biol Chem*. 275:36143-51.

Land, H., L.F. Parada, and R.A. Weinberg. 1983. Tumorigenic conversion of primary embryo fibroblasts requires at least two cooperating oncogenes. *Nature*. 304:596-602.

Lapointe, J., C. Li, J.P. Higgins, M. van de Rijn, E. Bair, K. Montgomery, M. Ferrari, L. Egevad, W. Rayford, U. Bergerheim, P. Ekman, A.M. DeMarzo, R. Tibshirani, D. Botstein, P.O. Brown, J.D. Brooks, and J.R. Pollack. 2004. Gene expression profiling identifies clinically relevant subtypes of prostate cancer. *Proc Natl Acad Sci U S A*. 101:811-6.

Lee, J.H., S.W. Lee, S.H. Choi, S.H. Kim, W.J. Kim, and J.Y. Jung. 2012. p38 MAP kinase and ERK play an important role in nitric oxide-induced apoptosis of the mouse embryonic stem cells. *Toxicol In Vitro*.

Leung, C.T., and J.S. Brugge. 2012. Outgrowth of single oncogene-expressing cells from suppressive epithelial environments. *Nature*. 482:410-3.

Li, J., L. Sun, C. Xu, F. Yu, H. Zhou, Y. Zhao, J. Zhang, J. Cai, C. Mao, L. Tang, Y. Xu, and J. He. 2012. Structure insights into mechanisms of ATP hydrolysis and the activation of human heat-shock protein 90. *Acta Biochim Biophys Sin (Shanghai)*. 44:300-6.

Linares, J.F., R. Amanchy, K. Greis, M.T. Diaz-Meco, and J. Moscat. 2011. Phosphorylation of p62 by cdk1 controls the timely transit of cells through mitosis and tumor cell proliferation. *Mol Cell Biol*. 31:105-17.

Lindsay, S.L., S. Ramsey, M. Aitchison, T. Renne, and T.J. Evans. 2007. Modulation of lamellipodial structure and dynamics by NO-dependent phosphorylation of VASP Ser239. *J Cell Sci*. 120:3011-21.

Luscher, B., and J. Vervoorts. 2012. Regulation of gene transcription by the oncoprotein MYC. *Gene*. 494:145-60.

MacLean, M., and D. Picard. 2003. Cdc37 goes beyond Hsp90 and kinases. *Cell Stress Chaperones*. 8:114-9.

Malliri, A., R.A. van der Kammen, K. Clark, M. van der Valk, F. Michiels, and J.G. Collard. 2002. Mice deficient in the Rac activator Tiam1 are resistant to Ras-induced skin tumours. *Nature*. 417:867-71.

Mantoni, T.S., R.R. Schendel, F. Rodel, G. Niedobitek, O. Al-Assar, A. Masamune, and T.B. Brunner. 2008. Stromal SPARC expression and patient survival after chemoradiation for non-resectable pancreatic adenocarcinoma. *Cancer Biol Ther*. 7:1806-15.

Martinek, N., J. Shahab, J. Sodek, and M. Ringuette. 2007. Is SPARC an evolutionarily conserved collagen chaperone? *J Dent Res*. 86:296-305.

Martinek, N., R. Zou, M. Berg, J. Sodek, and M. Ringuette. 2002. Evolutionary conservation and association of SPARC with the basal lamina in Drosophila. *Dev Genes Evol*. 212:124-33.

Marusyk, A., C.C. Porter, V. Zaberezhnyy, and J. DeGregori. 2010. Irradiation selects for p53-deficient hematopoietic progenitors. *PLoS Biol*. 8:e1000324.

Massberg, S., S. Gruner, I. Konrad, M.I. Garcia Arguinzonis, M. Eigenthaler, K. Hemler, J. Kersting, C. Schulz, I. Muller, F. Besta, B. Nieswandt, U. Heinzmann, U. Walter, and M. Gawaz. 2004. Enhanced in vivo platelet adhesion in vasodilator-stimulated phosphoprotein (VASP)-deficient mice. *Blood*. 103:136-42.

McClatchey, A.I. 2007. Neurofibromatosis. *Annu Rev Pathol*. 2:191-216.

McInroy, L., and A. Maatta. 2011. Plectin regulates invasiveness of SW480 colon carcinoma cells and is targeted to podosome-like adhesions in an isoform-specific manner. *Exp Cell Res*. 317:2468-78.

Meng, W., A. Huebner, A. Shabsigh, A. Chakravarti, and T. Lautenschlaeger. 2012. Combined RASSF1A and RASSF2A Promoter Methylation Analysis as Diagnostic Biomarker for Bladder Cancer. *Mol Biol Int*. 2012:701814.

Meng, X., V. Jerome, J. Devin, E.E. Baulieu, and M.G. Catelli. 1993. Cloning of chicken hsp90 beta: the only vertebrate hsp90 insensitive to heat shock. *Biochem Biophys Res Commun*. 190:630-6.

Miao, R.Q., J. Fontana, D. Fulton, M.I. Lin, K.D. Harrison, and W.C. Sessa. 2008. Dominant-negative Hsp90 reduces VEGF-stimulated nitric oxide release and migration in endothelial cells. *Arterioscler Thromb Vasc Biol*. 28:105-11.

Millson, S.H., A.W. Truman, A. Racz, B. Hu, B. Panaretou, J. Nuttall, M. Mollapour, C. Soti, and P.W. Piper. 2007. Expressed as the sole Hsp90 of yeast, the alpha and beta isoforms of human Hsp90 differ with regard to their capacities for activation of certain client proteins, whereas only Hsp90beta generates sensitivity to the Hsp90 inhibitor radicicol. *Febs J*. 274:4453-63.

Milstein, M., C.K. Mooser, H. Hu, M. Fejzo, D. Slamon, L. Goodglick, S. Dry, and J. Colicelli. 2007. RIN1 is a breast tumor suppressor gene. *Cancer Res*. 67:11510-6.

Minami, Y., H. Kawasaki, Y. Miyata, K. Suzuki, and I. Yahara. 1991. Analysis of native forms and isoform compositions of the mouse 90-kDa heat shock protein, HSP90. *J Biol Chem*. 266:10099-103.

Minard, M.E., L.S. Kim, J.E. Price, and G.E. Gallick. 2004. The role of the guanine nucleotide exchange factor Tiam1 in cellular migration, invasion, adhesion and tumor progression. *Breast Cancer Res Treat*. 84:21-32.

Mitin, N., K.L. Rossman, and C.J. Der. 2005. Signaling interplay in Ras superfamily function. *Curr Biol*. 15:R563-74.

Morata, G., and P. Ripoll. 1975. Minutes: mutants of drosophila autonomously affecting cell division rate. *Dev Biol*. 42:211-21.

Moreno, E., and K. Basler. 2004. dMyc transforms cells into super-competitors. *Cell*. 117:117-29.

Moreno, E., K. Basler, and G. Morata. 2002. Cells compete for decapentaplegic survival factor to prevent apoptosis in Drosophila wing development. *Nature*. 416:755-9.

Moulick, K., J.H. Ahn, H. Zong, A. Rodina, L. Cerchietti, E.M. Gomes DaGama, E. Caldas-Lopes, K. Beebe, F. Perna, K. Hatzi, L.P. Vu, X. Zhao, D. Zatorska, T. Taldone, P. Smith-Jones, M. Alpaugh, S.S. Gross, N. Pillarsetty, T. Ku, J.S. Lewis, S.M. Larson, R. Levine, H. Erdjument-Bromage, M.L. Guzman, S.D. Nimer, A. Melnick, L. Neckers, and G. Chiosis. 2011. Affinity-based proteomics reveal cancer-specific networks coordinated by Hsp90. *Nat Chem Biol*. 7:818-26.

Neckers, L. 2002. Hsp90 inhibitors as novel cancer chemotherapeutic agents. *Trends Mol Med*. 8:S55-61.

Neckers, L., and P. Workman. 2012. Hsp90 molecular chaperone inhibitors: are we there yet? *Clin Cancer Res*. 18:64-76.

Neto-Silva, R.M., S. de Beco, and L.A. Johnston. 2012. Evidence for a growth-stabilizing regulatory feedback mechanism between Myc and Yorkie, the Drosophila homolog of Yap. *Dev Cell*. 19:507-20.

Newbold, R.F., and R.W. Overell. 1983. Fibroblast immortality is a prerequisite for transformation by EJ c-Ha-ras oncogene. *Nature*. 304:648-51.

Norbury, C., J. Blow, and P. Nurse. 1991. Regulatory phosphorylation of the p34cdc2 protein kinase in vertebrates. *Embo J*. 10:3321-9.

Norman, M., K.A. Wisniewska, K. Lawrenson, P. Garcia-Miranda, M. Tada, M. Kajita, H. Mano, S. Ishikawa, M. Ikegawa, T. Shimada, and Y. Fujita. 2012. Loss of Scribble causes cell competition in mammalian cells. *J Cell Sci*. 125:59-66.

Ogata, M., Z. Naito, S. Tanaka, Y. Moriyama, and G. Asano. 2000. Overexpression and localization of heat shock proteins mRNA in pancreatic carcinoma. *J Nihon Med Sch*. 67:177-85.

Pagliarini, R.A., and T. Xu. 2003. A genetic screen in Drosophila for metastatic behavior. *Science*. 302:1227-31.

Pearce, L.R., D. Komander, and D.R. Alessi. 2010. The nuts and bolts of AGC protein kinases. *Nat Rev Mol Cell Biol*. 11:9-22.

Pedraza, L.G., R.A. Stewart, D.M. Li, and T. Xu. 2004. Drosophila Src-family kinases function with Csk to regulate cell proliferation and apoptosis. *Oncogene*. 23:4754-62.

Petrova, E., D. Soldini, and E. Moreno. 2011. The expression of SPARC in human tumors is consistent with its role during cell competition. *Commun Integr Biol*. 4:171-4.

Pfeifer, G.P., R. Dammann, and S. Tommasi. 2010. RASSF proteins. *Curr Biol*. 20:R344-5.

Pick, E., Y. Kluger, J.M. Giltnane, C. Moeder, R.L. Camp, D.L. Rimm, and H.M. Kluger. 2007. High HSP90 expression is associated with decreased survival in breast cancer. *Cancer Res*. 67:2932-7.

Podhajcer, O.L., L.G. Benedetti, M.R. Girotti, F. Prada, E. Salvatierra, and A.S. Llera. 2008. The role of the matricellular protein SPARC in the dynamic interaction between the tumor and the host. *Cancer Metastasis Rev*. 27:691-705.

Portela, M., S. Casas-Tinto, C. Rhiner, J.M. Lopez-Gay, O. Dominguez, D. Soldini, and E. Moreno. 2010. Drosophila SPARC is a self-protective signal expressed by loser cells during cell competition. *Dev Cell*. 19:562-73.

Potenza, N., C. Vecchione, A. Notte, A. De Rienzo, A. Rosica, L. Bauer, A. Affuso, M. De Felice, T. Russo, R. Poulet, G. Cifelli, G. De Vita, G. Lembo, and R. Di Lauro. 2005. Replacement of K-Ras with H-Ras supports normal embryonic development despite inducing cardiovascular pathology in adult mice. *EMBO Rep*. 6:432-7.

Price, P.J., W.A. Suk, P.C. Skeen, G.J. Spahn, and M.A. Chirigos. 1977. Geldanamycin inhibition of 3-methylcholanthrene-induced rat embryo cell transformation. *Proc Soc Exp Biol Med*. 155:461-3.

Prodromou, C. 2012. The 'active life' of Hsp90 complexes. *Biochim Biophys Acta*. 1823:614-23.

Pylayeva-Gupta, Y., E. Grabocka, and D. Bar-Sagi. 2011. RAS oncogenes: weaving a tumorigenic web. *Nat Rev Cancer*. 11:761-74.

Rajakulendran, T., M. Sahmi, M. Lefrancois, F. Sicheri, and M. Therrien. 2009. A dimerization-dependent mechanism drives RAF catalytic activation. *Nature*. 461:542-5.

Reinhard, M., M. Halbrugge, U. Scheer, C. Wiegand, B.M. Jockusch, and U. Walter. 1992. The 46/50 kDa phosphoprotein VASP purified from human platelets is a novel protein associated with actin filaments and focal contacts. *Embo J*. 11:2063-70.

Reinhard, M., K. Jouvenal, D. Tripier, and U. Walter. 1995. Identification, purification, and characterization of a zyxin-related protein that binds the focal adhesion and microfilament protein VASP (vasodilator-stimulated phosphoprotein). *Proc Natl Acad Sci U S A*. 92:7956-60.

Rentsendorj, O., T. Mirzapoiazova, D. Adyshev, L.E. Servinsky, T. Renne, A.D. Verin, and D.B. Pearse. 2008. Role of vasodilator-stimulated phosphoprotein in cGMP-mediated protection of human pulmonary artery endothelial barrier function. *Am J Physiol Lung Cell Mol Physiol*. 294:L686-97.

Retzlaff, M., M. Stahl, H.C. Eberl, S. Lagleder, J. Beck, H. Kessler, and J. Buchner. 2009. Hsp90 is regulated by a switch point in the C-terminal domain. *EMBO Rep*. 10:1147-53.

Rhiner, C., J.M. Lopez-Gay, D. Soldini, S. Casas-Tinto, F.A. Martin, L. Lombardia, and E. Moreno. 2010. Flower forms an extracellular code that reveals the fitness of a cell to its neighbors in Drosophila. *Dev Cell*. 18:985-98.

Richter, A.M., G.P. Pfeifer, and R.H. Dammann. 2009. The RASSF proteins in cancer; from epigenetic silencing to functional characterization. *Biochim Biophys Acta*. 1796:114-28.

Rowinsky, E.K. 2006. Lately, it occurs to me what a long, strange trip it's been for the farnesyltransferase inhibitors. *J Clin Oncol*. 24:2981-4.

Rudrapatna, V.A., R.L. Cagan, and T.K. Das. 2012. Drosophila cancer models. *Dev Dyn*. 241:107-18.

Sanchez, A., D. Tripathy, X. Yin, K. Desobry, J. Martinez, J. Riley, D. Gay, J. Luo, and P. Grammas. 2012. p38 MAPK: A Mediator of Hypoxia-Induced Cerebrovascular Inflammation. *J Alzheimers Dis*.

Sasaki, K., H. Yasuda, and K. Onodera. 1979. Growth inhibition of virus transformed cells in vitro and antitumor activity in vivo of geldanamycin and its derivatives. *J Antibiot (Tokyo)*. 32:849-51.

Saunders, R.M., M.R. Holt, L. Jennings, D.H. Sutton, I.L. Barsukov, A. Bobkov, R.C. Liddington, E.A. Adamson, G.A. Dunn, and D.R. Critchley. 2006. Role of vinculin in regulating focal adhesion turnover. *Eur J Cell Biol*. 85:487-500.

Schlegel, N., and J. Waschke. 2009. Impaired integrin-mediated adhesion contributes to reduced barrier properties in VASP-deficient microvascular endothelium. *J Cell Physiol*. 220:357-66.

Schulte, T.W., and L.M. Neckers. 1998. The benzoquinone ansamycin 17-allylamino-17-demethoxygeldanamycin binds to HSP90 and shares important biologic activities with geldanamycin. *Cancer Chemother Pharmacol*. 42:273-9.

Senoo-Matsuda, N., and L.A. Johnston. 2007. Soluble factors mediate competitive and cooperative interactions between cells expressing different levels of Drosophila Myc. *Proc Natl Acad Sci U S A*. 104:18543-8.

Sharrocks, A.D. 2001. The ETS-domain transcription factor family. *Nat Rev Mol Cell Biol*. 2:827-37.

Shen, Y., Q. Xie, M. Norberg, E. Sausville, G.V. Woude, and D. Wenkert. 2005. Geldanamycin derivative inhibition of HGF/SF-mediated Met tyrosine kinase receptor-dependent urokinase-plasminogen activation. *Bioorg Med Chem*. 13:4960-71.

Silvius, J.R., P. Bhagatji, R. Leventis, and D. Terrone. 2006. K-ras4B and prenylated proteins lacking "second signals" associate dynamically with cellular membranes. *Mol Biol Cell*. 17:192-202.

Simpson, P. 1979. Parameters of cell competition in the compartments of the wing disc of Drosophila. *Dev Biol*. 69:182-93.

Simpson, P., and G. Morata. 1981. Differential mitotic rates and patterns of growth in compartments in the Drosophila wing. *Dev Biol*. 85:299-308.

Sims, J.D., J. McCready, and D.G. Jay. 2011. Extracellular heat shock protein (Hsp)70 and Hsp90alpha assist in matrix metalloproteinase-2 activation and breast cancer cell migration and invasion. *PLoS One*. 6:e18848.

Smrcka, A.V., J.H. Brown, and G.G. Holz. 2012. Role of phospholipase Cepsilon in physiological phosphoinositide signaling networks. *Cell Signal*. 24:1333-43.

Sreeramulu, S., S.L. Gande, M. Gobel, and H. Schwalbe. 2009. Molecular mechanism of inhibition of the human protein complex Hsp90-Cdc37, a kinome chaperone-cochaperone, by triterpene celastrol. *Angew Chem Int Ed Engl*. 48:5853-5.

Stefanatos, R.K., and M. Vidal. 2011. Tumor invasion and metastasis in Drosophila: a bold past, a bright future. *J Genet Genomics*. 38:431-8.

Stengel, K., and Y. Zheng. 2011. Cdc42 in oncogenic transformation, invasion, and tumorigenesis. *Cell Signal*. 23:1415-23.

Stoker, M. 1964. Regulation of Growth and Orientation in Hamster Cells Transformed by Polyoma Virus. *Virology*. 24:165-74.

Swanson, K.D., J.M. Winter, M. Reis, M. Bentires-Alj, H. Greulich, R. Grewal, R.H. Hruban, C.J. Yeo, Y. Yassin, O. Iartchouk, K. Montgomery, S.P. Whitman, M.A. Caligiuri, M.L. Loh, D.G. Gilliland, A.T. Look, R. Kucherlapati, S.E. Kern, M. Meyerson, and B.G. Neel. 2008. SOS1 mutations are rare in human malignancies: implications for Noonan Syndrome patients. *Genes Chromosomes Cancer*. 47:253-9.

Swarthout, J.T., S. Lobo, L. Farh, M.R. Croke, W.K. Greentree, R.J. Deschenes, and M.E. Linder. 2005. DHHC9 and GCP16 constitute a human protein fatty acyltransferase with specificity for H- and N-Ras. *J Biol Chem*. 280:31141-8.

Tall, G.G., M.A. Barbieri, P.D. Stahl, and B.F. Horazdovsky. 2001. Ras-activated endocytosis is mediated by the Rab5 guanine nucleotide exchange activity of RIN1. *Dev Cell*. 1:73-82.

Tamori, Y., C.U. Bialucha, A.G. Tian, M. Kajita, Y.C. Huang, M. Norman, N. Harrison, J. Poulton, K. Ivanovitch, L. Disch, T. Liu, W.M. Deng, and Y. Fujita. 2010. Involvement of Lgl and Mahjong/VprBP in cell competition. *PLoS Biol*. 8:e1000422.

Tan, I., J. Lai, J. Yong, S.F. Li, and T. Leung. 2011. Chelerythrine perturbs lamellar actomyosin filaments by selective inhibition of myotonic dystrophy kinase-related Cdc42-binding kinase. *FEBS Lett*. 585:1260-8.

Tan, I., C.H. Ng, L. Lim, and T. Leung. 2001. Phosphorylation of a novel myosin binding subunit of protein phosphatase 1 reveals a conserved mechanism in the regulation of actin cytoskeleton. *J Biol Chem*. 276:21209-16.

Travers, J., S. Sharp, and P. Workman. 2012. HSP90 inhibition: two-pronged exploitation of cancer dependencies. *Drug Discov Today*. 17:242-52.

Trichet, L., C. Sykes, and J. Plastino. 2008. Relaxing the actin cytoskeleton for adhesion and movement with Ena/VASP. *J Cell Biol*. 181:19-25.

Trisciuoglio, D., C. Gabellini, M. Desideri, E. Ziparo, G. Zupi, and D. Del Bufalo. 2010. Bcl-2 regulates HIF-1alpha protein stabilization in hypoxic melanoma cells via the molecular chaperone HSP90. *PLoS One*. 5:e11772.

Tyler, D.M., W. Li, N. Zhuo, B. Pellock, and N.E. Baker. 2007. Genes affecting cell competition in Drosophila. *Genetics*. 175:643-57.

Uhlirova, M., and D. Bohmann. 2006. JNK- and Fos-regulated Mmp1 expression cooperates with Ras to induce invasive tumors in Drosophila. *Embo J*. 25:5294-304.

Vanhaesebroeck, B., J. Guillermet-Guibert, M. Graupera, and B. Bilanges. 2010. The emerging mechanisms of isoform-specific PI3K signalling. *Nat Rev Mol Cell Biol*. 11:329-41.

Vidal, M. 2010. The dark side of fly TNF: an ancient developmental proof reading mechanism turned into tumor promoter. *Cell Cycle*. 9:3851-6.

Vidal, M., D.E. Larson, and R.L. Cagan. 2006. Csk-deficient boundary cells are eliminated from normal Drosophila epithelia by exclusion, migration, and apoptosis. *Dev Cell*. 10:33-44.

Vidal, M., S. Warner, R. Read, and R.L. Cagan. 2007. Differing Src signaling levels have distinct outcomes in Drosophila. *Cancer Res*. 67:10278-85.

Vigil, D., J. Cherfils, K.L. Rossman, and C.J. Der. 2010. Ras superfamily GEFs and GAPs: validated and tractable targets for cancer therapy? *Nat Rev Cancer*. 10:842-57.

Vincent, J.P., G. Kolahgar, M. Gagliardi, and E. Piddini. 2011. Steep differences in wingless signaling trigger Myc-independent competitive cell interactions. *Dev Cell*. 21:366-74.

Wennerberg, K., K.L. Rossman, and C.J. Der. 2005. The Ras superfamily at a glance. *J Cell Sci*. 118:843-6.

Whitesell, L., E.G. Mimnaugh, B. De Costa, C.E. Myers, and L.M. Neckers. 1994. Inhibition of heat shock protein HSP90-pp60v-src heteroprotein complex formation by benzoquinone ansamycins: essential role for stress proteins in oncogenic transformation. *Proc Natl Acad Sci U S A*. 91:8324-8.

Wiche, G., and L. Winter. 2011. Plectin isoforms as organizers of intermediate filament cytoarchitecture. *Bioarchitecture*. 1:14-20.

Wilkinson, S., H.F. Paterson, and C.J. Marshall. 2005. Cdc42-MRCK and Rho-ROCK signalling cooperate in myosin phosphorylation and cell invasion. *Nat Cell Biol*. 7:255-61.

Wu, J.M., L. Xiao, X.K. Cheng, L.X. Cui, N.H. Wu, and Y.F. Shen. 2003. PKC epsilon is a unique regulator for hsp90 beta gene in heat shock response. *J Biol Chem*. 278:51143-9.

Yeatman, T.J. 2004. A renaissance for SRC. *Nat Rev Cancer*. 4:470-80.

Zaidel-Bar, R., C. Ballestrem, Z. Kam, and B. Geiger. 2003. Early molecular events in the assembly of matrix adhesions at the leading edge of migrating cells. *J Cell Sci*. 116:4605-13.

Zhang, D., L. Xu, F. Cao, T. Wei, C. Yang, G. Uzan, and B. Peng. 2010. Celastrol regulates multiple nuclear transcription factors belonging to HSP90's clients in a dose- and cell type-dependent way. *Cell Stress Chaperones*. 15:939-46.

Zhang, S.L., J. Yu, X.K. Cheng, L. Ding, F.Y. Heng, N.H. Wu, and Y.F. Shen. 1999. Regulation of human hsp90alpha gene expression. *FEBS Lett*. 444:130-5.

Zhang, T., A. Hamza, X. Cao, B. Wang, S. Yu, C.G. Zhan, and D. Sun. 2008. A novel Hsp90 inhibitor to disrupt Hsp90/Cdc37 complex against pancreatic cancer cells. *Mol Cancer Ther*. 7:162-70.

Zhang, T., Y. Li, Y. Yu, P. Zou, Y. Jiang, and D. Sun. 2009. Characterization of celastrol to inhibit hsp90 and cdc37 interaction. *J Biol Chem*. 284:35381-9.

Zhao, R., and W.A. Houry. 2005. Hsp90: a chaperone for protein folding and gene regulation. *Biochem Cell Biol*. 83:703-10.

Zhao, Z.S., Y.Y. Wang, Y.Q. Chu, Z.Y. Ye, and H.Q. Tao. 2010. SPARC is associated with gastric cancer progression and poor survival of patients. *Clin Cancer Res*. 16:260-8.

Ziosi, M., L.A. Baena-Lopez, D. Grifoni, F. Froldi, A. Pession, F. Garoia, V. Trotta, P. Bellosta, S. Cavicchi, and A. Pession. 2012. dMyc functions downstream of Yorkie to promote the supercompetitive behavior of hippo pathway mutant cells. *PLoS Genet*. 6.

Zuzga, D.S., J. Pelta-Heller, P. Li, A. Bombonati, S.A. Waldman, and G.M. Pitari. 2011. Phosphorylation of vasodilator-stimulated phosphoprotein Ser239 suppresses filopodia and invadopodia in colon cancer. *Int J Cancer*. 130:2539-48.